

論文 / 著書情報  
Article / Book Information

題目(和文)	夏季の西部北極海における溶存メタンの時空間分布
Title(English)	Spatial and temporal distribution of dissolved methane in the summertime western Arctic Ocean
著者(和文)	工藤久志
Author(English)	Kushi Kudo
出典(和文)	学位:博士(理学), 学位授与機関:東京工業大学, 報告番号:甲第10751号, 授与年月日:2018年3月26日, 学位の種別:課程博士, 審査員:吉田 尚弘,大河内 直彦,笠井 康子,豊田 栄,山田 桂太
Citation(English)	Degree:Doctor (Science), Conferring organization: Tokyo Institute of Technology, Report number:甲第10751号, Conferred date:2018/3/26, Degree Type:Course doctor, Examiner:,,,,
学位種別(和文)	博士論文
Type(English)	Doctoral Thesis

Ph. D thesis

Spatial and temporal distribution of dissolved methane in the  
summertime western Arctic Ocean

A dissertation submitted in partial fulfillment of the requirement for the degree  
DOCTOR OF SCIENCE

Kushi Kudo

Department of Environmental Chemistry and Engineering  
Tokyo Institute of Technology

2018

## Abstract

Methane (CH<sub>4</sub>) is a trace gas playing an important role in the global carbon cycles and climate change as a greenhouse gas. Recent Arctic warming and decreasing sea-ice could promote release of CH<sub>4</sub> from sediment on the continental shelf and microbes, and provide a strong positive climate feedback. However, dynamics of dissolved CH<sub>4</sub> in the Arctic Ocean are still uncertain, especially in the western part (Bering Strait, Chukchi Sea and Canada Basin). Therefore, this thesis describes the horizontal and vertical distributions of concentration and stable carbon isotope ratio ( $\delta^{13}\text{C}$  value) of CH<sub>4</sub> in the western Arctic Ocean.

Surface layer samples analyzed by this study were supersaturated with CH<sub>4</sub> in comparison to the atmosphere. Furthermore, the concentrations in 2013 were 2–3 times higher than in 2012. This reason might be considered as vertical transportation of CH<sub>4</sub> from bottom layer to surface layer due to weaker stratification by freshwater.

In coastal shelf area in 2012, concentrations in bottom layer were higher (up to 55.9 nmol kg<sup>-1</sup>), whereas  $\delta^{13}\text{C}$  values were lower (down to -63.8‰). This might indicate that CH<sub>4</sub> in bottom layer was produced mainly by organic matter degradation in seafloor sediment via methanogen. On the other hands, gradients of concentration and  $\delta^{13}\text{C}$  value of dissolved CH<sub>4</sub> were not found in 2013. This fact supported that effect by vertical mixing were stronger in 2013.

At deeper stations in the Canada Basin (seafloor > 300 m depth) in 2012, the maxima of CH<sub>4</sub> concentration were detected at depths of 10–50 m and 100–200 m, although  $\delta^{13}\text{C}$  values were lowest at 50 m depth. The shallower CH<sub>4</sub> maximum coincided with the DO maximum, suggesting CH<sub>4</sub> production by plankton activity or sinking particles. The deeper CH<sub>4</sub> maximum corresponded to the nutrient maximum, suggesting horizontal advection of shelf water from the coastal shelf area.

In fixed station observation in 2013, vertical mixing at windy condition produced the highest CH<sub>4</sub> concentration in surface layer (17.2 nmol kg<sup>-1</sup> with  $\delta^{13}\text{C} = -52.9\text{‰}$ ), which suggested vertically transportation of CH<sub>4</sub> from bottom of mixed layer to surface layer.

From the results, the dynamic variation of dissolved CH<sub>4</sub> in the western Arctic Ocean in summer 2012 and 2013 with area, depth and years were carefully studied and its mechanism was evaluated quantitatively.

## Contents

<b>Chapter 1: Introduction</b>	<b>1</b>
1.1 Methane (CH <sub>4</sub> ) dynamics in the Arctic Ocean	1
1.1.1 General introduction of oceanic CH <sub>4</sub>	2
1.1.2 Situation of the Arctic Ocean	3
1.2 Purpose of this study	4
Figures and Tables	6
<b>Chapter 2: Methods</b>	<b>10</b>
2.1 Sampling	10
2.2 Measurement	11
2.3 Calculation	12
Figures and Tables	16
<b>Chapter 3: Results</b>	<b>21</b>
3.1 Horizontal distributions of CH <sub>4</sub> in the surface seawater	21
3.1.1 September–October 2012	21
3.1.2 August–October 2013	22
3.2 Vertical distributions of CH <sub>4</sub> in the continental shelf area	22
3.2.1 September–October 2012	22
3.2.2 August–October 2013	23
3.3 Vertical distributions of deeper area (from off point Barrow to the Canada Basin in 2012)	24
3.4 Temporal change in FPO in 2013	24
Figures and Tables	26
<b>Chapter 4: Discussion</b>	<b>50</b>
4.1 Dissolved CH <sub>4</sub> in surface water	50
4.1.1 September–October 2012	50
4.1.2 August–October 2013	51
4.2 Continental shelf area	52
4.2.1 Chukchi Sea	52
4.2.2 Bering Strait	55
4.3 Deeper area (from off point Barrow to the Canada Basin in 2012)	56
4.3.1 Shallower CH <sub>4</sub> maximum	57
4.3.2 Deeper CH <sub>4</sub> maximum	58

<b>4.4 Temporal change in FPO in 2013</b>	<b>61</b>
<b>Figures and Tables</b>	<b>64</b>
<b>Chapter 5: Conclusion</b>	<b>76</b>
<b>5.1 Summary of this study</b>	<b>76</b>
<b>5.2 Future works</b>	<b>77</b>
<b>Acknowledgement</b>	<b>79</b>
<b>References</b>	<b>81</b>

## **Chapter 1: Introduction**

### **1.1 Methane (CH<sub>4</sub>) dynamics in the Arctic Ocean**

Because of recent global warming, a sea-ice decrease can be measured in the Arctic Ocean especially during summer (McGuire et al. 2009, 2010; Arrigo et al. 2011; Permentier et al. 2013). During 1979–2012, the respective rates of decrease of the annual mean Arctic sea-ice extent and the summer sea-ice minimum have been 3.5–4.1% per decade and 9.4–13.6% per decade (IPCC 2013; Figure 1-1). Sea-ice extent was minimalized in September 2012 (IPCC 2013; Permentier et al. 2013; Harada et al. 2016; Figure 1-2, 3). These sea-ice decreases affect heat, light and freshwater cycles in this area, accelerating primary production and seafloor sediments (McGuire et al. 2009, 2010; Arrigo et al. 2011; Hioki et al. 2014, Harada 2016). These phenomena might accelerate the release of greenhouse gases. Especially, the release of methane (CH<sub>4</sub>) has been regarded as predominant because of its greater storage capacity in Arctic areas (35–365 Pg CH<sub>4</sub>) (IPCC 2007, 2013; McGuire et al. 2009, 2010; Dlugokencky et al. 2009, 2011).

Terrestrial and oceanic CH<sub>4</sub> in Arctic areas are potentially important sources to the atmosphere. Their flux is estimated at 32–112 Tg C yr<sup>-1</sup> (McGuire et al. 2009, 2010; Figure 1-4). In the Arctic Ocean, CH<sub>4</sub> production has been reported via processes of CH<sub>4</sub> release from seafloor sediments in the Beaufort Sea, Eastern Siberian Sea, Laptev Sea, and off the Svalbard islands (Kvenvolden et al. 1993b; Damm et al. 2005, 2008; Shakhova et al. 2005, 2010, 2014; Myhre et al. 2016), in addition to aerobic CH<sub>4</sub> production by the phytoplankton metabolite

dimethylsulfoniopropionate (DMSP:  $(\text{CH}_3)_2\text{S}^+\text{CH}_2\text{CH}_2\text{COO}^-$ ) in the central Arctic Ocean (Damm et al. 2010). These  $\text{CH}_4$  production processes and dynamics of dissolved  $\text{CH}_4$  affect the budget, influencing not only the Arctic climate but also global climate (e.g. IPCC 2013).

#### 1.1.1 General introduction of oceanic $\text{CH}_4$

Earlier studies revealed the characteristic stable carbon isotope ratio ( $\delta^{13}\text{C}$ , see section 2.2 for definition) of oceanic  $\text{CH}_4$  produced by various processes. (1) Biogenic sources such as sedimentary organic matter and  $\text{CH}_4$  clathrate hydrate, are divided into two pathways :1.  $\text{CO}_2$  reduction pathway ( $\text{CO}_2 + 4\text{H}_2 \rightarrow \text{CH}_4 + 2\text{H}_2\text{O}$ , mainly occurring in seawater) and 2. acetate fermentation pathway ( $\text{CH}_3\text{COOH} \rightarrow \text{CH}_4 + \text{CO}_2$ , mainly occurring in freshwater). In seawater, acetate is used as a substance of sulfate-reducing bacteria. Therefore,  $\text{CH}_4$  formation occurs almost entirely via the  $\text{CO}_2$  reduction pathway in seawater (e.g. Whiticar 1999). The  $\delta^{13}\text{C}$  values of  $\text{CH}_4$  produced by  $\text{CO}_2$  reduction were reported as  $-110$  to  $-60\text{‰}$  (Whiticar et al. 1986, 1999; Kvenvolden et al. 1993a; Kanster et al. 1998). The reported  $\delta^{13}\text{C}$  values of  $\text{CH}_4$  produced by acetate fermentation are  $-65$  to  $-50\text{‰}$  (Whiticar et al. 1986, 1999). (2) Thermogenic processes in hydrothermal systems produce  $\text{CH}_4$  with  $\delta^{13}\text{C}$  values of  $-50$  to  $-20\text{‰}$  (Whiticar et al. 1986, 1999). (3) In aerobic environments, methanogenic archaea living within anaerobic cavities of the zooplankton gut or inside sinking particles produce  $\text{CH}_4$ . Their respective reported  $\delta^{13}\text{C}$  values are  $-61$  to  $-54\text{‰}$  (Sasakawa et al. 2008) and  $-37$  to  $+6\text{‰}$  (Sasakawa et al. 2008). Oceanic  $\text{CH}_4$  is consumed mainly by microbial  $\text{CH}_4$  oxidation, and then the  $\delta^{13}\text{C}$  value

becomes higher (e.g. Sansone et al. 2001; Yoshikawa et al. 2014) (Figure 1-5).

### 1.1.2 Situation of the Arctic Ocean

In the Arctic Ocean, reports of several studies have described the concentration and  $\delta^{13}\text{C}$  of  $\text{CH}_4$ . MacDonald (1976) observed vertical profile of  $\text{CH}_4$  concentration in 1974 and 1975 in the Beaufort Sea. That study found concentrations near equilibrium with the atmosphere (approx.  $3.5 \text{ nmol L}^{-1}$ ) in surface waters but concentrations considerably higher than saturation near the bottom layer (up to  $50 \text{ nmol L}^{-1}$ ) during the sea-ice melted season. Shakhova et al. (2005) measured  $\text{CH}_4$  concentration in the East Siberian and Laptev Seas in the summers of 2003 and 2004. They found that  $\text{CH}_4$  concentrations in the surface layer were 2.1 to  $28.2 \text{ nmol L}^{-1}$  in 2003 and approx. 5 to  $110 \text{ nmol L}^{-1}$  in plume areas in 2004. In the bottom layer, it was approx.  $5\text{--}87 \text{ nmol L}^{-1}$  in 2003 and approx.  $5\text{--}154 \text{ nmol L}^{-1}$  in 2004. Kvenvolden et al. (1993b) observed that micro bubbles in sea ice in the Beaufort Sea have a high concentration of  $\text{CH}_4$ , with  $\delta^{13}\text{C}$  of  $-78.4\text{‰}$ . Damm et al. (2005, 2008, 2010, 2015) reported that sources of  $\text{CH}_4$  in Pacific-derived water (Pdw) ( $\delta^{13}\text{C} < -46\text{‰}$ ) and Atlantic-derived water (Adw) ( $\delta^{13}\text{C} = -43$  to  $-41\text{‰}$ ) in the central Arctic Ocean differ. They inferred a  $\text{CH}_4$  surplus in Pdw and mixing between the local marine background ( $-38\text{‰}$ ) and the atmospheric reservoir ( $-47\text{‰}$ ) in Adw. Savvichev et al. (2007) observed  $\text{CH}_4$  profiles in the water column and bottom sediments of the Bering Strait and Chukchi Sea. They found that the  $\text{CH}_4$  content in the water column of the Chukchi Sea varied from 8 to  $31 \text{ nmol L}^{-1}$ , and that the  $\text{CH}_4$  formation rate from bottom sediments varied from  $0.25$  to  $16 \text{ nmol dm}^{-3} \text{ day}^{-1}$ .



Fenwick et al. (2017) observed dissolved CH<sub>4</sub> with its concentration of 0.7–30.5 nmol L<sup>-1</sup> ( $\delta^{13}\text{C} = -42$  to  $-33\text{‰}$ ) in the Bering Sea and Chukchi Sea in summer 2015. They concluded that dissolved CH<sub>4</sub> was produced mainly from seafloor sediments via the decomposition of organic carbon. Then microbial CH<sub>4</sub> oxidation occurred. Lapham et al. (2017) reported that CH<sub>4</sub> concentrations in Barrow Canyon were 5–74 nmol L<sup>-1</sup> in August 2012. They inferred that CH<sub>4</sub> was produced mainly from sedimentary source.

## 1.2 Purpose of this study

In this study, I focused on the western Arctic Ocean (Bering Sea, Chukchi Sea and Canada Basin) because this area occupied 22% of total shelf volume of the Arctic Ocean, and the most rapid retreat of sea-ice has been observed (Harada et al. 2016; Figure 1-3). Therefore, I thought that distribution of dissolved CH<sub>4</sub> in the western Arctic Ocean was important for clarifying CH<sub>4</sub> dynamics in the Arctic Ocean and Arctic climate change. Nevertheless, data of CH<sub>4</sub> obtained in the western Arctic Ocean are almost nonexistent. Few studies have used  $\delta^{13}\text{C}$  of CH<sub>4</sub>, which provides information about CH<sub>4</sub> production and consumption processes, including its concentration (e.g. Kvenvolden et al. 1993b). Therefore, identification of the influence on CH<sub>4</sub> amounts, its production and consumption processes, and its cycle (e.g. McGuire et al. 2009) in the Arctic Ocean remains difficult.

Therefore, the present study surveys and analyzes the distribution of CH<sub>4</sub> dissolved in the surface water and the water column of the western Arctic Ocean. I investigated CH<sub>4</sub> production and consumption processes by first elucidating the CH<sub>4</sub>

concentration and  $\delta^{13}\text{C}$ .

## Figures and tables

### Figures

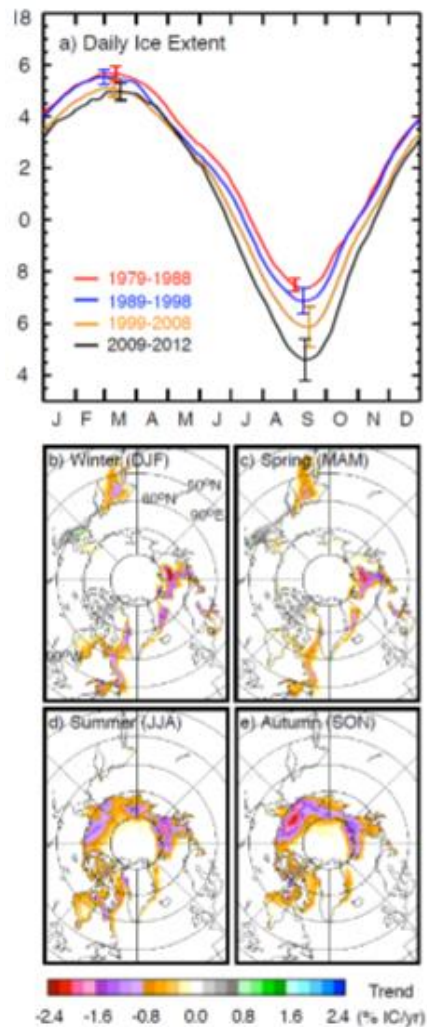


**Figure 1-1.** (a) Plots of decadal averages of daily sea ice extent in the Arctic (1979 to 1988 in red, 1989 to 1998 in blue, 1999 to 2008 in gold) and a four-year average daily ice extent from 2009 to 2012 in black. Maps ice concentration trends (1979–2012) in (b) winter, (c) spring, (d) summer and (e) autumn (updated from Comiso, 2010) (IPCC 2013).

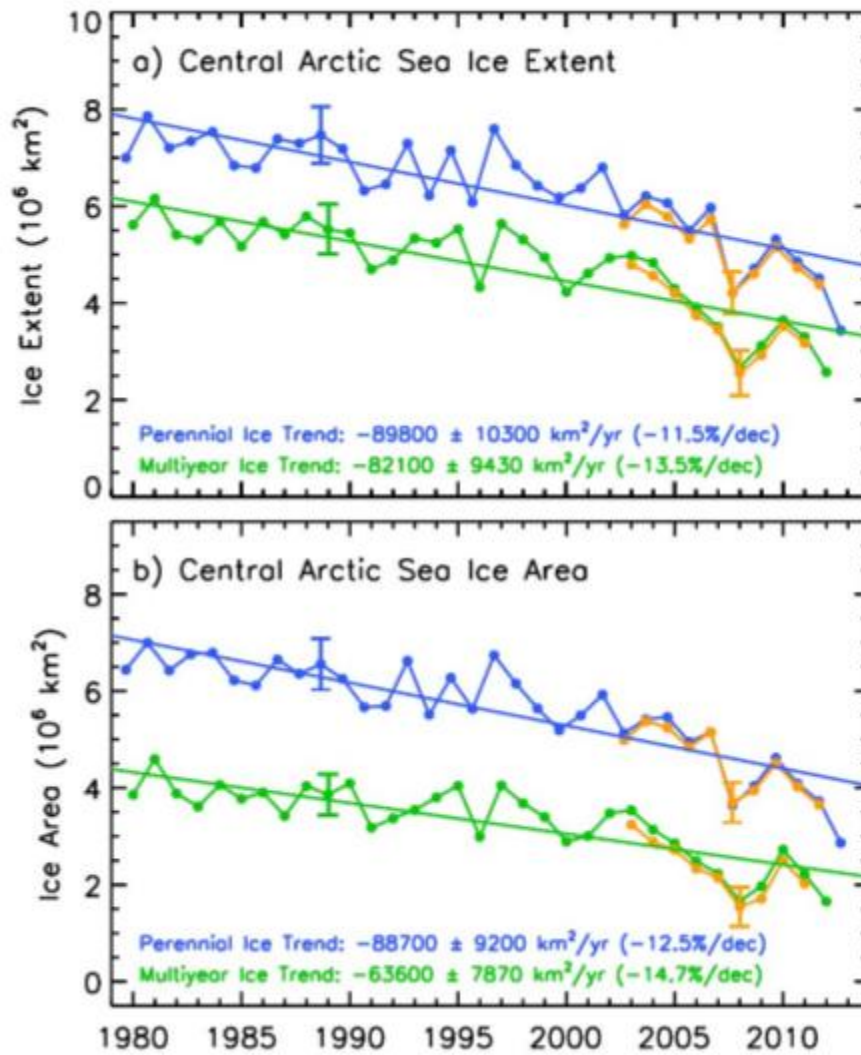


**Figure 1-2.** Annual perennial (blue) and multiyear (green) sea ice extent (a) and sea ice area (b) in the Central Arctic from 1979 to 2012 as derived from satellite passive microwave data. Perennial ice values are derived from summer ice minimum values, while the multiyear ice values are averages of those from December, January and February. The gold lines (after 2002) are from AMSR-E data (updated from Comiso, 2012) (IPCC 2013).

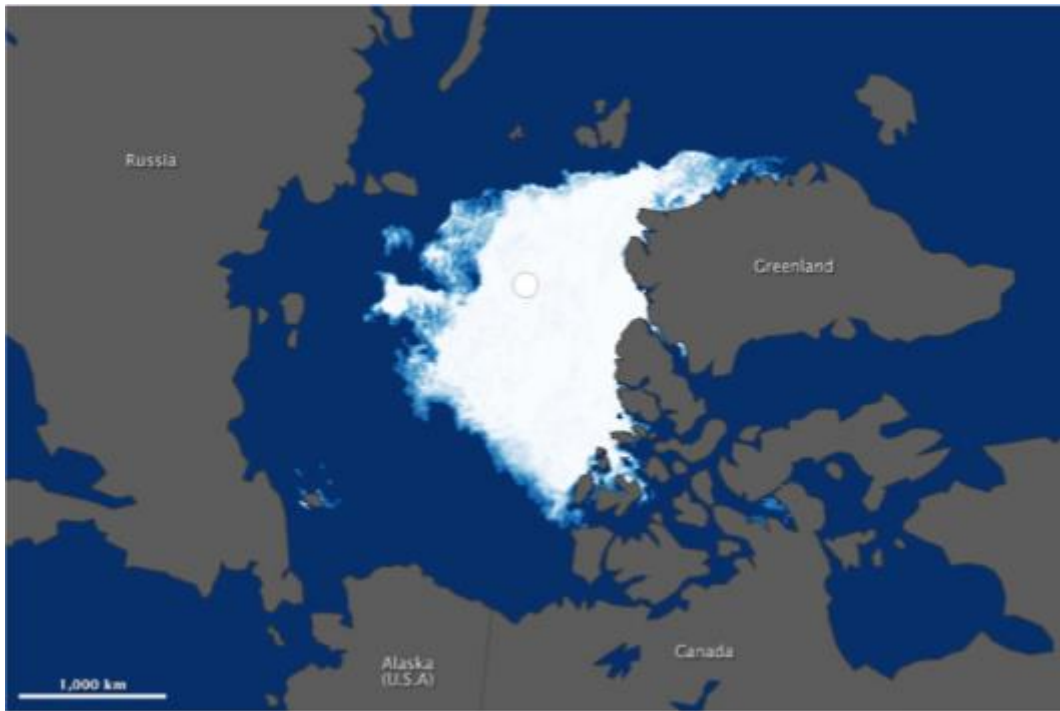


**Figure 1-3.** Map of the Arctic Ocean with the sea-ice condition acquired 13 September 2012 (Harada et al. 2016).

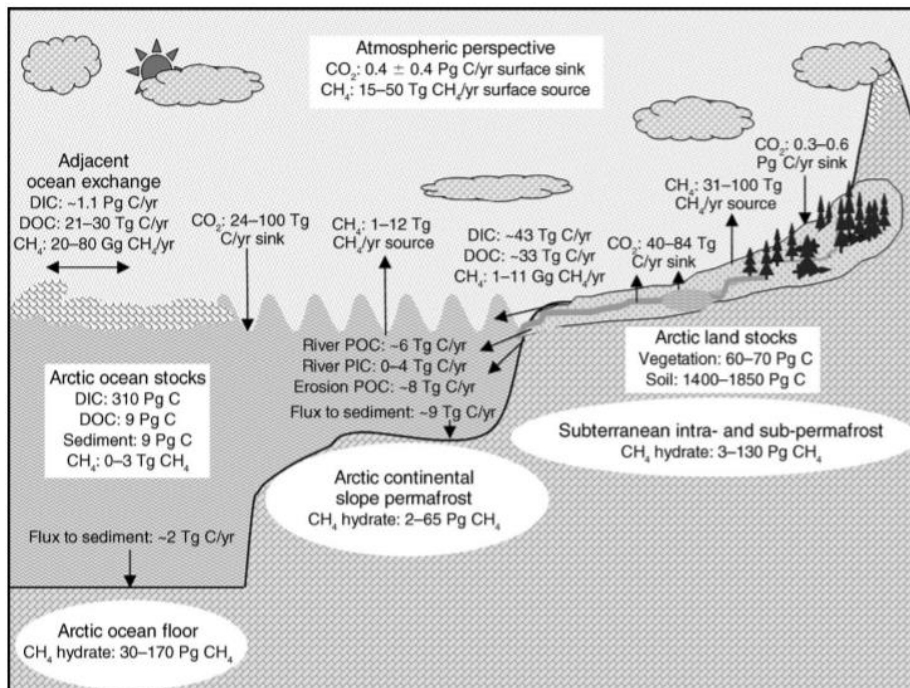


**Figure 1-4.** The current state of the Arctic carbon cycle based on a synthesis of the information. Values shown are the ranges uncertainty (McGuire et al. 2009, 2010).

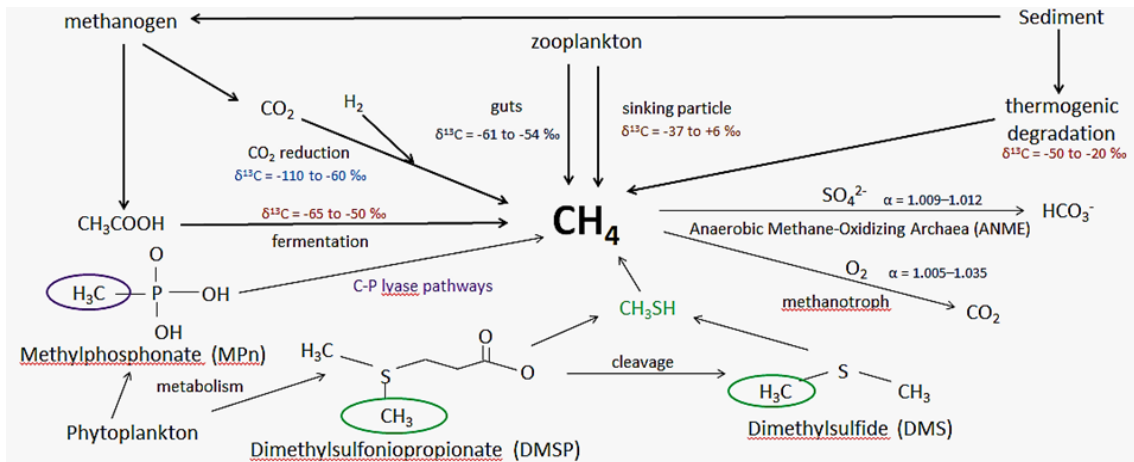


**Figure 1-5.** Production and consumption pathways of oceanic CH<sub>4</sub> (Coleman and Risatti 1981; Whiticar et al. 1986, 1999; Alperin et al. 1988; Karl and Titblook 1994; Martens et al. 1999; Tsunogai et al. 2000; Sansone et al. 2001; Yoshida et al. 2004; Sasakawa et al.,2008; Karl et al. 2008; Damm et al. 2010; Florez-Leiva et al. 2013)

## Chapter 2: Methods

### 2.1 Sampling

During the MR12-E03 and MR13-06 cruises of R/V Mirai (JAMSTEC, Japan), as a part of GRENE Arctic Climate Change Research Project, we collected seawater samples at 26 and 14 stations (St.) in the western Arctic Ocean from 15 September to 4 October and from 28 August to 7 October in 2012 and 2013, respectively. The period of from August to October was important because minimum of sea-ice extent has been observed in mid-September (especially in 2012) and effect from sea-ice forming has been often observed toward October (Figure 1-1a). Therefore, I focused on this period in this study. During the sampling period, sea ice was almost free around the sampling stations. Furthermore, fixed point observation was held at 72.75°N, 192.75°E in the northern Chukchi Sea shelf (St. 41 in MR13-06 cruise) in from 10 to 26 September and 1 October in 2013 for considering impact of forming sea-ice to sea-air interaction and biological activity (Nishino, S., 2013, R/V Mirai Cruise Report MR13-06, edited by S. Nishino 226pp., JAMSTEC, Yokosuka, Japan). Sea-ice has nearing to this point in October. Therefore, I choose this point as fixed point observation. Samples were collected using a CTD-CAROUSEL system (Sea-Bird Electronics, Bellevue, WA, USA) equipped with 12-L Niskin bottles (Figure 2-2) at 2–6 depths at the continental shelf stations and 5–20 depths at deeper stations. Samples were subsampled, respectively, into 30 and 125 ml glass vials for analysis of CH<sub>4</sub> concentration and stable carbon isotope ratio. Special care was taken to avoid air contamination. These samples were sterilized by adding saturated mercuric chloride (HgCl<sub>2</sub>) solution (final HgCl<sub>2</sub> concentration was

ca. 0.5%; Karl and Tilbrook 1995; Watanabe et al. 1995) and were sealed with rubber stoppers and aluminum caps. They were stored in refrigerator (dark 277 K) until analysis.

Furthermore, conductivity, temperature and depth (CTD) were conducted on this cruise and we used this data for dissolved oxygen (DO) and nutrients concentration, total carbon (TCarbon), total alkalinity (TA), water temperature, salinity and potential density. Surface water samples were taken at 5 m depth from sea surface in order to compare with on board spectroscopic monitoring system for dissolved CH<sub>4</sub> operated by Meteorological Research Institute (MRI). Vertical sampling of the water column was conducted at several deep stations. Sampling locations and depth are shown in Figures 2-1 and Tables 2-1.

## **2.2 Measurement**

The concentration and stable carbon isotope ratio of dissolved CH<sub>4</sub> were measured, respectively, using gas chromatography with flame ionization detection (GC-FID) and gas chromatography-combustion-isotope ratio mass spectrometry (GC-C-IRMS). Outlines of these equipment are shown in Figures 2-3. For each measurement, the dissolved CH<sub>4</sub> was extracted with a purge and trap unit. We extracted the dissolved CH<sub>4</sub> using a glass gas extraction bottle (125 mL) and a trap cooled with liquid N<sub>2</sub> (170 mm long column packed with Polapak-Q and glass wool) based on a description by Tsunogai et al. (1998, 2000). Then the dissolved CH<sub>4</sub> was injected into the GC by He carrier gas. For isotopic measurements, CH<sub>4</sub> was separated from interfering components (CO) using a column packed with Molecular Sieves 5A (10 mm ID × 500 mm length,



30/60 mesh, GL Sciences, Inc., Tokyo, Japan) before it was concentrated in a cryofocusing trap. The  $\delta^{13}\text{C}$  value was calculated as shown below.

$$\delta^{13}\text{C} = \left( \left( \frac{^{13}\text{C}}{^{12}\text{C}} \right)_{\text{sample}} / \left( \frac{^{13}\text{C}}{^{12}\text{C}} \right)_{\text{VPDB}} - 1 \right) \times 1000 \quad (1)$$

Therein, VPDB stands for Vienna Peedee Belemnite, in the international standard of the  $^{13}\text{C}/^{12}\text{C}$  ratio.

I used two working standards. For concentration measurements, we used 2.08 ppm  $\text{CH}_4$  in purified Air (Taiyo Nissan Co.). For isotope measurements, 1000 ppm  $\text{CH}_4$  in He (Taiyo Nissan Co.) with  $\delta^{13}\text{C} = -39.56\text{‰}$  was used (Yamada et al. 2005). Precision of the concentration and  $\delta^{13}\text{C}$  value of  $\text{CH}_4$  were estimated respectively as  $<5\%$  ( $n = 5$ ,  $1\sigma$ ) and  $0.3\text{‰}$ , respectively ( $n = 6$ ,  $1\sigma$ ) based on repeated analyses of the standards. The differences between measured concentration and  $\delta^{13}\text{C}$  of duplicate seawater samples were, respectively,  $0.1\text{--}0.7 \text{ nmol kg}^{-1}$  and  $0.1\text{--}0.8\text{‰}$ .

### 2.3 Calculation

We calculated the oversaturation ratio (SR) of dissolved  $\text{CH}_4$  using its solubility (Weisenberg and Guinasso 1979) of

$$\text{SR}(\%) = \left( \left[ \text{CH}_4 \right]_w / \left[ \text{CH}_4 \right]_a - 1 \right) \times 100 \quad (2)$$

where  $[CH_4]_w$  denotes the measured concentration and  $[CH_4]_a$  represents the equilibrium concentration calculated from the atmospheric concentration of  $CH_4$  (1.89 ppmv: Database of JAMSTEC), seawater temperature ( $T$ , in K), and salinity ( $S$ , ‰) as

$$\ln[CH_4]_a = \ln f_G + A_1 + A_2(100/T) + A_3 \ln(T/100) + A_4(T/100) + S[B_1 + B_2(T/100) + B_3(T/100)^2] \quad (3)$$

where  $A_1 = -417.5023$ ,  $A_2 = 599.8626$ ,  $A_3 = 380.3636$ ,  $A_4 = -62.0764$ ,  $B_1 = -0.064236$ ,  $B_2 = 0.034980$ , and  $B_3 = -0.0052732$ .

Sea-air  $CH_4$  flux ( $F_{CH_4}$ ,  $\mu\text{mol m}^{-2} \text{day}^{-1}$ ) was calculated according to a description by Wanninkhof (1992).

$$F_{CH_4} = k_w \times ([CH_4]_{w(0-10m)} - [CH_4]_a) \quad (4)$$

Therein  $[CH_4]_{w(0-10m)}$  stands for the measured  $CH_4$  concentration in the surface 0–10 m seawater. Also  $k_w$  denotes the gas transfer velocity, which depends on the wind speed ( $v$ ,  $\text{m s}^{-1}$ ) at 10 m overseas height and which is calculated using the equation below.

$$k_w = 0.31v^2 \sqrt{(S_c/660)^{-1}} \quad (5)$$

In that equation,  $S_c$  represents the Schmidt number of  $CH_4$  in seawater, which depends on the atmospheric temperature ( $T$ , in  $^{\circ}\text{C}$ ) and which is calculated as presented below.

$$Sc = 2039.2 - 120.31T + 3.4029T^2 - 0.040437T^3 \quad (6)$$

The atmospheric temperature and wind speeds in equations (5) and (6) were taken from the integrated meteorological dataset obtained during the MR12-E03 cruise (Japan Agency for Marine-Earth Science and Technology (2016) Data Research System for Whole Cruise Information in JAMSTEC. <http://www.godac.jamstec.go.jp/darwin/>).

Assuming that CH<sub>4</sub> dissolved in excess (SR > 0) is a mixture of atmospheric CH<sub>4</sub> and CH<sub>4</sub> produced in the water column, we calculated the δ<sup>13</sup>C value of the excess CH<sub>4</sub> (δ<sup>13</sup>C<sub>ex</sub>) based on the mass balance as shown below (Sasakawa et al. 2008).

$$\delta^{13}C_{ex} = (\delta^{13}C \times [CH_4] - \delta^{13}C_a \times [CH_4]_a) / [CH_4]_{ex} \quad (7)$$

In that equation, δ<sup>13</sup>C<sub>a</sub> represents the δ<sup>13</sup>C value of the atmospheric equilibrium (= -47‰ VPDB: Quay et al. 1991; Grant and Whiticar 2002)

We also examined the possibility of microbial oxidation of CH<sub>4</sub> in the water column using the following equation (Coleman et al. 1981).

$$\delta^{13}C = \delta^{13}C_{t_0} + 1000 \times (1/\alpha - 1) \times \ln([CH_4] / [CH_4]_{t_0}) \quad (8)$$

In that equation, t<sub>0</sub> stands for the initial state before oxidation of CH<sub>4</sub>. Also, α denotes the kinetic isotope fractionation factor. Eq. (8) is applicable if we assume that

the CH<sub>4</sub> concentration is controlled simply by microbial oxidation in a closed system.

## Figures and tables

### Figures

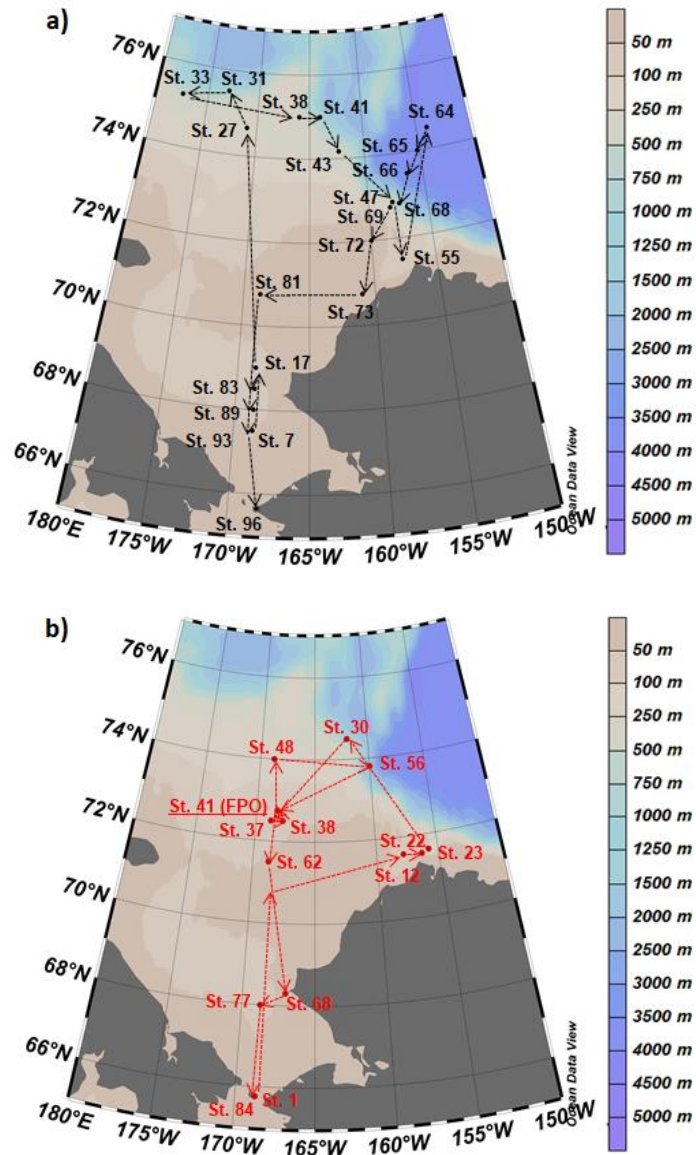
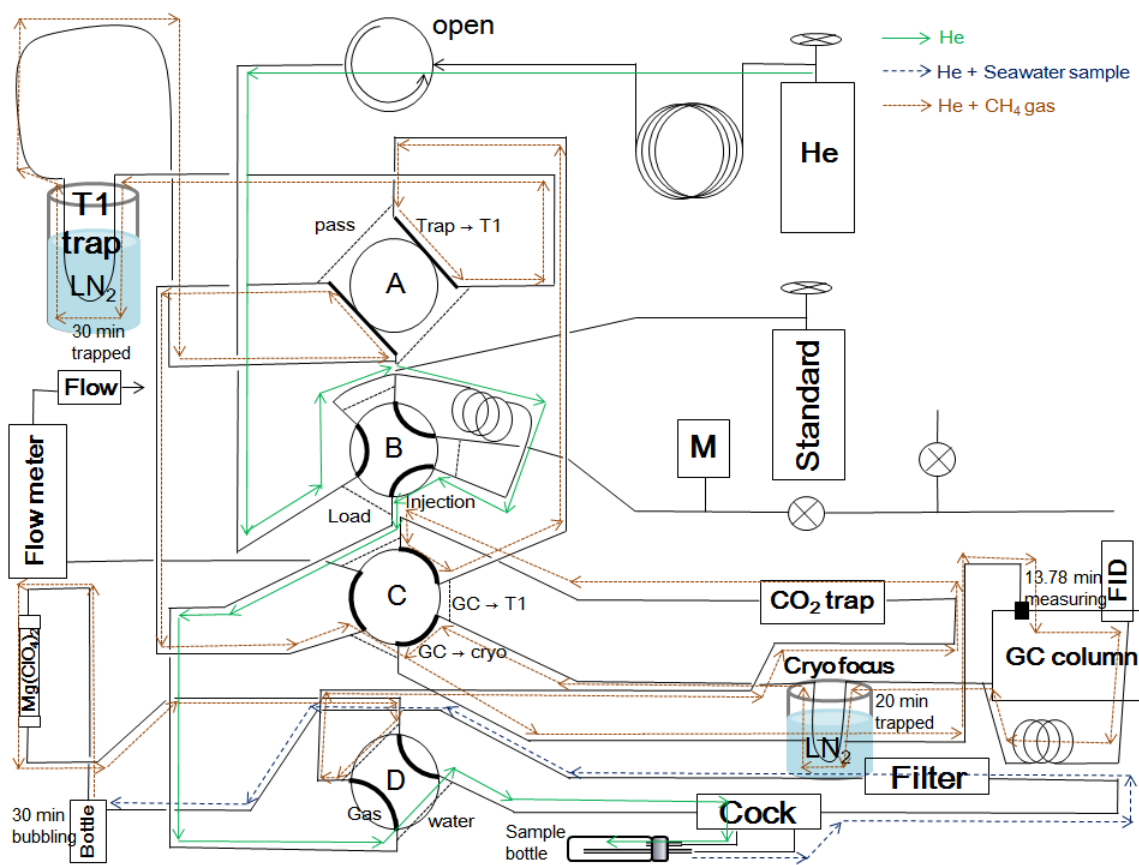


**Figure 2-1.** Map of sampling stations (a) MR12-E03 (2012) and (b) MR13-06 (2013). Broken arrows represent the cruise track of R/V Mirai. St. 41 of MR13-06 cruise was station of fixed point observation (FPO) which was held at 72.75°N, 192.75°E in the northern Chukchi Sea shelf in from 10 to 26 September and 1 October in 2013.



**Figure 2-2.** Picture of 12-L Niskin bottles.

(a)



(b)

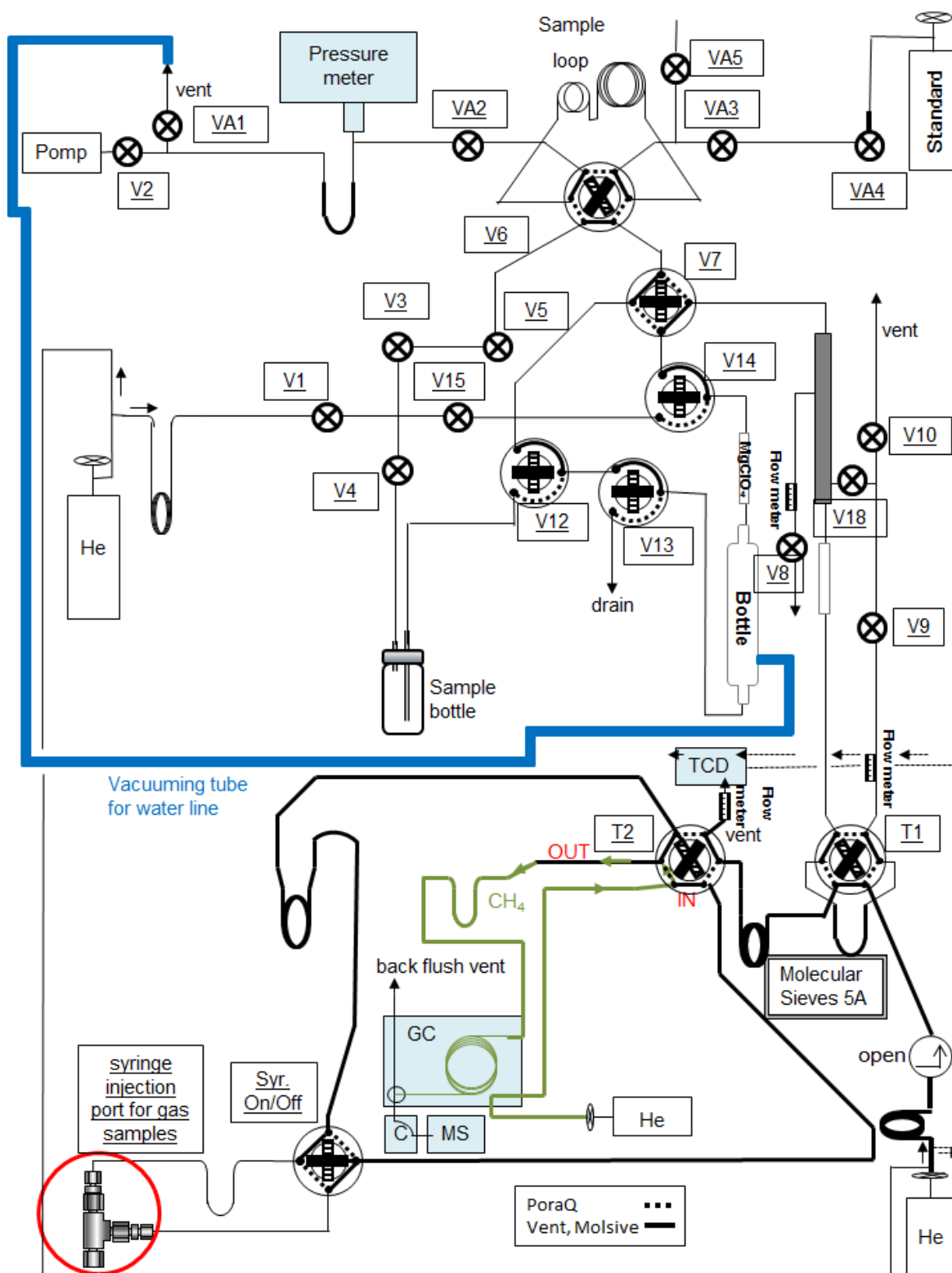


Figure 2-3. Outline of (a) GC-FID and (b) GC-C-IRMS.

## Tables

**Table 2-1.** Sampling time, location and station number information of (a) MR12-E03 and (b) MR13-06 cruises.

(a)

Station number	Sampling date	Latitude [°N]	Longitude [°E]	Sampling depth [m]
7	2012/9/14 10:20	67.5024	191.2523	5
17	2012/9/15 11:01	69.0004	191.2477	5
27	2012/9/17 7:31	74.6727	189.072	5
31	2012/9/18 3:31	75.5032	186.9634	5
33	2012/9/19 4:21	75.2353	182.4839	5
38	2012/9/20 10:37	74.9998	194.0015	5
41	2012/9/22 9:13	75	195.9984	5
43	2012/9/23 7:21	74.1725	197.6589	5
47	2012/9/24 7:53	72.8254	202.5969	5
55	2012/9/25 6:17	71.4946	202.3605	5
64	2012/9/29 3:33	74.4975	205.9901	5, 10, 25, 50, 75, 100, 125, 150, 175, 200, 225, 250, 300, 350, 400, 450, 500, 600, 700, 800, 900, 1000, 1100, 1200, 1300, 140, 1500, 1750, 2000, 2000, 2250, 2500, 2750, 3000, 3250, 3800, 3911
65	2012/9/29 9:21	73.998	204.7851	5, 3500, 3913
66	2012/9/29 19:32	73.4908	203.5829	5, 10, 25, 50, 75, 100, 125, 150, 200, 250, 300, 400, 600, 800, 1000, 1500, 2000, 3000, 3500, 3744
68	2012/9/30 4:42	72.8647	202.0353	5, 10, 20, 30, 40, 50, 60, 75, 100, 125, 150, 175, 200, 225, 250, 300, 400, 500, 600, 800, 1000, 1585
69	2012/9/30 7:29	72.7466	201.8035	5, 20, 50, 100, 303
72	2012/9/30 18:01	72.0002	200.0011	5, 21
73	2012/10/1 9:08	70.7501	199.0035	0, 5
81	2012/10/2 5:59	70.7514	191.2609	0, 5
83	2012/10/3 13:01	68.502	191.2488	5, 46
89	2012/10/3 22:17	67.9992	191.2537	5, 52
93	2012/10/4 4:29	67.5007	191.2487	0, 5, 40
96	2012/10/4 22:11	65.6525	191.7459	0, 5, 36



(b)

Station number	Sampling date	Latitude [°N]	Longitude [°E]	Sampling depth [m]
1	2013/8/31 19:51	65.7697	191.2483	0, 10, 20, 30, 45
12	2013/9/3 7:34	71.5808	202.1557	0, 10, 20, 40, 50, 58
22	2013/9/4 13:56	71.5468	203.6457	0, 10, 20, 30, 40, 50, 75, 100, 125, 150, 157
23	2013/9/4 16:22	71.627	204.2397	0, 10, 20, 30, 40, 50, 75, 100, 125, 150, 175, 200, 225
30	2013/9/7 22:34	74.5003	198.0157	5, 25, 50, 75, 100, 150, 200, 250, 300, 350, 400, 500, 600, 700, 800, 900, 1000, 1100, 1200, 1300, 1400, 1500, 1600, 1614
37	2013/9/10 9:36	72.501	191.2505	0, 10, 20, 30, 40, 49
38	2013/9/10 14:56	72.5012	192.252	0, 10, 20, 30, 40, 47
41#10	2013/9/13 2:40	72.7498	191.7548	0, 10, 20, 30, 40, 51
41#14	2013/9/14 2:41	72.7508	191.753	0, 10, 20, 30, 40, 45, 51
41#21	2013/9/15 20:42	72.7512	191.7458	0, 10, 20, 30, 40, 45, 51
41#25	2013/9/16 20:42	72.7515	191.7467	0, 20, 30, 40, 45, 51
41#33	2013/9/18 20:41	72.7487	191.7497	0, 10, 20, 30, 40, 45, 51
41#41	2013/9/20 20:45	72.7488	191.7592	0, 10, 20, 30, 40, 45, 51
41#43	2013/9/21 8:46	72.7517	191.7605	0, 10, 20, 30, 40, 45, 51
41#51	2013/9/23 8:43	72.7497	191.7532	0, 5, 10, 20, 30, 40, 45, 51
41#57	2013/9/24 20:42	72.7505	191.7507	0, 10, 20, 30, 40, 45, 51
48	2013/9/26 6:43	74.0025	191.2492	5, 10, 20, 30, 40, 50, 75, 100, 125, 150, 174
56	2013/9/27 12:25	73.8005	200.0103	5, 10, 20, 30, 40, 50, 75, 100, 125, 150, 175, 200, 225, 250, 300, 400, 500, 600, 800, 100, 1500, 2000, 2500, 2682
41#63	2013/10/1 2:43	72.751	191.7528	0, 10, 20, 30, 40, 45, 51
62	2013/10/2 2:05	71.5003	191.2533	0, 10, 20, 30, 40, 43
68	2013/10/2 22:56	68.3013	192.9542	0, 5, 10, 20, 31
77	2013/10/3 20:31	68.0008	191.2438	0, 10, 20, 30, 40, 45, 50
84	2013/10/4 18:23	65.7633	191.2427	0, 10, 20, 30, 40, 45

## Chapter 3: Results

### 3.1 Horizontal distributions of CH<sub>4</sub> in the surface seawater

#### 3.1.1 September–October 2012

The respective distributions of concentration, oversaturation ratio (SR), sea–air CH<sub>4</sub> flux ( $F_{\text{CH}_4}$ ), and  $\delta^{13}\text{C}$  values of dissolved CH<sub>4</sub> in seawater are presented in Figures 3-1a–3-1d. Information related to wind speed, air temperature, dissolved and atmospheric equilibrium CH<sub>4</sub> concentration, sea–air CH<sub>4</sub> flux, and values of  $\delta^{13}\text{C}$  and  $\delta^{13}\text{C}_{\text{ex}}$  of dissolved CH<sub>4</sub> in the surface water and atmospheric CH<sub>4</sub> is shown in Table 3-1a.

Surface water was found to be supersaturated with CH<sub>4</sub> at all stations (SR = 5.1–206.2%, Fig. 3-1b, Table 3-1). In general, CH<sub>4</sub> concentrations were higher at the stations at continental shelf areas ( $5.5 \pm 0.4 \text{ nmol kg}^{-1}$ , average and  $1\sigma$ ) than at the stations at deeper areas ( $4.7 \pm 0.1 \text{ nmol kg}^{-1}$ ). Especially high CH<sub>4</sub> concentrations were observed off point Barrow (up to  $10.3 \text{ nmol kg}^{-1}$ ).

The  $\delta^{13}\text{C}$  values of dissolved CH<sub>4</sub> were  $-55.0$  to  $-41.1\text{‰}$  (average and  $1\sigma$ :  $-47.1 \pm 1.3\text{‰}$ ) (Table 3-1a, Fig. 3-1c). The  $\delta^{13}\text{C}$  values at continental shelf areas (average,  $\delta^{13}\text{C} = -48.9 \pm 2.2\text{‰}$ ) were lower than the values of atmospheric equilibrium CH<sub>4</sub> ( $-47\text{‰}$ ) whereas the  $\delta^{13}\text{C}$  values in deeper areas ( $-45.3 \pm 1.3\text{‰}$ ) were often higher than the values of atmospheric equilibrium CH<sub>4</sub>. Especially low  $\delta^{13}\text{C}$  values (down to  $-55.9\text{‰}$ ) were observed off point Barrow. Calculated  $\delta^{13}\text{C}_{\text{ex}}$  values were  $-67.2$  to  $-14.8\text{‰}$ .

### 3.1.2 August–October 2013

Distribution of concentration, oversaturation ratio (SR), sea–air CH<sub>4</sub> flux ( $F_{CH_4}$ ), and  $\delta^{13}C$  values of dissolved CH<sub>4</sub> in 2013 are presented in Figs. 3-2a–3-2d. Information related to wind speed, air temperature, dissolved and atmospheric equilibrium CH<sub>4</sub> concentration, sea–air CH<sub>4</sub> flux, and values of  $\delta^{13}C$  and  $\delta^{13}C_{ex}$  of dissolved CH<sub>4</sub> in the surface water and atmospheric CH<sub>4</sub> in 2013 is shown in Table 3-1b.

Surface water was also found to be supersaturated with CH<sub>4</sub> at all stations in 2013 (SR = 44.1–984.1%, Fig. 3-2b, Table 3-1). Same as in 2012, CH<sub>4</sub> concentrations were higher at the stations at continental shelf areas ( $11.3 \pm 1.7 \text{ nmol kg}^{-1}$ ) than at the stations at deeper areas ( $9.4 \pm 3.5 \text{ nmol kg}^{-1}$ ). These concentrations were 2–3 times higher than in 2012.

The  $\delta^{13}C$  values of dissolved CH<sub>4</sub> were  $-52.9$  to  $-40.4\text{‰}$  ( $-47.4 \pm 1.0\text{‰}$ ) (Table 3-1, Fig. 3-2c). Same as in 2012, the  $\delta^{13}C$  values at continental shelf areas ( $-47.8 \pm 1.0\text{‰}$ ) were lower than the values of atmospheric equilibrium CH<sub>4</sub> ( $-47\text{‰}$ ) whereas the  $\delta^{13}C$  values in deeper areas ( $-43.9 \pm 0.4\text{‰}$ ) were often higher than the values of atmospheric equilibrium CH<sub>4</sub>. Calculated  $\delta^{13}C_{ex}$  values were  $-62.7$  to  $-37.3\text{‰}$ .

## 3.2 Vertical distributions of CH<sub>4</sub> in the continental shelf area

### 3.2.1 September–October 2012

Figure 3-3a–3-3f and table 3-2a present vertical distributions of dissolved CH<sub>4</sub>, DO,

and physical parameters of seawater in the continental shelf area (St. 72, 83, 89, and 96). In the Chukchi Sea (St. 72, 83, and 89), CH<sub>4</sub> concentrations increased with depth (surface, [CH<sub>4</sub>] = 4.1–6.1 nmol kg<sup>-1</sup>, SR = 14.0–65.5%; bottom, [CH<sub>4</sub>] = 16.9–55.9 nmol kg<sup>-1</sup>, SR = 398.1–1386.8% (Figs. 3-3a–3-3b)), whereas δ<sup>13</sup>C-CH<sub>4</sub> values decreased with depth (surface, –55.0 to –49.4‰; bottom, –63.8 to –61.3‰) (Fig. 3-3c). However, in the Bering Strait in October (St. 96), the vertical gradient of concentration and δ<sup>13</sup>C value was weak, showing almost homogeneous vertical distribution (surface, [CH<sub>4</sub>] = 5.1 nmol kg<sup>-1</sup>, SR = 48.0%, δ<sup>13</sup>C-CH<sub>4</sub> = –48.2‰; bottom, [CH<sub>4</sub>] = 6.3 nmol kg<sup>-1</sup>, SR = 80.2%, δ<sup>13</sup>C-CH<sub>4</sub> = –47.4‰) (Figs. 3-3a–3-3c).

### 3.2.2 August–October 2013

Figure 3-4a–3-4f and Table 3-2b present vertical distributions of dissolved CH<sub>4</sub>, DO, and physical parameters of seawater in the continental shelf area (St. 1, 62, 68, 77 and 84). In Chukchi Sea (St. 62, 68, and 77), gradient of CH<sub>4</sub> concentration with depth was not seen (surface, [CH<sub>4</sub>] = 9.3–15.9 nmol kg<sup>-1</sup>, SR = 187.2–367.8%; bottom, [CH<sub>4</sub>] = 10.4–13.5 nmol kg<sup>-1</sup>, SR = 206.7–273.2% (Figs. 3-4a–3-4b)), whereas δ<sup>13</sup>C value changed with depth (surface, δ<sup>13</sup>C = –51.9 to –40.4‰; bottom, δ<sup>13</sup>C = –84.2 to –57.1‰ (Fig. 3-4c)). In Bering Strait (St. 1 and 84), profile of concentration and δ<sup>13</sup>C value was different from in 2012 (surface, [CH<sub>4</sub>] = 7.4–37.4 nmol kg<sup>-1</sup>, SR = 145.3–984.1%, δ<sup>13</sup>C = –42.9 to –42.0‰; bottom, [CH<sub>4</sub>] = 10.0–10.4 nmol kg<sup>-1</sup>, SR = 183.7–202.3%, δ<sup>13</sup>C = –42.9 to –26.9‰ (Figs. 3-4a–3-4c)).

### **3.3 Vertical distributions of CH<sub>4</sub> in deeper area (from off point Barrow to the Canada Basin in 2012)**

Figures 3-5a–3-5i and table 3-3 present vertical distributions of CH<sub>4</sub>, DO, physical parameters, and the N<sup>\*\*</sup> value at St. 66, 68, and 69. Defined as a linear combination of nitrate and phosphate ( $N^{**} = 0.87 \times (([\text{NO}_3^-] + [\text{NO}_2^-] + [\text{NH}_4^+]) - 16 [\text{PO}_4^{3-}] + 2.9)$   $\mu\text{mol kg}^{-1}$ ) was proposed to investigate the distribution of nitrogen fixation and denitrification. Gruber and Sarmiento 1997; Nishino et al. 2005). Correlations between CH<sub>4</sub> and phosphate and those between CH<sub>4</sub> and potential density area shown in Figs 3-5h–3-5i. Depth–latitude sections of CH<sub>4</sub> and DO from off point Barrow to the Canada Basin are presented in Figs. 3-6a–3-6d.

In general, the CH<sub>4</sub> concentration maximum was observed at 10–50 m depth ([CH<sub>4</sub>]: up to 17.7 nmol kg<sup>-1</sup>, SR: up to 415.1%). At St. 68 and 69, there was another maximum was found at 100–200 m depth ([CH<sub>4</sub>], up to 21.8 nmol kg<sup>-1</sup>, SR, up to 477.2%). However, the  $\delta^{13}\text{C}$  values showed a minimum at around 50 m depth and increased gradually below that depth (10–50 m depth, –65.1 to –43.5‰; 100–200 m depth, –58.3 to –25.7‰) at St. 66 and 69, although the secondary minimum was observed at St. 68. Dissolved CH<sub>4</sub> concentrations were almost all less than 5 nmol kg<sup>-1</sup> and SR < 0 at several depths below 700 m depth.  $\delta^{13}\text{C}$  values were close to –40 to –30‰ below 700 m depth.

### **3.4 Temporal change in fixed-point observation in 2013**

Figures 3-7a–3-7b, Figures 3-8a–3-8b and Table 3-4 present temporal and vertical

distributions of dissolved CH<sub>4</sub>, respectively. Seawater was saturated with CH<sub>4</sub>. Seawater was found to be supersaturated with CH<sub>4</sub> at always. These concentrations in bottom layer ([CH<sub>4</sub>] = 10.9–61.0 nmol kg<sup>-1</sup>; SR = 188.3–1510.3%) were generally higher than in surface layer ([CH<sub>4</sub>] = 4.9–17.2 nmol kg<sup>-1</sup>; SR = 44.1–400.3%), whereas δ<sup>13</sup>C values in bottom layer (–58.2 to –24.1‰; δ<sup>13</sup>C<sub>ave</sub> = –51.9 ± 3.5‰) generally were lower than in surface layer (–52.9 to –43.6‰; δ<sup>13</sup>C<sub>ave</sub> = –50.0 ± 0.9‰). However, dramatically higher δ<sup>13</sup>C values (> –25‰) than atmospheric equilibrium were sometimes found in bottom layer.

## Figures and tables

### Figures

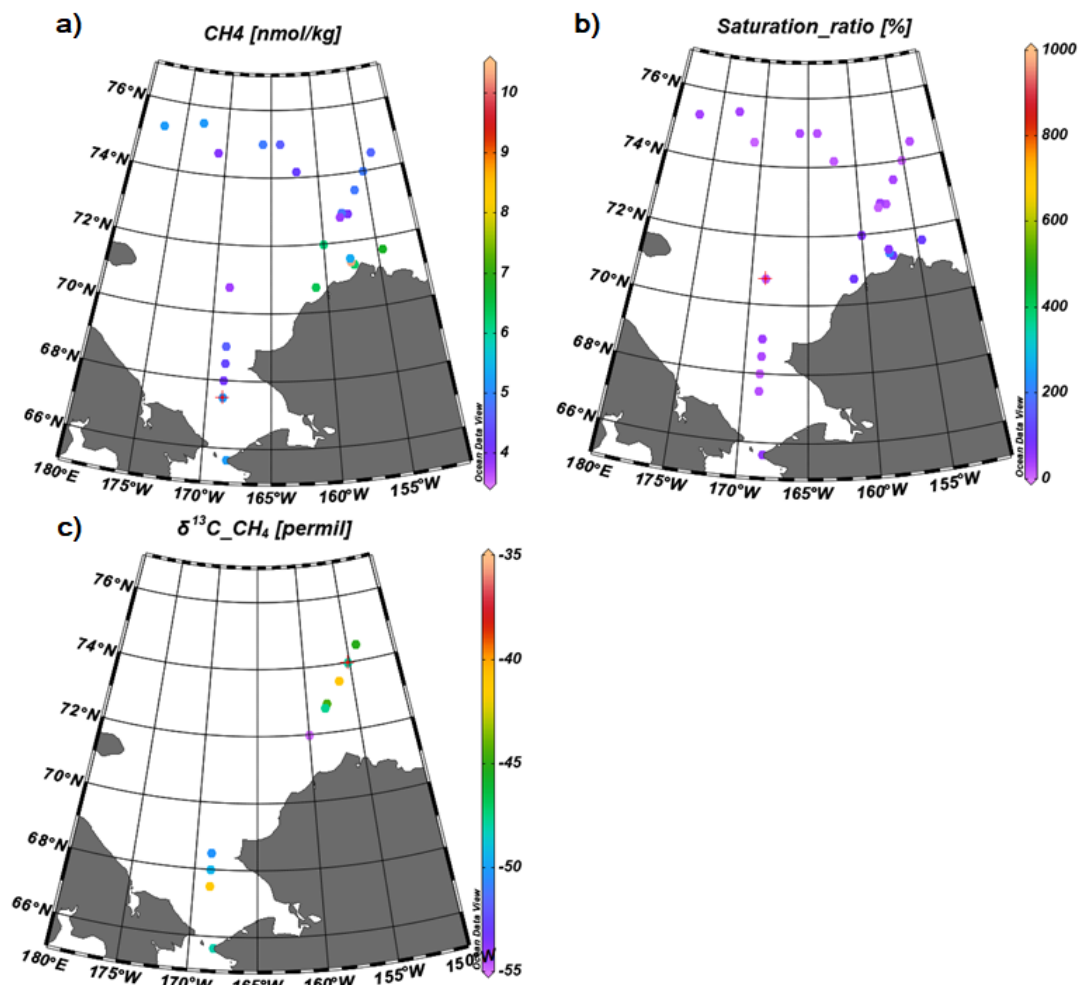


**Figure 3-1.** Horizontal distribution of (a) concentration, (b) over-saturation ratio (SR), and (c)  $\delta^{13}\text{C}$  values of dissolved CH<sub>4</sub> in surface seawater (0–10 m depth) in 2012.

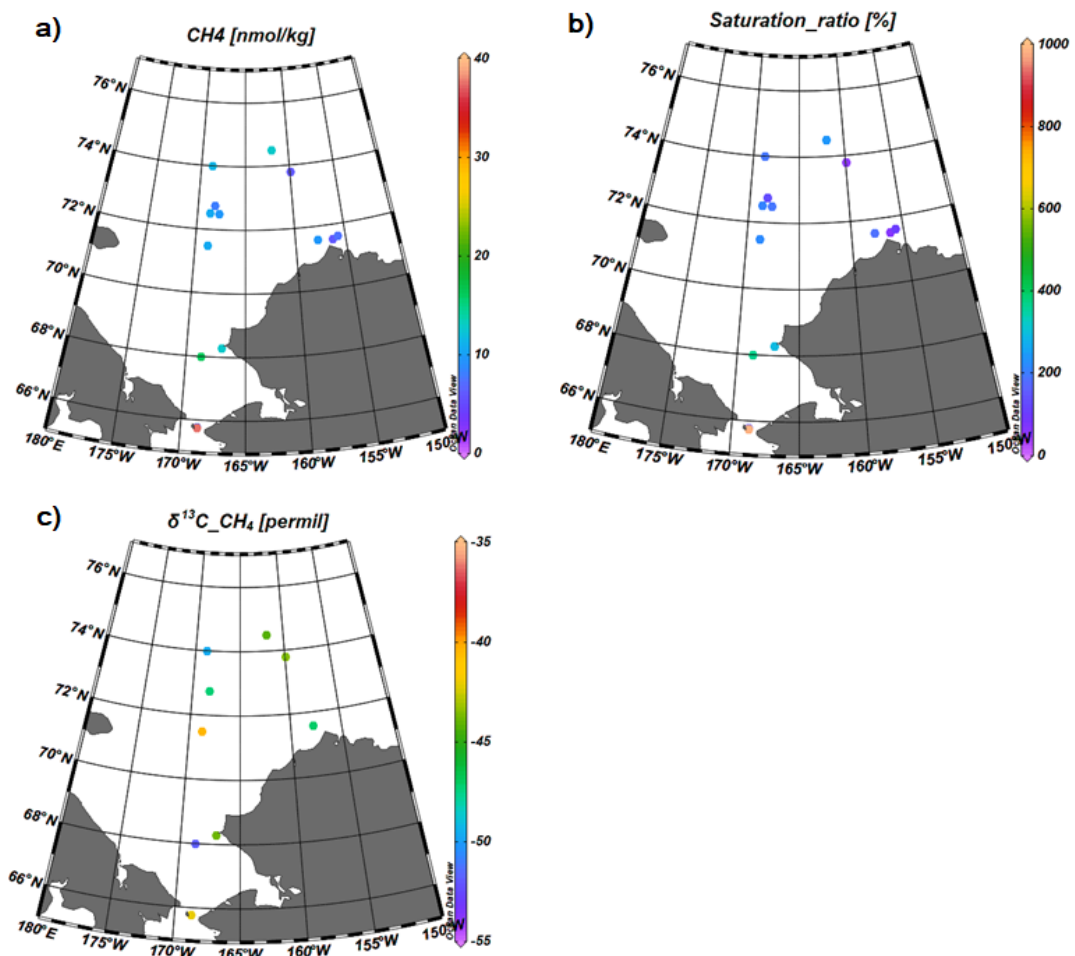


**Figure 3-2.** Horizontal distribution of (a) concentration, (b) over-saturation ratio (SR), and (c)  $\delta^{13}\text{C}$  values of dissolved CH<sub>4</sub> in surface seawater (0–10 m depth) in 2013.



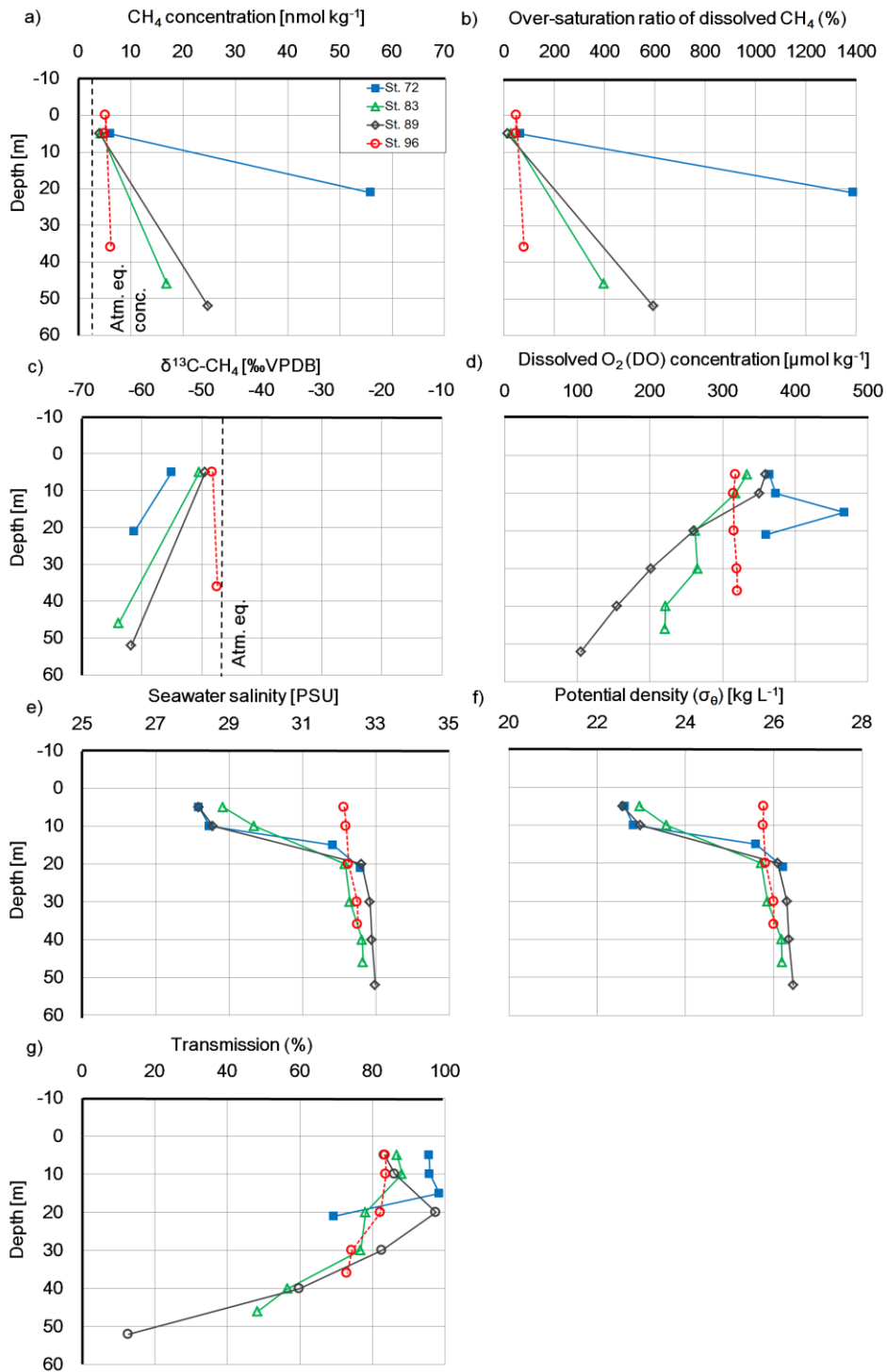


**Figure 3-3.** Vertical distributions of (a) concentration, (b) SR, and (c)  $\delta^{13}\text{C}$  values of dissolved  $\text{CH}_4$ , (d) DO concentration, (e) seawater salinity, (f) potential density and (g) transmission in the continental shelf area in 2012 (Chukchi Sea: St. 72, 83, and 89; Bering Strait: St. 96).

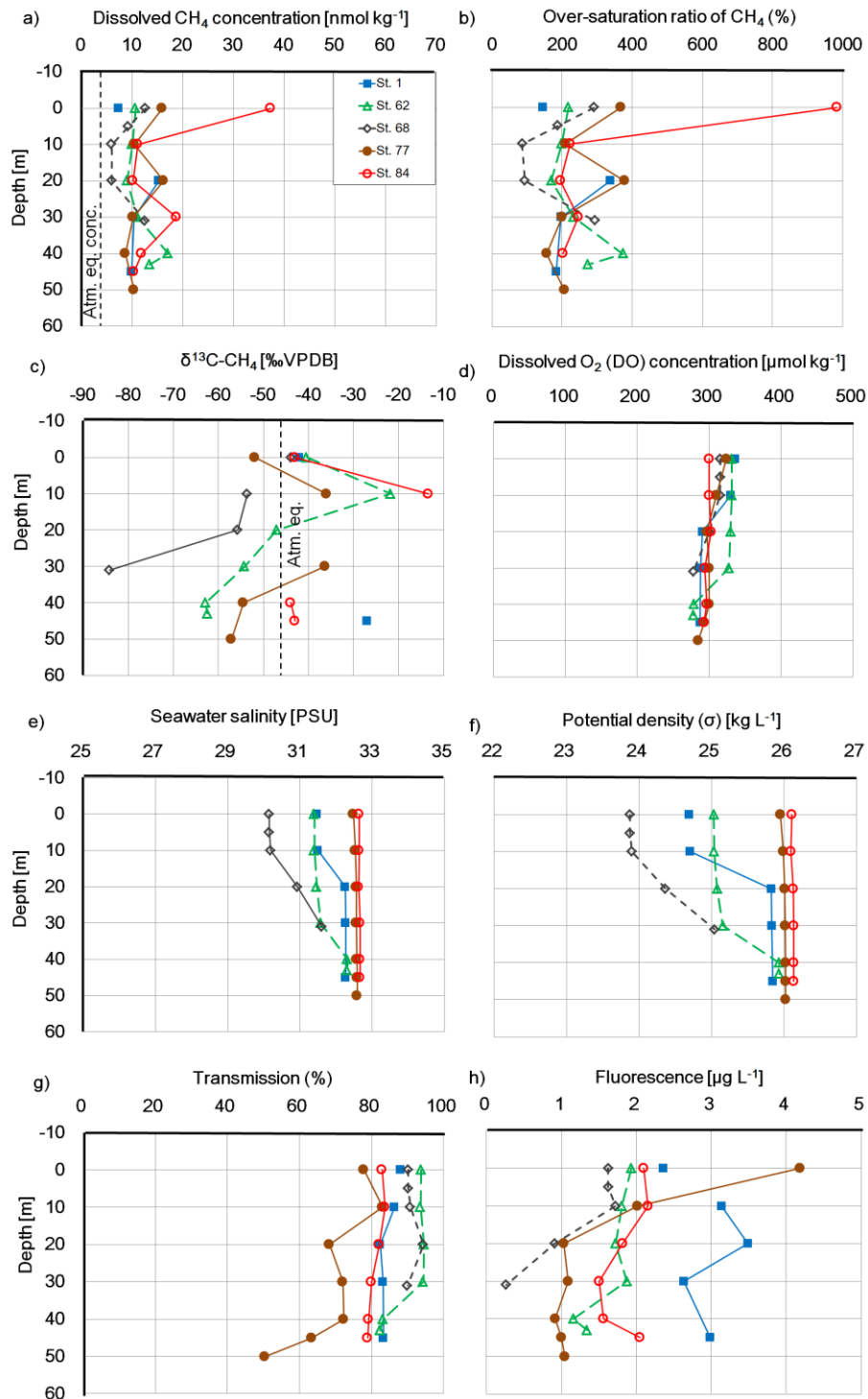


**Figure 3-4.** Vertical distributions of (a) concentration, (b) SR, and (c)  $\delta^{13}\text{C}$  values of dissolved  $\text{CH}_4$ , (d) DO concentration, (e) seawater salinity, (f) potential density, (g) transmission and (h) fluorescence concentration in the continental shelf area in 2013 (Chukchi Sea: St. 62, 68, and 77; Bering Strait: St. 1 and 84).

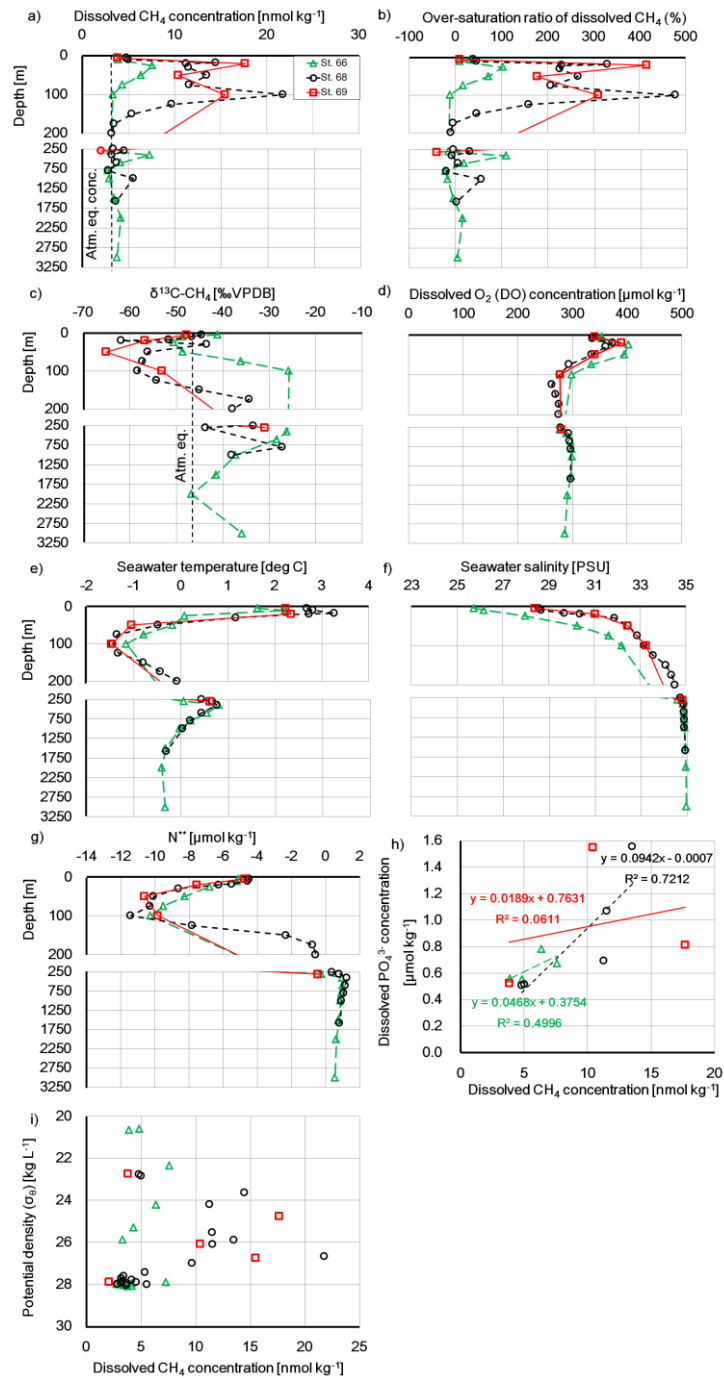


**Figure 3-5.** Vertical distributions of (a) concentration, (b) SR, and (c)  $\delta^{13}\text{C}$  values of dissolved  $\text{CH}_4$ , (d) DO concentration (e) seawater temperature, (f) seawater salinity, and (g)  $\text{N}^{**}$  value and correlation diagram of (h) dissolved  $\text{CH}_4$  concentration–dissolved phosphate concentration and (i) correlation diagram of dissolved  $\text{CH}_4$  concentration–potential density ( $\sigma_\theta$ ) in the Canada Basin. Data of DO concentration, seawater temperature, seawater salinity,  $\text{PO}_4^{3-}$  concentration and potential density ( $\sigma_\theta$ ) were referred from the JAMSTEC database.

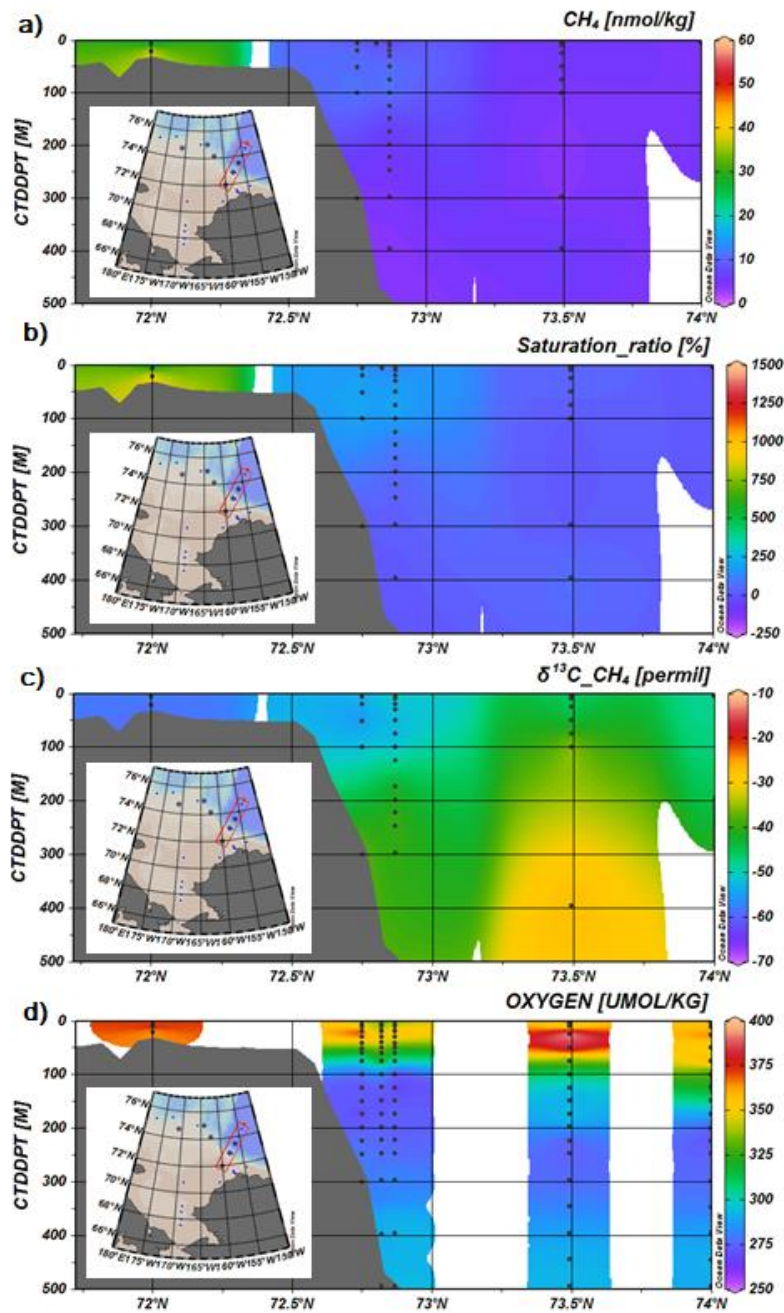


**Figure 3-6.** Spatial distributions of (a) concentration, (b) SR, (c)  $\delta^{13}\text{C}$  of dissolved  $\text{CH}_4$ , and (d) DO concentration in the deeper area. Data of DO concentration were referred from the JAMSTEC database.

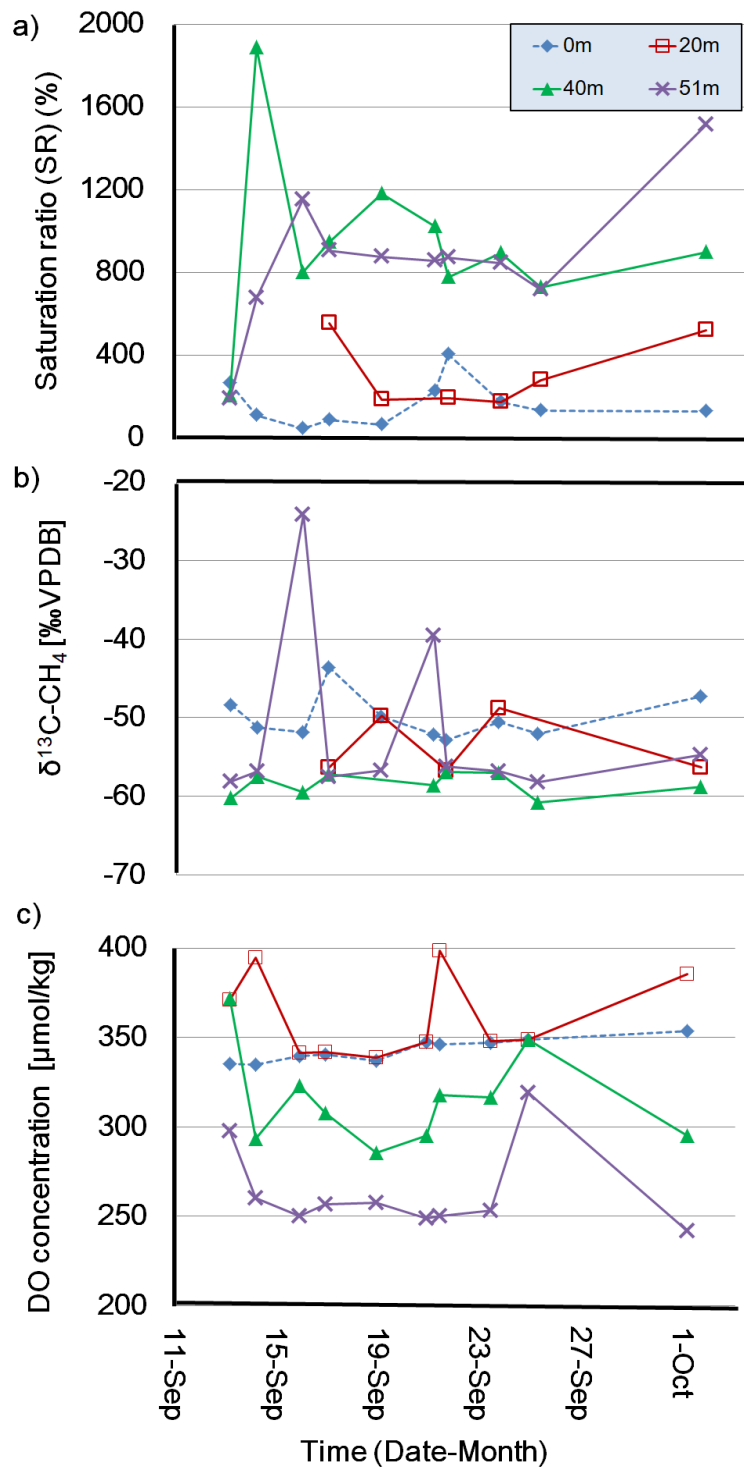


**Figure 3-7.** Temporal changing of (a) CH<sub>4</sub> concentration, (b)  $\delta^{13}\text{C}$  value and (c) DO concentration at 0, 20, 40, and 51 m depths in fixed-point observation (FPO) (St. 41 of MR13-06 cruise). Data of DO concentration were referred from the JAMSTEC database.

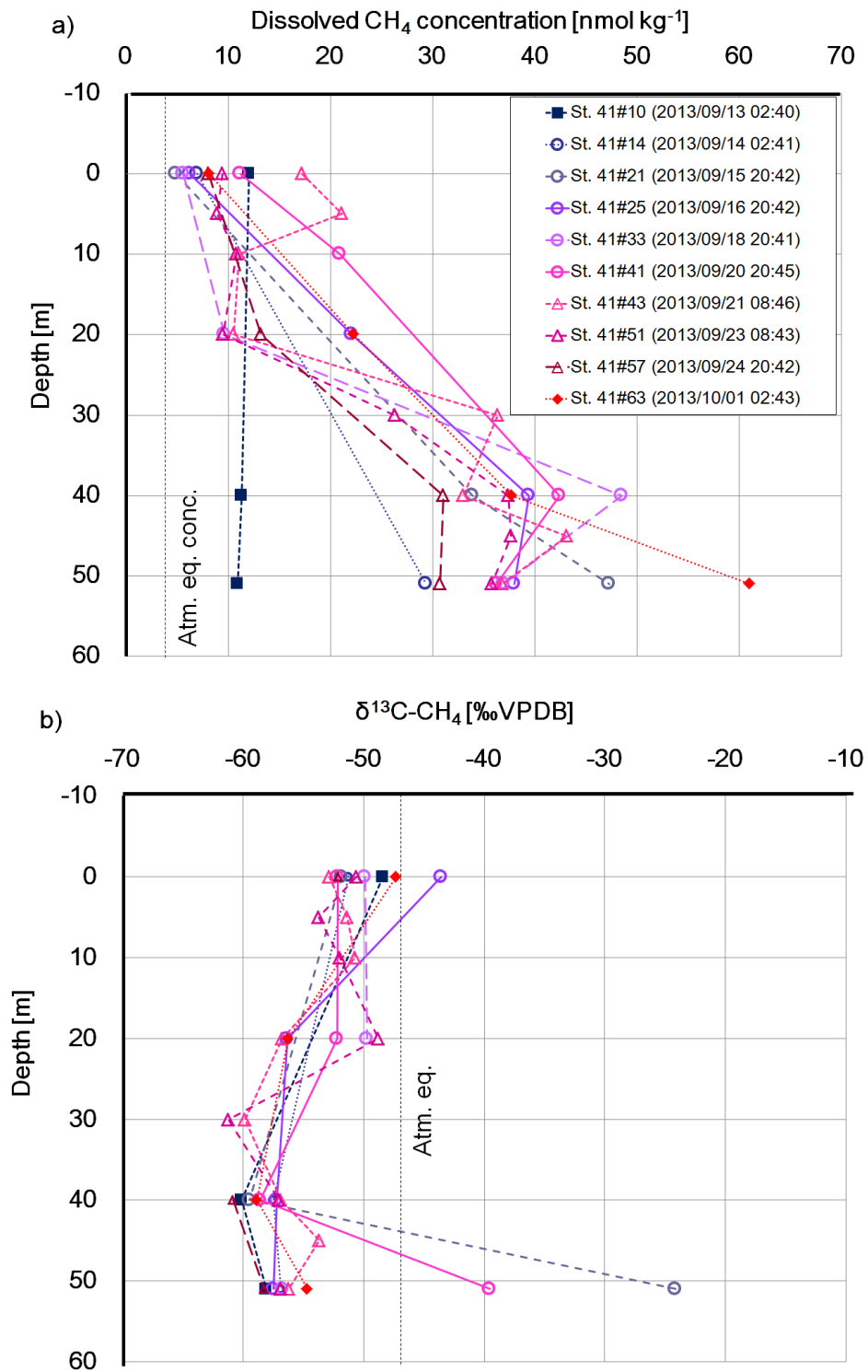


**Figure 3-8.** Vertical distribution of (a) CH<sub>4</sub> concentration and (b) δ<sup>13</sup>C value at 0, 20, 40, and 51 m depths in fixed-point observation (FPO).

## Tables

**Table 3-1.** Information of wind speed, air temperature, dissolved and atmospheric equilibrium CH<sub>4</sub> concentration, sea-air CH<sub>4</sub> flux, and values of  $\delta^{13}\text{C-CH}_4$  and  $\delta^{13}\text{C-CH}_{4\text{ex}}$  of dissolved CH<sub>4</sub> in surface water and atmospheric CH<sub>4</sub> on (a) MR12-E03 and (b) MR13-06 cruises. Data of wind speed, air temperature was based on database of JAMSTEC.

(a)

Station number	Sampling date	Latitude (°N)	Longitude (°E)	Seafloor depth (m)
7	2012/09/14 10:20	67.5024	191.2523	50
17	2012/09/15 11:01	69.0004	191.2477	53
27	2012/09/17 07:31	74.6727	189.0720	233
31	2012/09/18 03:31	75.5032	186.9634	1262
33	2012/09/19 04:21	75.2353	182.4839	721
38	2012/09/20 10:37	74.9998	194.0015	487
41	2012/09/22 09:13	75.0000	195.9984	690
43	2012/09/23 07:21	74.1725	197.6589	984
47	2012/09/24 07:53	72.8254	202.5969	1008
-	2012/09/24 22:12	71.3225	202.6777	
-	2012/09/25 04:46	71.3975	202.3812	
55	2012/09/25 06:17	71.4946	202.3605	87
-	2012/09/27 09:32	71.6444	205.437	
64	2012/9/29 3:33	74.4975	205.9901	3852
65	2012/09/29 09:21	73.998	204.7851	3855
66	2012/9/29 19:32	73.4908	203.5829	3684
68	2012/9/30 4:42	72.8647	202.0353	1573
69	2012/09/30 07:29	72.7466	201.8035	312
72	2012/9/30 18:01	72.0002	200.0011	30
73	2012/10/01 09:08	70.7501	199.0035	45
81	2012/10/02 05:59	70.7514	191.2609	38
83	2012/10/03 13:01	68.502	191.2488	54
89	2012/10/03 22:17	67.9992	191.2537	59
93	2012/10/04 04:29	67.5007	191.2487	51
96	2012/10/04 22:11	65.6525	191.7459	45

Station number	Wind speed ( $v$ ) (h = 24 m) ( $\text{m s}^{-1}$ )	Wind speed ( $v$ ) (h = 10 m) ( $\text{m s}^{-1}$ )	Air temperature ( $^{\circ}\text{C}$ )
7	8.1	7.5	1.3
17	2.8	2.6	1.9
27	11.1	10.3	-0.8
31	12.9	12.0	-2.4
33	8.7	8.0	-0.9
38	3.3	3.1	-1.0
41	5.2	4.8	-0.3
43	7.6	7.1	-1.1
47	2.5	2.3	1.9
-	13.0	12.1	1.3
-	13.3	12.3	1.7
55	13.0	12.1	1.3
-	4.3	4.0	-0.6
64	3.4	0.7	-2.7
65	6.0	5.6	-2.2
66	3.8	0.2	-1.2
68	2.6	0.2	-1.2
69	4.0	3.7	-1.1
72	3.9	0.7	-1.5
73	3.8	3.5	1.9
81	8.1	7.5	2.8
83	9.3	8.6	1.6
89	4.0	3.7	1.8
93	5.6	5.2	0.8
96	11.6	10.7	4.0



Station number	Dissolved CH <sub>4</sub> conc <sub>ave 0-10 m</sub> (nmol kg <sup>-1</sup> )	Atmospheric equilibrium CH <sub>4</sub> concentration (nmol kg <sup>-1</sup> )
7	4.9	3.7
17	4.6	3.3
27	4.0	3.8
31	5.2	3.8
33	5.2	3.8
38	4.9	3.8
41	4.6	3.8
43	4.3	3.8
47	4.1	3.4
-	6.3	3.3
-	10.3	3.4
55	5.4	3.4
-	6.8	3.4
64	4.7	3.9
65	4.9	3.7
66	4.9	3.7
68	4.8	3.5
69	3.8	3.5
72	6.1	3.7
73	6.4	3.4
81	3.8	3.3
83	4.3	3.4
89	4.1	3.6
93	4.4	3.6
96	5.1	3.5

Station number	Over-saturation ratio of CH <sub>4</sub> (SR) (%)	Sea-air CH <sub>4</sub> flux ( $\mu$ mol m <sup>-2</sup> day <sup>-1</sup> )
7	32.2	1.4
17	40.9	0.2
27	5.1	0.3
31	34.6	4.3
33	36.9	2.0
38	28.0	0.2
41	21.5	0.4
43	12.8	0.5
47	20.7	0.1
-	87.3	9.1
-	206.2	22.4
55	59.5	6.1
-	99.8	1.2
64	21.6	0.7
65	32.6	0.8
66	33.0	0.2
68	39.0	0.2
69	8.6	0.1
72	65.5	0.7
73	88.2	0.8
81	13.0	0.3
83	27.6	1.4
89	14.0	0.1
93	21.4	0.6
96	48.0	3.8

Station number	$\delta^{13}\text{C-CH}_4$ ave 0-10 m depth (‰)	$\delta^{13}\text{C-CH}_4$ air (‰)	$\delta^{13}\text{C-CH}_4$ ex (‰)
7			
17			
27			
31			
33			
38			
41			
43			
47			
-			
-			
55			
-			
64	-45.2	-47	-36.8
65	-48.1	-47	-51.5
66	-41.1	-47	-23.2
68	-44.5	-47	-38.2
69	-47.7	-47	-56.4
72	-55.0	-47	-67.2
73			
81			
83	-50.4	-47	-62.5
89	-49.4	-47	-66.7
93	-41.3	-47	-14.8
96	-48.2	-47	-50.6

(b)

Station number	Sampling date	Latitude°(N)	Longitude°(E)	Seafloor depth (m)
1	2013/8/31 19:51	65.7697	191.2483	52
12	2013/9/3 7:34	71.5808	202.1557	64
22	2013/9/4 13:56	71.5468	203.6457	159
23	2013/9/4 16:22	71.6270	204.2397	235
30	2013/9/7 22:34	74.5003	198.0157	1631
37	2013/9/10 9:36	72.5010	191.2505	58
38	2013/9/10 14:56	72.5012	192.2520	52
41#10	2013/9/13 2:40	72.7498	191.7548	51
41#14	2013/9/14 2:41	72.7508	191.7530	51
41#21	2013/9/15 20:42	72.7512	191.7458	51
41#25	2013/9/16 20:42	72.7515	191.7467	51
41#33	2013/9/18 20:41	72.7487	191.7497	51
41#41	2013/9/20 20:45	72.7488	191.7592	51
41#43	2013/9/21 8:46	72.7517	191.7605	51
41#51	2013/9/23 8:43	72.7497	191.7532	51
41#57	2013/9/24 20:42	72.7505	191.7507	51
48	2013/9/26 6:43	74.0025	191.2492	180
56	2013/9/27 12:25	73.8005	200.0103	2652
41#63	2013/10/1 2:43	72.7510	191.7528	51
62	2013/10/2 2:05	71.5003	191.2533	48
68	2013/10/2 22:56	68.3013	192.9542	38
77	2013/10/3 20:31	68.0008	191.2438	58
84	2013/10/4 18:23	65.7633	191.2427	51

Station number	Wind speed (v) (h = 24 m) (m s <sup>-1</sup> )	Wind speed (v) (h = 10 m) (m s <sup>-1</sup> )	Air temperature [degC]
1	8.2	7.6	6.9
12	13.9	12.9	0.9
22	10.4	9.7	2.9
23	9.9	9.1	2.9
30	11.2	10.3	-1.3
37	6.4	5.9	0.9
38	5.5	5.1	-0.1
41#10	1.2	1.1	2.4
41#14	7.2	6.7	0.1
41#21	6.7	6.2	-3.0
41#25	5.4	5.0	-1.0
41#33	7.6	7.0	-3.3
41#41	12.8	11.8	-2.2
41#43	9.7	8.9	-2.1
41#51	7.6	7.1	-2.0
41#57	6.1	5.6	-0.4
48	4.0	3.7	-3.4
56	7.3	6.8	0.0
41#63	6.0	5.6	-1.4
62	9.3	8.6	-0.8
68	1.0	0.9	-0.2
77	2.9	2.7	1.0
84	-	-	-

Station number	Dissolved CH <sub>4</sub> conc <sub>ave 0-5 m</sub> [nmol kg <sup>-1</sup> ]	Atmospheric equilibrium CH <sub>4</sub> concentration [nmol kg <sup>-1</sup> ]
1	7.4	3.0
12	9.6	3.4
22	5.7	3.6
23	7.2	3.6
30	12.8	3.9
37	10.5	3.4
38	9.6	3.3
41#10	12.0	3.3
41#14	6.9	3.3
41#21	4.9	3.4
41#25	6.3	3.4
41#33	5.6	3.4
41#41	11.2	3.4
41#43	19.2	3.4
41#51	9.2	3.5
41#57	8.1	3.5
48	11.4	3.9
56	5.9	3.8
41#63	8.1	3.6
62	10.7	3.4
68	11.0	3.2
77	15.9	3.4
84	37.4	3.4

Station number	Over-saturation ratio of CH <sub>4</sub> (%)	Sea-air CH <sub>4</sub> flux [ $\mu$ mol m <sup>-2</sup> day <sup>-1</sup> ]
1	145.3	4.7
12	182.2	22.3
22	61.6	4.6
23	100.3	6.7
30	233.4	22.5
37	212.4	5.5
38	187.8	3.6
41#10	261.7	0.2
41#14	107.6	3.6
41#21	44.1	1.4
41#25	84.8	1.6
41#33	64.2	2.6
41#41	224.1	25.9
41#43	456.7	30.3
41#51	163.8	6.8
41#57	130.8	3.3
48	191.0	2.6
56	57.0	2.2
41#63	125.4	3.3
62	217.2	12.6
68	238.2	0.2
77	367.8	1.9
84	984.1	-

Station number	$\delta^{13}\text{C-CH}_4$ ave 0-5 m [‰]	$\delta^{13}\text{C-CH}_4$ air [‰]	$\delta^{13}\text{C-CH}_4$ ex [‰]
1	-42.0	-47	-38.6
12	-47.2		-47.3
22			
23			
30	-44.3		-43.2
37	-44.2		-42.8
38	-		-
41#10	-48.4		-48.9
41#14	-51.3		-55.2
41#21	-51.8		-62.7
41#25	-43.6		-39.6
41#33	-49.9		-54.4
41#41	-52.1		-54.4
41#43	-52.9		-54.3
41#51	-50.6		-52.7
41#57	-52.1		-55.9
48	-		-
56	-43.5		-37.4
41#63	-47.3		-47.5
62	-40.4		-37.3
68	-43.9	-42.8	
77	-51.9	-53.2	
84	-42.9	-42.5	

(Wind speed ( $\text{m s}^{-1}$ ) and Air temperature ( $^{\circ}\text{C}$ ) were based on database of JAMSTEC.)

**Table 3-2.** Vertical profiles of concentration and values of  $\delta^{13}\text{C-CH}_4$  of dissolved  $\text{CH}_4$ , and DO concentration, seawater temperature, seawater salinity, potential density ( $\sigma_\theta$ ) and fluorescence concentration (only in 2013) in continental shelf area of (a) MR12-E03 and (b) MR13-06 cruises. Data of DO concentration, seawater temperature, seawater salinity, and potential density ( $\sigma_\theta$ ) were referred from the JAMSTEC database.

(a)

Station number	Depth (m)	Dissolved $\text{CH}_4$ conc. ( $\text{nmol kg}^{-1}$ )	Over-saturation ratio of $\text{CH}_4$ (SR) (%)	$\delta^{13}\text{C}$ (‰)
72	5	6.1	65.5	-55.0
	10	-	-	-
	15	-	-	-
	21	55.9	1386.8	-61.3
83	5	4.3	27.6	-50.4
	10	-	-	-
	20	-	-	-
	30	-	-	-
	40	-	-	-
	46	16.9	398.1	-63.8
89	5	4.1	14.0	-49.4
	10	-	-	-
	20	-	-	-
	30	-	-	-
	40	-	-	-
	52	24.8	593.4	-61.7
96	0	5.2	50.2	-
	5	5.1	48.0	-48.2
	10	-	-	-
	20	-	-	-
	30	-	-	-
	36	6.3	80.2	-47.4

Station number	Depth (m)	DO conc. ( $\mu\text{mol kg}^{-1}$ )	Seawater temperature ( $^\circ\text{C}$ )	Seawater salinity (PSU)	Potential density ( $\sigma_\theta$ ) ( $\text{kg L}^{-1}$ )	Transmission (%)
72	5	364.3	0.5	28.2	22.6	95.71
	10	373.5	0.6	28.5	22.8	95.72
	15	467.6	-1.0	31.8	25.6	98.44
	21	359.8	-1.2	32.6	26.2	69.34
83	5	333.9	3.3	28.8	23.0	86.81
	10	317.5	3.9	29.7	23.6	88.09
	20	261.8	1.9	32.2	25.7	78.17
	30	265.3	1.3	32.3	25.9	76.8
	40	221.6	0.6	32.6	26.2	56.63
	46	220.6	0.6	32.7	26.2	48.43
89	5	359.1	1.6	28.2	22.6	83.34
	10	350.5	1.7	28.6	23.0	86.12
	20	260.3	1.6	32.6	26.1	97.5
	30	200.9	1.3	32.8	26.3	82.62
	40	154.5	1.2	32.9	26.3	59.85
	52	104.9	0.8	33.0	26.4	12.77
96	0	-	-	-	-	-
	5	317.8	1.6	32.1	25.8	83.55
	10	315.0	1.5	32.2	25.8	83.76
	20	315.4	1.5	32.3	25.8	82.29
	30	319.6	1.6	32.5	26.0	74.34
	36	320.0	1.6	32.5	26.0	72.97



(b)

Station number	Depth (m)	Dissolved CH <sub>4</sub> conc. (nmol kg <sup>-1</sup> )	Over-saturation ratio of CH <sub>4</sub> (SR) (%)	δ <sup>13</sup> C (‰)
1	0	7.4	145.3	-42.0
	10	-	-	-
	20	15.3	337.7	-
	30	10.4	197.1	-
	45	10.0	183.7	-26.9
62	0	10.7	217.2	-40.4
	10	10.1	198.4	-21.7
	20	9.1	169.2	-47.0
	30	11.1	232.4	-54.2
	40	17.1	373.5	-62.8
	43	13.5	273.2	-62.4
68	0	12.7	290.4	-43.9
	5	9.3	187.2	-
	10	6.0	85.8	-53.5
	20	6.0	93.6	-55.7
	31	12.6	293.2	-84.2
77	0	15.9	367.8	-51.9
	10	10.5	209.0	-36.0
	20	16.3	377.8	-
	30	10.2	199.7	-36.3
	40	8.7	156.0	-54.4
	45	-	-	-
84	0	37.4	984.1	-42.9
	10	11.2	223.1	-13.3
	20	10.2	195.6	-
	30	18.8	195.6	-43.6
	40	11.9	245.1	-43.9
	45	10.4	202.3	-42.9

Station number	Depth (m)	DO conc. (μmol kg <sup>-1</sup> )	Seawater temperature (°C)	Seawater salinity (PSU)	Potential density (σ <sub>θ</sub> ) (kg L <sup>-1</sup> )	Transmission (%)	Fluorescence (μg L <sup>-1</sup> )
1	0	336.1	7.0	31.5	24.7	88.1	2.4
	10	330.2	6.7	31.5	24.7	86.4	3.1
	20	290.8	1.3	32.3	25.8	82.4	3.5
	30	288.2	1.3	32.3	25.8	83.2	2.6
	45	287.5	1.2	32.3	25.8	83.4	3.0
62	0	331.4	2.8	31.4	25.0	93.8	1.9
	10	331.6	2.8	31.4	25.0	93.7	1.8
	20	329.8	2.9	31.5	25.1	94.6	1.7
	30	327.3	3.0	31.6	25.2	94.4	1.9
	40	278.5	0.2	32.3	25.9	83.3	1.2
	43	278.3	0.2	32.3	25.9	82.4	1.3
68	0	315.6	4.5	30.2	23.9	90.2	1.6
	5	315.6	4.7	30.2	23.9	90.2	1.6
	10	315.3	4.7	30.2	23.9	90.9	1.7
	20	300.1	5.8	30.9	24.4	94.5	0.9
	31	277.9	4.6	31.6	25.0	90.1	0.3
77	0	324.2	2.2	32.5	26.0	77.9	4.2
	10	309.9	2.1	32.5	26.0	83.2	2.0
	20	296.7	2.1	32.6	26.0	68.4	1.0
	30	300.1	2.1	32.6	26.0	72.0	1.1
	40	299.9	2.2	32.6	26.0	72.3	0.9
	45	293.2	2.2	32.6	26.0	63.5	1.0
	50	284.5	2.2	32.6	26.0	50.4	1.0
84	0	299.7	1.7	32.6	26.1	83.0	2.1
	10	299.7	1.7	32.6	26.1	83.8	2.2
	20	302.7	1.7	32.6	26.1	82.1	1.8
	30	293.8	1.6	32.7	26.1	80.0	1.5
	40	296.5	1.6	32.7	26.1	79.3	1.6
	45	293.0	1.6	32.7	26.1	79.0	2.0

**Table 3-3.** Vertical profiles of concentration and values of  $\delta^{13}\text{C}$ - $\text{CH}_4$  of dissolved  $\text{CH}_4$ , and DO concentration, seawater temperature, seawater salinity potential density ( $\sigma_\theta$ ) and  $\text{N}^{**}$  values in deeper area (Canada Basin) of MR12-E03 cruise. Data of DO concentration, seawater temperature, seawater salinity, potential density ( $\sigma_\theta$ ) and  $\text{N}^{**}$  values were referred from the JAMSTEC database.

Station number	Depth (m)	Dissolved $\text{CH}_4$ conc. ( $\text{nmol kg}^{-1}$ )	Over-saturation ratio of $\text{CH}_4$ (SR) (%)	$\delta^{13}\text{C}$ (‰)
66	5	4.9	33.0	-41.1
	10	3.9	9.1	-48.6
	25	7.6	102.5	-50.5
	50	6.4	71.6	-48.5
	75	4.3	15.9	-36.1
	100	3.3	-12.3	-25.7
	300	3.0	-14.9	-27.5
	400	7.3	109.3	-26.2
	600	4.2	18.6	-28.3
	800	2.8	-21.4	-
	1000	3.0	-16.4	-37.2
	1500	3.4	-4.2	-41.4
	2000	4.2	15.8	-46.7
3000	3.8	4.7	-35.9	
68	5	4.8	39.0	-44.5
	10	5.0	45.8	-46.6
	18	14.5	329.4	-51.6
	20	11.3	230.7	-61.8
	30	11.5	227.0	-43.5
	50	13.5	266.3	-56.1
	75	11.6	206.9	-57.2
	100	21.8	477.2	-58.3
	125	9.7	158.5	-54.2
	150	5.4	46.1	-45.0
	175	3.4	-5.0	-34.3
	200	3.2	-10.4	-37.9
	225	4.1	17.1	-35.2
	250	3.4	-4.3	-33.4
	300	4.6	30.6	-43.7
	400	3.2	-7.1	-
	600	3.7	6.0	-
800	2.9	-19.4	-27.2	
1000	5.5	55.6	-38.0	
1583	3.7	2.1	-39.8	
69	5	3.8	8.6	-47.7
	20	17.7	415.1	-56.7
	50	10.4	177.3	-65.1
	100	15.5	310.0	-53.1
	303	2.1	-40.9	-30.9

Station number	Depth (m)	DO conc. ( $\mu\text{mol kg}^{-1}$ )	Seawater temperature ( $^{\circ}\text{C}$ )	Seawater salinity (PSU)	Potential density ( $\sigma_{\theta}$ ) ( $\text{kg L}^{-1}$ )	$\text{N}^{**}$ ( $\mu\text{mol kg}^{-1}$ )
66	5	353.5	1.6	25.7	20.6	-5.1
	10	353.7	2.2	26.2	20.7	-5.2
	25	402.1	0.1	28.0	22.4	-6.8
	50	394.8	-0.2	30.2	24.2	-8.3
	75	334.1	-0.8	31.6	25.3	-9.5
	100	298.4	-1.2	32.2	25.9	-10.3
	300	276.5	0.1	34.6	27.8	-0.2
	400	288.4	0.8	34.8	27.9	1.0
	600	296.0	0.6	34.9	28.0	1.0
	800	298.1	0.2	34.9	28.0	0.9
	1000	298.9	0.0	34.9	28.0	0.9
	1500	297.5	-0.3	34.9	28.1	0.8
2000	290.7	-0.4	34.9	28.1	0.6	
3000	285.9	-0.3	35.0	28.1	0.6	
68	5	338.5	2.7	28.6	22.8	-4.5
	10	336.4	2.8	28.7	22.8	-4.6
	18	345.8	3.3	29.7	23.6	-5.5
	20	373.2	2.7	30.4	24.2	-6.3
	30	361.1	1.2	31.9	25.5	-8.6
	50	334.8	-0.5	32.5	25.9	-10.1
	75	293.4	-1.4	32.9	26.1	-10.3
	100	276.4	-1.4	33.2	26.7	-11.4
	125	262.3	-1.3	33.6	27.0	-7.8
	150	269.1	-0.8	34.1	27.4	-2.3
	175	275.2	-0.4	34.4	27.6	-0.8
	200	274.4	-0.1	34.5	27.7	-0.6
	225	271.2	0.2	34.6	27.8	-0.6
	250	278.2	0.4	34.7	27.8	0.4
	300	283.7	0.7	34.8	27.9	0.8
	400	292.8	0.8	34.8	27.9	1.3
	600	294.9	0.4	34.9	28.0	1.2
800	297.0	0.2	34.9	28.0	1.1	
1000	297.6	0.0	34.9	28.0	1.0	
1583	296.5	-0.3	34.9	28.1	0.8	
69	5	340.9	2.2	28.4	22.7	-4.7
	20	389.4	2.3	31.0	24.8	-7.6
	50	340.8	-1.0	32.4	26.1	-10.6
	100	277.2	-1.5	33.3	26.8	-9.8
	303	279.8	0.6	34.8	27.9	-0.5

**Table 3-4.** Vertical profiles of concentration and values of  $\delta^{13}\text{C}$ - $\text{CH}_4$  of dissolved  $\text{CH}_4$ , and DO concentration, seawater temperature, seawater salinity, potential density ( $\sigma_\theta$ ) and transmission in fixed-point observation (FPO). Data of DO concentration, seawater temperature, seawater salinity, potential density ( $\sigma_\theta$ ) and transmission were referred from the JAMSTEC database.

Station number	Depth (m)	Dissolved $\text{CH}_4$ conc. ( $\text{nmol kg}^{-1}$ )	Over-saturation ratio of $\text{CH}_4$ (SR) (%)	$\delta^{13}\text{C}$ (‰)
41#10	0	12.0	261.7	-48.4
	10	-	-	-
	20	-	-	-
	30	-	-	-
	40	11.3	200.8	-60.1
	51	10.9	188.3	-58.1
41#14	0	6.9	107.6	-51.3
	10	-	-	-
	20	-	-	-
	30	-	-	-
	40	76.7	1884.8	-57.5
	51	29.3	675.2	-56.9
41#21	0	4.9	44.1	-51.8
	10	-	-	-
	20	-	-	-
	30	-	-	-
	40	33.9	799.9	-59.5
	51	47.3	1147.9	-24.2
41#25	0	6.3	84.8	-43.6
	20	22.1	553.3	-56.3
	30	-	-	-
	40	39.4	944.3	-57.2
	45	-	-	-
	51	38.0	902.8	-57.5
41#33	0	5.6	64.2	-49.9
	10	-	-	-
	20	9.6	183.5	-49.7
	30	-	-	-
	40	48.5	1181.2	-
	51	37.0	875.3	-56.7
41#41	0	11.2	224.1	-52.1
	10	20.9	510.0	-52.2
	20	-	-	-
	30	-	-	-
	40	42.4	1020.8	-58.5
	51	36.2	855.1	-39.5
41#43	0	17.2	400.3	-52.9
	5	21.1	513.1	-51.4
	10	11.0	219.7	-50.7
	20	10.6	190.9	-56.8
	30	36.4	867.5	-59.8
	40	33.0	774.9	-56.9
	51	43.1	1038.3	-53.7
		36.8	871.7	-56.2

Station number	Depth (m)	Dissolved CH <sub>4</sub> conc. (nmol kg <sup>-1</sup> )	Over-saturation ratio of CH <sub>4</sub> (SR) (%)	δ <sup>13</sup> C (‰)
41#51	0	9.4	171.4	-50.6
	5	8.9	156.2	-53.7
	10	10.8	211.2	-52.0
	20	9.5	172.9	-48.8
	30	26.3	607.1	-61.2
	40	37.4	892.4	-57.0
	45	37.6	899.2	-
	51	35.8	842.7	-56.8
41#57	0	8.1	130.8	-52.1
	10	-	-	-
	20	13.2	278.4	-
	30	-	-	-
	40	31.0	725.9	-60.8
	45	-	-	-
	51	30.7	715.3	-58.2
41#63	0	8.1	125.4	-47.3
	10	-	-	-
	20	22.3	519.5	-56.3
	30	-	-	-
	40	37.7	897.4	-58.8
	45	-	-	-
	51	61.0	1510.3	-54.7

Station number	Depth (m)	DO conc. ( $\mu\text{mol kg}^{-1}$ )	Seawater temperature ( $^{\circ}\text{C}$ )	Seawater salinity (PSU)	Potential density ( $\sigma_{\theta}$ ) ( $\text{kg L}^{-1}$ )	Transmission (%)
41#10	0	335.0	3.4	31.2	24.8	97.3
	10	334.3	3.3	31.1	24.8	97.1
	20	371.0	2.2	31.5	25.1	96.3
	30	378.7	-0.9	32.3	26.0	98.3
	40	372.0	-1.1	32.5	26.1	98.5
	51	297.7	-1.3	32.6	26.2	98.7
41#14	0	334.9	3.2	31.1	24.8	96.9
	10	335.1	3.2	31.2	24.8	96.8
	20	394.5	1.6	31.8	25.4	96.1
	30	430.9	-0.7	32.3	26.0	97.6
	40	293.2	-1.4	32.5	26.2	98.0
	45	315.3	-1.3	32.6	26.2	98.5
41#21	0	339.7	2.6	31.4	25.0	96.6
	10	339.6	2.6	31.4	25.0	96.6
	20	341.2	2.6	31.4	25.0	96.5
	30	385.7	-1.0	32.4	26.0	98.0
	40	322.9	-1.2	32.5	26.2	98.4
	45	324.7	-1.2	32.6	26.2	98.5
41#25	0	340.3	2.6	31.3	25.0	96.5
	20	341.6	2.7	31.4	25.1	96.4
	30	398.4	-0.9	32.4	26.0	98.0
	40	307.7	-1.3	32.6	26.2	98.4
	45	288.8	-1.3	32.6	26.2	98.4
	51	256.7	-1.4	32.8	26.4	78.0
41#33	0	336.7	2.5	31.4	25.0	96.0
	10	336.8	2.7	31.4	25.0	96.0
	20	338.7	2.6	31.5	25.1	96.0
	30	395.8	-0.9	32.3	26.0	95.8
	40	285.4	-1.3	32.5	26.2	97.4
	45	287.6	-1.3	32.6	26.2	98.0
41#41	0	347.3	2.0	31.7	25.3	95.5
	10	346.7	2.1	31.7	25.3	95.5
	20	347.3	2.1	31.7	25.3	95.4
	30	384.3	-0.9	32.4	26.0	97.1
	40	295.1	-1.3	32.5	26.2	96.7
	45	266.4	-1.4	32.7	26.3	93.2
41#43	0	346.3	2.0	31.6	25.3	95.3
	5	346.3	2.0	31.6	25.3	95.3
	10	345.7	2.0	31.6	25.3	95.3
	20	398.6	0.1	32.1	25.8	95.5
	30	356.5	-1.1	32.5	26.1	96.3
	40	317.6	-1.3	32.6	26.2	97.6
41#51	0	347.2	1.8	31.6	25.3	95.1
	5	347.2	1.8	31.6	25.3	95.1
	10	347.2	1.8	31.6	25.3	95.2
	20	347.9	1.8	31.6	25.3	94.8
	30	417.5	-0.8	32.4	26.0	97.0
	40	316.7	-1.2	32.5	26.1	97.4
41#57	0	348.8	1.6	31.6	25.3	95.1
	10	348.9	1.6	31.6	25.3	95.1
	20	348.9	1.6	31.6	25.3	95.1
	30	405.2	-0.8	32.3	25.9	97.4
	40	348.5	-1.1	32.5	26.1	97.4
	45	300.5	-1.3	32.5	26.2	97.7
41#63	0	353.3	0.7	31.1	24.9	93.9
	10	347.1	1.8	31.3	25.1	94.0
	20	385.6	0.5	31.7	25.4	94.6
	30	370.3	-1.1	32.4	26.0	96.5
	40	295.2	-1.3	32.5	26.2	96.8
	45	310.7	-1.2	32.6	26.2	91.7
51	242.0	-1.5	32.7	26.3	69.3	

Station number	Depth (m)	DO conc. ( $\mu\text{mol kg}^{-1}$ )	Seawater temperature ( $^{\circ}\text{C}$ )	Seawater salinity (PSU)	Potential density ( $\sigma_{\theta}$ ) ( $\text{kg L}^{-1}$ )	Transmission (%)
41#51	0	347.2	1.8	31.6	25.3	95.1
	5	347.2	1.8	31.6	25.3	95.1
	10	347.2	1.8	31.6	25.3	95.2
	20	347.9	1.8	31.6	25.3	94.8
	30	417.5	-0.8	32.4	26.0	97.0
	40	316.7	-1.2	32.5	26.1	97.4
	45	322.8	-1.2	32.6	26.2	97.5
41#57	0	348.8	1.6	31.6	25.3	95.1
	10	348.9	1.6	31.6	25.3	95.1
	20	348.9	1.6	31.6	25.3	95.1
	30	405.2	-0.8	32.3	25.9	97.4
	40	348.5	-1.1	32.5	26.1	97.4
	45	300.5	-1.3	32.5	26.2	97.7
41#63	0	353.3	0.7	31.1	24.9	93.9
	10	347.1	1.8	31.3	25.1	94.0
	20	385.6	0.5	31.7	25.4	94.6
	30	370.3	-1.1	32.4	26.0	96.5
	40	295.2	-1.3	32.5	26.2	96.8
	45	310.7	-1.2	32.6	26.2	91.7
51	242.0	-1.5	32.7	26.3	69.3	

## Chapter 4: Discussion

### 4.1 Dissolved CH<sub>4</sub> dynamics in surface water

#### 4.1.1 September–October 2012

The value of  $F_{\text{CH}_4}$  calculated from the observed CH<sub>4</sub> concentration suggests that the western Arctic Ocean behaves as a potential CH<sub>4</sub> source to the atmosphere during the sea-ice free period. In addition,  $\delta^{13}\text{C}_{\text{ex}}$  values of dissolved CH<sub>4</sub> in surface seawater indicate that biological processes produce excess CH<sub>4</sub>.

In the continental shelf area, dissolved oxygen (DO) concentrations (mean,  $339.5 \pm 5.1 \mu\text{mol kg}^{-1}$ ) were lower than in the deeper area (mean,  $360.0 \pm 5.1 \mu\text{mol kg}^{-1}$ ) (JAMSTEC database). Furthermore, higher nutrient concentrations (up to 30.7, 2.04, 4.50, 14.1, and  $0.240 \mu\text{mol kg}^{-1}$  respectively for silicate, phosphate, ammonia, nitrate, and nitrite) produced by decomposition of organic matter deposited at the sediments (Nishino et al. 2005), were also found in this area, which suggests that excess CH<sub>4</sub> in the surface water is produced mainly by methanogens in seafloor sediments.

In the deeper area near the Canada Basin, higher DO concentration and lower pCO<sub>2</sub> were observed. Higher chlorophyll-a (Chl. a) concentration ( $> 0.5 \text{ mg L}^{-1}$ ) was found near St. 68 and 69 (JAMSTEC database; Cruise report of MR12-E03 cruise). These tendencies indicate that photosynthesis by phytoplankton occurs well in this area, and that CH<sub>4</sub> might be produced mainly by phytoplankton. and zoo plankton activities in this area.

Therefore, dynamics of dissolved CH<sub>4</sub> differ between the coastal shelf area and

deeper area. We discuss details related to this issue in section 4. 2.

#### 4.1.2 August–October 2013

The value of SR of CH<sub>4</sub> in 2013 also becomes positive. This suggests that the western Arctic Ocean in 2013 also behaves as a potential CH<sub>4</sub> source to the atmosphere during the sea-ice free period.  $\delta^{13}\text{C}_{\text{ex}}$  values of dissolved CH<sub>4</sub> in surface water in 2013 also indicate that biological processes mainly produce excess CH<sub>4</sub>.

SR values in 2013 were higher than in 2012. Especially, higher SR values were often observed in coastal shelf area, which did not depend on sampling date and place in both years (Figures 4-1 and 4-2). On the other hand,  $\delta^{13}\text{C}$  values were not so different in both years and lower  $\delta^{13}\text{C}$  values than atmospheric equilibrium were often observed at higher CH<sub>4</sub> concentration. Thus, I supposed that CH<sub>4</sub> has been produced from same source with different amount between both years.

Figure 4-3 presents a total alkalinity–salinity (TA–S) diagram in surface seawater in 2012 and 2013 (JAMSTEC database). This diagram showed that TA and salinity in 2013 were higher than in 2012. This tendency suggested that seawater in 2012 was affected strongly by freshwater. During the period of August–October. sea-ice extent in 2013 was stronger than 2012, which supported weaker effect by freshwater in 2013. It also suggests that CH<sub>4</sub> was well mixed between bottom water and surface water because of a weak influence by sea-ice melt water and stratification.

Therefore, higher CH<sub>4</sub> concentration in 2013 might be caused by vertical mixing of bottom CH<sub>4</sub> with weaker stratification. We discuss details related to this issue in section 4.2.1.



## 4.2 Continental shelf area

### 4.2.1 Chukchi Sea

Concentrations of CH<sub>4</sub> were higher in bottom water (16.9–55.9 nmol kg<sup>-1</sup>) than in surface water (4.1–6.1 nmol kg<sup>-1</sup>), although concentrations of DO were lower in bottom water (104.9–359.8 nmol kg<sup>-1</sup>) than in surface water (333.9–364.3 nmol kg<sup>-1</sup>) in the Chukchi Sea (St. 72, 83, and 89). Similar profiles have been observed in other Arctic Ocean areas, indicating that sediments are a major CH<sub>4</sub> source to shelf waters (Macdonald et al. 1976; Damm et al. 2005; Shakhova et al. 2005, 2010, 2014; Savvichev et al. 2007). Savvichev et al. (2007) reported that CH<sub>4</sub> concentrations in bottom layer were two times higher than in the surface layer in the Chukchi Sea. They also estimated the rates of methanogenesis from seafloor sediments in the Chukchi Sea to be as high as 67 μmol m<sup>-2</sup>: dramatically higher than the rates of methane oxidation (approx. 3 μmol m<sup>-2</sup>).

The δ<sup>13</sup>C values in bottom water (–63.8 to –61.3‰) were lower than in surface water (–55.0 to –49.4‰). This result indicates that CH<sub>4</sub> is supplied from resuspension of seafloor sediments, in which particle organic matter (POM) is decomposed by methanogenic activity via CO<sub>2</sub> reduction pathways. In bottom water, the transmission decreased, indicating an accumulation of organic matter and its decomposition at the bottom (Nishino et al. 2016). These δ<sup>13</sup>C values in bottom water were within the range of reported values of the CO<sub>2</sub> reduction pathway (δ<sup>13</sup>C = –110 to –60‰: Whiticar et al. 1986, 1999; Sugimoto and Wada 1993; Kanster et al. 1998). Furthermore, the Chukchi Sea holds point Barrow (near St. 72) and the hollow called Hope Valley (near St. 83 and

89), where sediments are readily accumulated and where positive apparent oxygen utilization (AOU) and positive correlation between CH<sub>4</sub> and CO<sub>2</sub> (Database of JAMSTEC) are reported (Verzhbitsky et al. 2008; Yamada et al. 2015, Nishino et al. 2016).

A thermocline and pycnocline were found at 10–20 m depths at these stations. Myhre et al. (2016) reported that CH<sub>4</sub> release from seafloor sediments west of Svalbard substantially increased its concentrations in the ocean, but this release has limited influence on atmospheric CH<sub>4</sub> levels because of the pycnocline, except for the case in which physical processes (e.g., storms) remove this dynamic barrier (Myhre et al. 2016). When excess CH<sub>4</sub> in the seawater is transported, it is affected simultaneously by oxidation, dilution and mixing with atmosphere, in addition to loss into the atmosphere (Damm et al. 2005). In the Chukchi Sea, a markedly higher CH<sub>4</sub> production rate than CH<sub>4</sub> oxidation rate has been reported (Savvichev et al. 2007). Therefore, we examine the effects of mixing with atmospheric CH<sub>4</sub> at these stations using the relation between inverse of CH<sub>4</sub> concentration (1/[CH<sub>4</sub>]) and δ<sup>13</sup>C (Figure 4-4). At these stations, data from 5 m depth almost fall on the mixing line between the bottom layer and atmosphere. Therefore CH<sub>4</sub> was produced by methanogenic activity in seafloor sediments and was partially transported strongly to the surface, affected mainly by mixing between atmospheric CH<sub>4</sub>. Fenwick et al. (2017) observed dissolved CH<sub>4</sub> in the Bering Sea and Chukchi Sea in July–October 2015. They concluded that this CH<sub>4</sub> was produced from methanogens in seafloor sediments from the decomposition of organic carbon. Then microbial CH<sub>4</sub> oxidation occurred, as inferred from information related to the concentration (0.7–30.5 nmol L<sup>-1</sup>) and δ<sup>13</sup>C (from –42 to –33‰) of CH<sub>4</sub> (Figure 4-5). The vertical gradients of CH<sub>4</sub> concentrations and the CH<sub>4</sub> concentrations in bottom

water (approx. 10–31 nmol L<sup>-1</sup>) reported by Fenwick et al. (2017) were respectively weaker and lower than our data. Furthermore, they observed higher  $\delta^{13}\text{C}$  values than those found in the present study. These differences might derive from CH<sub>4</sub> release from seafloor sediments and the strength of stratification by sea-ice melt water. Lapham et al. (2017) reported using data from August 2012 that most of the water column CH<sub>4</sub> profiles in Barrow Canyon exhibited an increase with depth (5–74 nmol L<sup>-1</sup>), suggesting that mainly sedimentary sources produced CH<sub>4</sub>. The  $\delta^{13}\text{C}$  profiles obtained in the same area during this study agree with such sedimentary CH<sub>4</sub> production.

In 2013, gradient of concentrations and  $\delta^{13}\text{C}$  values of dissolved CH<sub>4</sub> with depth were not found in Chukchi Sea (St. 62, 68 and 77). Figures 3-1e and 3-2e show vertical distribution of potential density ( $\sigma_\theta$ ) in continental shelf area in 2012 and 2013, respectively. These figures support that strength of stratification by sea-ice melt water was weaker in 2013, indicating stronger vertical mixing between bottom layer and surface layer. This weak stratification in the Chukchi Sea enhanced vertical mixing to supply nutrients to the surface water, as observed in the nitrate and ammonium profiles in 2012 and 2013 (Nishino et al. 2016). Nishino et al. (2016) found that strongly nutrients supply in 2013 caused higher algal biomass and primary productivity. Their estimations of primary productivity were 0.3 and 1.6 C m<sup>-2</sup> d<sup>-1</sup> in 2012 and 2013, respectively.

Thus, I supposed that difference of primary productivity between both years affected CH<sub>4</sub> dynamics. Therefore, I examine the effects of mixing between atmospheric CH<sub>4</sub> and three end-members ((1) sinking particles from zooplankton (Zs) ( $\delta^{13}\text{C}$  = from –37 to +6‰: Sasakawa et al. 2008) and (2) zooplankton guts (Zg) ( $\delta^{13}\text{C}$  = from –61 to –54‰: Sasakawa et al. 2008). Methane from these endmembers was produced

originally by (3) methanogens via the CO<sub>2</sub> reduction pathway (C<sub>M</sub>) ( $\delta^{13}\text{C}$  = from -110 to -60‰: Whiticar et al. 1986; Whiticar 1999; Sugimoto and Wada 1993). The CH<sub>4</sub> is partly consumed by microbial CH<sub>4</sub> oxidation with <sup>13</sup>C enrichment of remaining CH<sub>4</sub> within these anaerobic microenvironments (Oremland 1979; Karl and Titbrook 1994; Holmes et al. 2000; Sasakawa et al. 2008.) using the relation between inverse of CH<sub>4</sub> concentration (1/[CH<sub>4</sub>]) and  $\delta^{13}\text{C}$  value at the Chukchi Sea (Figure 4-2). In 2012, CH<sub>4</sub> was produced mainly by organic matter in seafloor sediments and mixed with atmosphere in surface layer. In 2013, CH<sub>4</sub> was produced mainly by organic matter in seafloor sediments and transported between bottom layer and surface layer with influence by zooplankton activity. Therefore, difference of CH<sub>4</sub> dynamics between both years might be caused by strength of not only stratification but also primary production (Figure 4-6). Vertical difference of CH<sub>4</sub> were not regarded as measurement error due to difference of concentrations and  $\delta^{13}\text{C}$  values were larger, respectively, than 5% and 0.3‰.

#### 4.2.2 Bering Strait

In the Bering Strait in October in 2012 (St. 96), the concentration and  $\delta^{13}\text{C}$  values of CH<sub>4</sub> in seawater become almost homogeneous from the surface water to bottom water, showing values close to those expected under equilibrium with the atmosphere. Furthermore, DO concentration and potential density also become homogeneous from the surface water to bottom water (Fig. 3-3d-3-3e; Database of JAMSTEC). These tendencies suggest that CH<sub>4</sub> is well mixed between bottom water and surface water because of surface water cooling in mid-October, in addition to a small influence by

sea-ice melt water. Only a single profile was obtained in this region. Nevertheless, these facts might suggest weaker CH<sub>4</sub> emissions in the Bering Strait than in the Chukchi Sea.

In Bering Strait in 2013 (St. 1 and 84), profile of concentration and  $\delta^{13}\text{C}$  of CH<sub>4</sub> become variable. DO concentration, seawater salinity, potential density and transmission become homogeneous from the surface water to bottom water in St. 84 (Fig. 3-4d–3-4g; Database of JAMSTEC). The highest CH<sub>4</sub> concentration (37.4 nmol kg<sup>-1</sup>) and  $\delta^{13}\text{C}$  value (–13.3‰) is observed in 0 and 10 m depth in St. 84. In surface layer in St. 84, profile of fluorescence concentration becomes higher than in 20–30 m depth (Fig. 3-4h), which indicates that phytoplankton is enriched in surface layer. This enriched phytoplankton may be consumed by zooplankton. Figure 4-7 shows that  $\delta^{13}\text{C}$  of y-segment of mixing line between atmospheric equilibrium and 0 m depth is –42.5‰ and mixing line between atmospheric equilibrium and 10 m depth is +1.8‰. This suggests that CH<sub>4</sub> may be produced from zooplankton guts in 0 m, which may be partly consumed by microbial CH<sub>4</sub> oxidation described as in 4.1.1, and then sinking particles may emitted <sup>13</sup>C enriched CH<sub>4</sub> in 10 m. These tendencies suggest that CH<sub>4</sub> is well mixed between bottom layer and surface layer same as in 2012 and may be well influenced by plankton activity in surface layer (Figure 4-8).

### **4.3 Deeper area (from off point Barrow to the Canada Basin in 2012)**

Two CH<sub>4</sub> concentration maxima were observed at 10–50 m depth and 100–200 m depth, whereas the DO concentration maximum was observed only at around 10–50 m depth. Nutrient concentration maxima were observed only at around 100–200 m depth. In the following sections, we discuss about CH<sub>4</sub> production processes in the shallower

(10–50 m) and deeper (100–200 m) CH<sub>4</sub> maxima.

#### 4.3.1 Shallower CH<sub>4</sub> maximum

At 10–50 m depth, the CH<sub>4</sub> concentration increased,  $\delta^{13}\text{C}$  decreased concomitantly with depth. Positive correlation was found between CH<sub>4</sub> and phosphate concentrations (Figs. 3-5h). Apparent correlation between dissolved CH<sub>4</sub> and phosphate concentrations has been also observed in Pacific-derived water (Pdw) in the central Arctic Ocean (Slope:  $y = 0.1161x - 0.1473$ ,  $R^2 = 0.8823$ ) (Damm et al. 2010). Damm et al. (2010) also found negative correlation between dissolved CH<sub>4</sub> and DMSP, a metabolite of phytoplankton in the Pdw. They proposed that CH<sub>4</sub> was produced by bacteria from DMSP in nitrate-depleted and phosphate-rich aerobic water. During our observations in the western Arctic Ocean, nitrate deficits and phosphate concentration were greater ( $N^*$  values and phosphate concentrations were, respectively,  $-11.9$  to  $-4.5 \mu\text{mol kg}^{-1}$  and  $0.5$  to  $1.6 \mu\text{mol kg}^{-1}$ ) than in the Pdw reported by Damm et al. (2010) ( $N^* = -1.5$  to  $+1 \mu\text{mol kg}^{-1}$  and  $[\text{PO}_4^{3-}] = 0.4$ – $0.9 \mu\text{mol kg}^{-1}$ , respectively). Therefore, it is likely that at least a part of the excess CH<sub>4</sub> was produced from DMSP, although we have no data for DMSP. However, accumulation of particle organic carbon (POC) and Chl. *a* was observed near St. 68 immediately above the pycnocline (0–60 m depth; Yamada et al. 2015). This fact suggests that CH<sub>4</sub> is also produced by methanogenic activity in zooplankton guts or sinking particles from zooplankton. Figure 4-9 shows mixing between atmospheric equilibrium and three end-members: (1) sinking particles from zooplankton (Zs) ( $\delta^{13}\text{C} =$  from  $-37$  to  $+6\%$ ; Sasakawa et al. 2008) and (2) zooplankton guts (Zg) ( $\delta^{13}\text{C} =$  from  $-61$  to  $-54\%$ ; Sasakawa et al. 2008). Methane from these endmembers was produced

originally by (3) methanogens via the CO<sub>2</sub> reduction pathway (C<sub>M</sub>) ( $\delta^{13}\text{C}$  = from -110 to -60‰: Whiticar et al. 1986; Whiticar 1999; Sugimoto and Wada 1993). The CH<sub>4</sub> is partly consumed by microbial CH<sub>4</sub> oxidation with <sup>13</sup>C enrichment of remaining CH<sub>4</sub> within these anaerobic microenvironments (Oremland 1979; Karl and Titbrook 1994; Holmes et al. 2000; Sasakawa et al. 2008). Figure 4-9 suggests that CH<sub>4</sub> is produced by methanogenic activity within zooplankton guts or sinking particles in addition to DMSP at 10–50 m depth in summer Canada Basin. Rau et al. (1982) reported  $\delta^{13}\text{C}$  values of organic carbon of ocean plankton ranged from -30 to -17‰. Suppose <sup>13</sup>C was not fractionated, CH<sub>4</sub> production from DMSP might be suitable. The largest  $\delta^{13}\text{C}$  values (-43‰) are still lower than those of sinking particles, which indicates that CH<sub>4</sub> was produced mainly from zooplankton guts and methanogens, and that it was not well oxidized within sinking particles. Furthermore, if one assumes a decrease in CH<sub>4</sub> concentrations from CH<sub>4</sub> maxima (10–50 m depth) to 0–10 m depth results from CH<sub>4</sub> oxidation, then the  $\alpha$  values are calculated as  $\alpha = 1.021$ ,  $1.006$ , and  $1.006$ , respectively at St. 66, 68, and 69 (Figure 4-10). Those calculated values agree with values of biological aerobic–anaerobic CH<sub>4</sub> oxidation reported from earlier studies (1.005–1.035; Coleman et al. 1981, Alperin et al. 1988, Martens et al. 1999, Tsunogai et al. 2000, Sansone et al. 2001). This fact indicates that CH<sub>4</sub> produced by zooplankton-/phytoplankton activity might be transported vertically from 10–50 m depth to 0–10 m depth: then it is oxidized by biological oxidation.

#### 4.3.2 Deeper CH<sub>4</sub> maximum

At 100–200 m depth, the concentration and  $\delta^{13}\text{C}$  values of dissolved CH<sub>4</sub> in

seawater became lower and higher as dissolved CH<sub>4</sub> gas left the bottom of the continental shelf area off point Barrow (St. 72), except at around St. 68 (Figs. 3-5a–3-5c, Table 4-1). This dissolved CH<sub>4</sub> might be transported laterally along the extended shelf water and Alaskan Continental Current (Hioki et al. 2014; Gong and Pickart 2015; Zhang et al. 2015). Hioki et al. (2014) measured dissolved Fe, humic-like fluorescent, dissolved organic matter, and nutrient concentrations in waters above the continental shelf area (Chukchi Sea) and deeper area (Canada Basin) during the same cruise as this study (Figure 4-11). They inferred lateral transportation of these constituents from shelf sediments to basin regions (Hioki et al. 2014). Results of several earlier studies suggest that particles in the shelf region are transferred to the slope–basin region by water currents from the Bering Strait to the Canada Basin (Aagaard et al. 2006; Hopcroft et al. 2008; Yamada et al. 2015). Here, I suggest that dissolved CH<sub>4</sub> was also transported horizontally from the continental shelf to the Canada Basin (in 100–200 m depth).

Furthermore,  $\alpha$  values ( $\alpha = 1.006$  and  $1.018$ , respectively, at St. 72–69 and St. 68–66 (Table 4-1)), indicate that CH<sub>4</sub> was affected not only by dilution but also by CH<sub>4</sub> consumption from biological oxidation ( $\text{CH}_4 + 2\text{O}_2 \rightarrow \text{CO}_2 + 2\text{H}_2\text{O}$ ). In St. 72–69 CH<sub>4</sub> may 56.2% diluted and then consumed by biological oxidation with  $\alpha = 1.018$ .

I estimated life time of CH<sub>4</sub> ( $\tau$ ) and transportation time of CH<sub>4</sub> ( $t$ ) in St. 72–69 and St. 68–66 for verifying CH<sub>4</sub> consumption during transportation, using the rate equation as shown below (e.g. Jacob 1999; Valentine et al. 2001).

$$[\text{CH}_4] = [\text{CH}_4]_0 \exp(-kt) \quad (9)$$

$$\tau = 1/k \quad (10)$$



where  $k$  represents reaction rate constant of  $\text{CH}_4$  consumption from biological oxidation.

I assumed that  $\tau$  in these areas were 1.5 [years] ( $k = 2.1 \times 10^{-8} [\text{s}^{-1}]$ ), which were shorter than in atmospheric  $\text{CH}_4$  (approx. 10 [years],  $k = 6.0 \times 10^{-15} [\text{s}^{-1}]$ ) (e.g.: Jacob 1999; IPCC 2013)), according to Valrntine et al. (2001). Based on this value and eq. (9),  $t$  in St. 72–69 and St. 68–66 were 2.5 [years] and 3.4 [years]. However, these  $t$  values were longer than  $\tau$  value, which indicated that these  $t$  values were unfitted for horizontal transportation of  $\text{CH}_4$ . In these areas,  $\text{CH}_4$  might be also effect by lower  $\text{CH}_4$  concentration water mass with horizontal transportation. Therefore, these facts supported that  $\text{CH}_4$  was consumed during horizontal transportation.

If biogenic  $\text{CH}_4$  production occurred, then the isotopic enrichment around the  $\text{CH}_4$  concentration maximum zone indicated that the  $\text{CH}_4$  was produced elsewhere and that it subsequently underwent partial bacterial oxidation and isotopic fractionation (Coleman et al. 1981; Sansone et al. 2001). Sansone et al. (2001) suggested that the isotopically heavy  $\text{CH}_4$  was not from local production by methanogens, but was instead attributable to biological oxidation with  $\text{CH}_4$  advection from  $\text{CH}_4$  maxima occurring along the eastern margin of the Pacific. Furthermore, Yoshikawa et al. (2014) showed that the  $^{13}\text{C}$ -enriched  $\text{CH}_4$  ( $> -30\text{‰}$ ) originated not only from in-situ  $\text{CH}_4$  production and oxidation but also from the  $\text{CH}_4$  transported from the eastern upwelling region off Peru. However, when data from St. 68 and 69 obtained at the 100–200 m depth area were compared, the  $\text{CH}_4$  concentration was found be higher at St. 68 than at St. 69. A lower  $\delta^{13}\text{C}$  value was found at St. 68 than at St. 69 (Table 4-1), which indicates that in-situ  $\text{CH}_4$  production might occur by methanogen in particles. Therefore, after  $\text{CH}_4$  was

produced mainly by methanogens in continental shelf sediments, it was transported horizontally to the Canada Basin (100–200 m depth) with effects not only by biological oxidation but also by methanogens in particles (Figure 4-12).

#### **4.4. Temporal change in Fixed-point observation in 2013**

The distribution of concentrations and  $\delta^{13}\text{C}$  values of dissolved  $\text{CH}_4$  suggested that the seawater behaved as a  $\text{CH}_4$  source to the atmosphere and  $\text{CH}_4$  was produced mainly by organic matter degradation in sediment especially in bottom layer during FPO in 2013. The vertical distribution of potential density ( $\sigma_\theta$ ) shows that there was a pycnocline at around 20 m depth during the entire period of observation, which divided seawater into a warmer/fresher surface layer and a colder/saltier bottom layer (Figure 4-13). Thus,  $\text{CH}_4$  source might be different between surface layer and bottom layer. However, surface water showed two types of mixing processes: near-surface turbulence due to strong wind forcing and subsurface mixing due to internal gravity waves (Kawaguchi et al. 2015).

Kawaguchi et al. (2015) performed repeated microstructure measurements to reveal the temporal evolution of the surface mixed layer and mixing processes in the upper water column. During second week (between 19 to 26 September), mixed layer showed a remarkable thickening by nearly 10 m, reaching approx. 28 m thick for almost week. Regarding the mixing layer deepening during this term, a vertical mean flow associated with the strong wind forcing ( $v > 13 \text{ m s}^{-1}$ ) could weaken the stratification within the mixing layer (Figure 4-14). This fact suggested that the wind-supplied turbulent energy reached down to the mixing layer bottom and then eroded the

stratification there, resulting in the deepening of the pycnocline.

CH<sub>4</sub> in surface layer maximized (17.2 nmol kg<sup>-1</sup>) in 21 September when mixing layer was deepened by strong wind forcing. δ<sup>13</sup>C value in this time was -52.9‰. Figure 4-15 presented the relationship between 1/[CH<sub>4</sub>] and δ<sup>13</sup>C value, showing mixing between atmospheric CH<sub>4</sub> and three end-members (described in section 4.2.1.). This suggested that CH<sub>4</sub> might be produced by (1) zooplankton guts and/or (2) methanogen in mixed layer bottom and then influenced by zooplankton activity with transportation to surface layer (Figure 4-16a). On the other hands, CH<sub>4</sub> concentration maximum in bottom layer (61.0 nmol kg<sup>-1</sup>) was observed at 1 October, whereas δ<sup>13</sup>C value was -54.7‰, which was still higher than of methanogenic activity via CO<sub>2</sub> reduction pathways (δ<sup>13</sup>C value should be -110 to -60‰) and lower than particles (δ<sup>13</sup>C value should be -37 to +6‰). In this layer, DO concentration and the transmission were lower ([DO]: 242.0 μmol kg<sup>-1</sup>, transmission: 69.3%) than at other depths ([DO]: 295.2–385.6 μmol kg<sup>-1</sup>, transmission: 91.7–96.8%). These facts indicate that CH<sub>4</sub> may be produced mainly by (1) mixing between methanogen in sediments and particle from organic matter in sediments, which may not be well oxidized within particles described as 4.3.1 and/or (2) mixing between methanogen and thermogenic CH<sub>4</sub> (δ<sup>13</sup>C = -50 to -20‰: Whiticar 1999) from gas hydrate in deep sediments (Figure 4-16b).

In 40 m depth, dramatically higher CH<sub>4</sub> concentration (76.7 nmol kg<sup>-1</sup>, which SR was 1884.8%) was observed in September 14<sup>th</sup>. δ<sup>13</sup>C value in this time was -57.5‰. CH<sub>4</sub> might be produced by methanogen and/or zooplankton guts. However DO concentration in this time was 293.2 μmol kg<sup>-1</sup>, which was lower than in surface layer and indicated that CH<sub>4</sub> production from zooplankton guts was not corrected. This higher CH<sub>4</sub> concentration might be produced originality from gas hydrate in deeper sediment

through CH<sub>4</sub> seep with bubble. In gas hydrate, CH<sub>4</sub> is, respectively, produced by thermogenic degradation and microbial CH<sub>4</sub> (such as methanogen) in deeper and shallower sediment (Figure 4-17: Ruppel and Kessler 2017), and emitted to water column (e.g.; Kvenvolden et al. 1993b; Shakhova et al. 2010; Zhou et al. 2014). Because of low solubility of CH<sub>4</sub> to water, produced CH<sub>4</sub> is immediately becomes bubble (e.g. Rehder et al. 2002), and coalescence of CH<sub>4</sub> bubbles occurs in turbulent system (Prince and Blanch 1990). CH<sub>4</sub> bubbles emitted from deeper than the shallowest extent of gas hydrate stability in the water column develop an armor of gas hydrate (e.g. Rehder et al. 2002; Ruppel and Kessler 2017). Therefore, this higher CH<sub>4</sub> concentration might be produced from mixing between methanogen and thermogenic degradation, which was emitted from CH<sub>4</sub> hydrate in sediment and might develop an armor of gas hydrate, and this did not effect to surface layer and oversea atmosphere.

In bottom layer, dramatically higher  $\delta^{13}\text{C}$  values (e. g.;  $-24.1\%$ , at 15 September) than atmospheric equilibrium were observed in sometimes. These higher  $\delta^{13}\text{C}$  values were accompanied by higher CH<sub>4</sub> concentration ( $> 35 \text{ nmol kg}^{-1}$ ) than other depths. Furthermore, DO concentration and the transmission were lower ([DO]: approx.  $250 \mu\text{mol kg}^{-1}$ , transmission: 58–75%) than other depths. These facts indicated that these higher  $\delta^{13}\text{C}$  values may be caused by (1) particles, which was well oxidized within this and/or (2) strongly effect by thermogenic degradation in deeper sediments.

## Figures and tables

### Figures

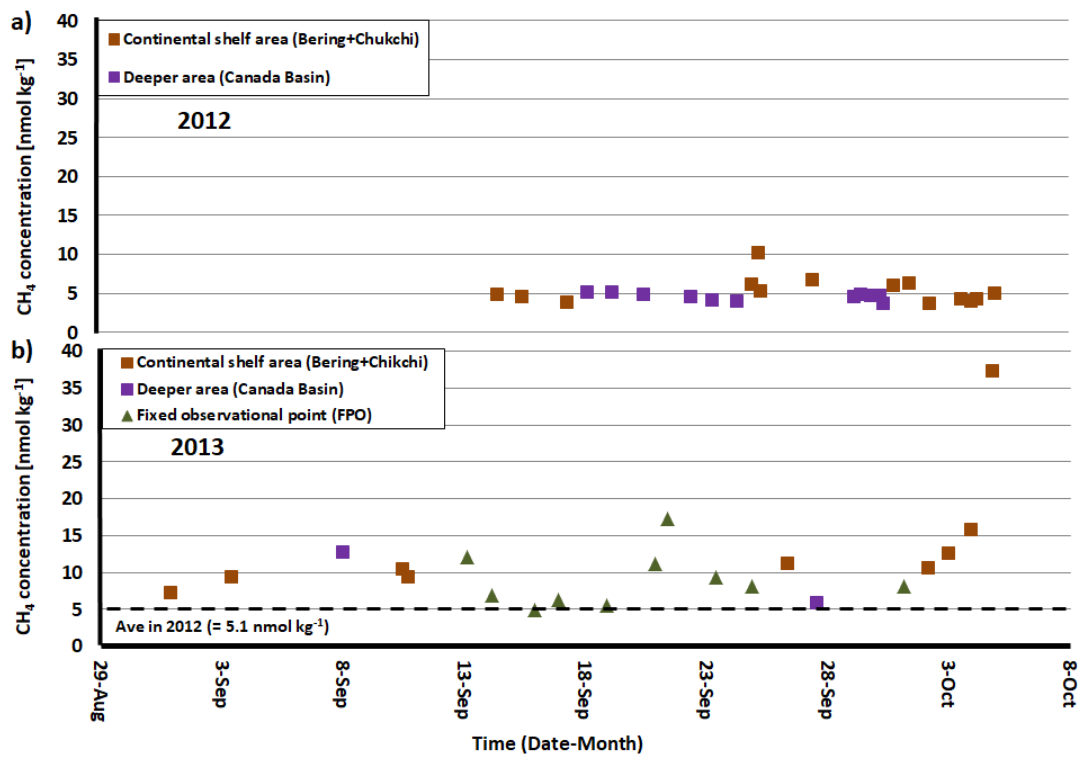


**Figure 4-1.** Temporal distribution of dissolved CH<sub>4</sub> concentration in surface water in (a) 2012 and (b) 2013.

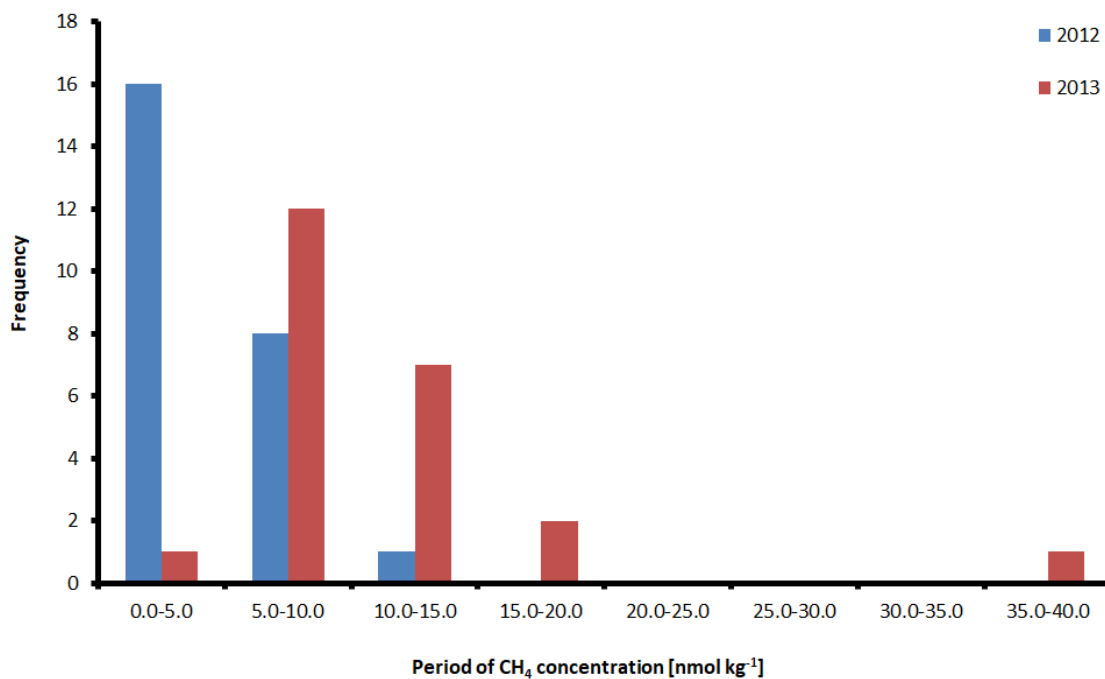


**Figure 4-2.** Histogram of dissolved CH<sub>4</sub> concentration in surface water in (a) 2012 and (b) 2013.

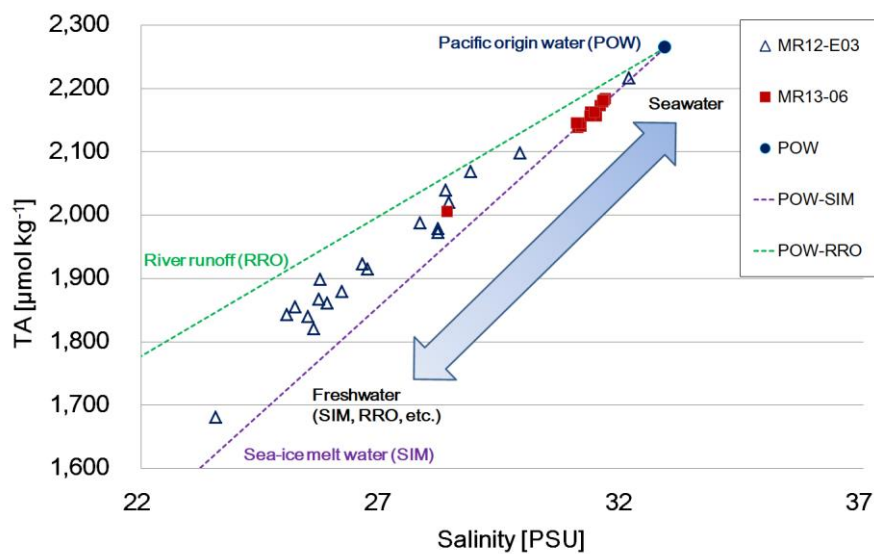


**Figure 4-3.** TA-S diagram in the surface seawater on MR12-E03 cruise (Based on database of JAMSTEC)

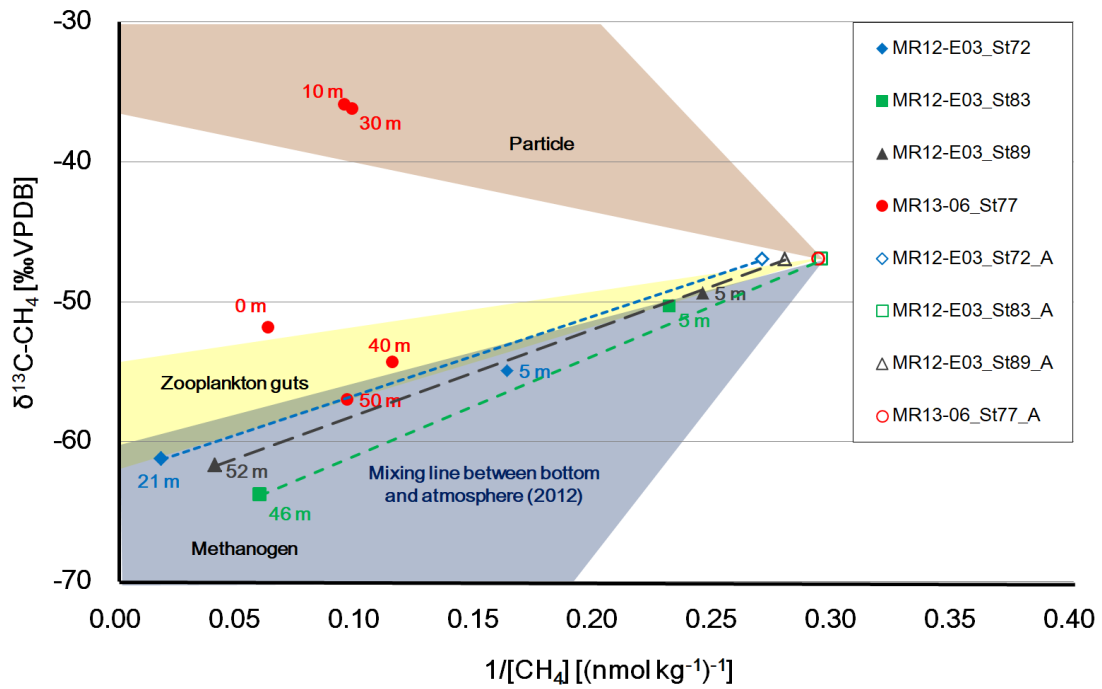


**Figure 4-4.** Relationship between inverse of dissolved  $\text{CH}_4$  concentration ( $1/[\text{CH}_4]$ ) and three end-members (Zs: sinking particle from zooplankton body ( $\delta^{13}\text{C}$  = from -37 to +6‰VPDB: Sasakawa et al., 2008); Zg: zooplankton guts ( $\delta^{13}\text{C}$  = from -61 to -54‰VPDB: Sasakawa et al., 2008); M: methanogen ( $\text{CO}_2$  reduction pathway) ( $\delta^{13}\text{C}$  = from -110 to -60‰VPDB: Whiticar et al., 1986, 1999; Sugimoto and Wada 1993)) in Chukchi Sea in 2012 (at stations 72, 83, and 89) and 2013 (at station 77). Data from dissolved  $\text{CH}_4$  are drawn as closed symbols and calculated values for the surface water equilibrated with the atmosphere (A) are drawn as open symbols. Straight lines show mixing lines between the bottom layer  $\text{CH}_4$  and atmospheric equilibrium in 2012.

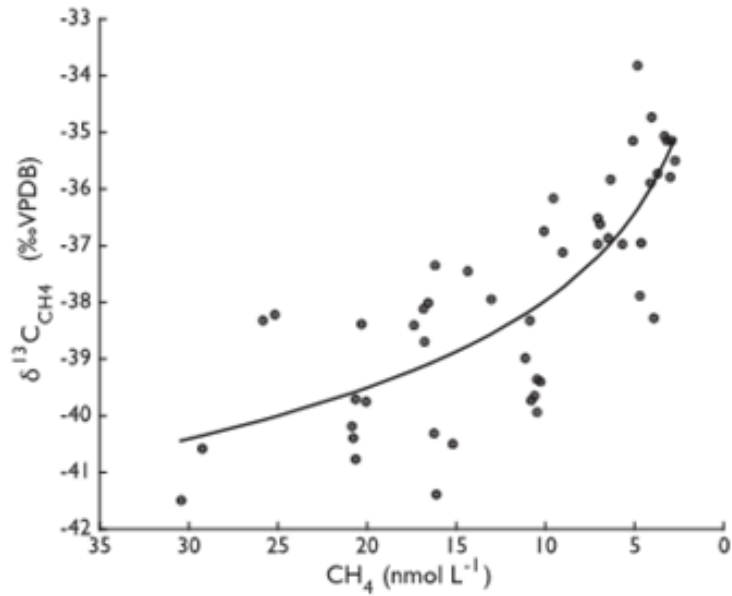


**Figure 4-5.** CH<sub>4</sub> oxidation curve calculated using a Rayleigh distillation model with an initial concentration of 31 nmol L<sup>-1</sup>, a δ<sup>13</sup>C<sub>CH<sub>4</sub></sub> value of -40‰VPDB, and an isotopic fractionation factor (α) of 1.002. Data is from the Bering and Chukchi Seas (Fenwick et al. 2017).

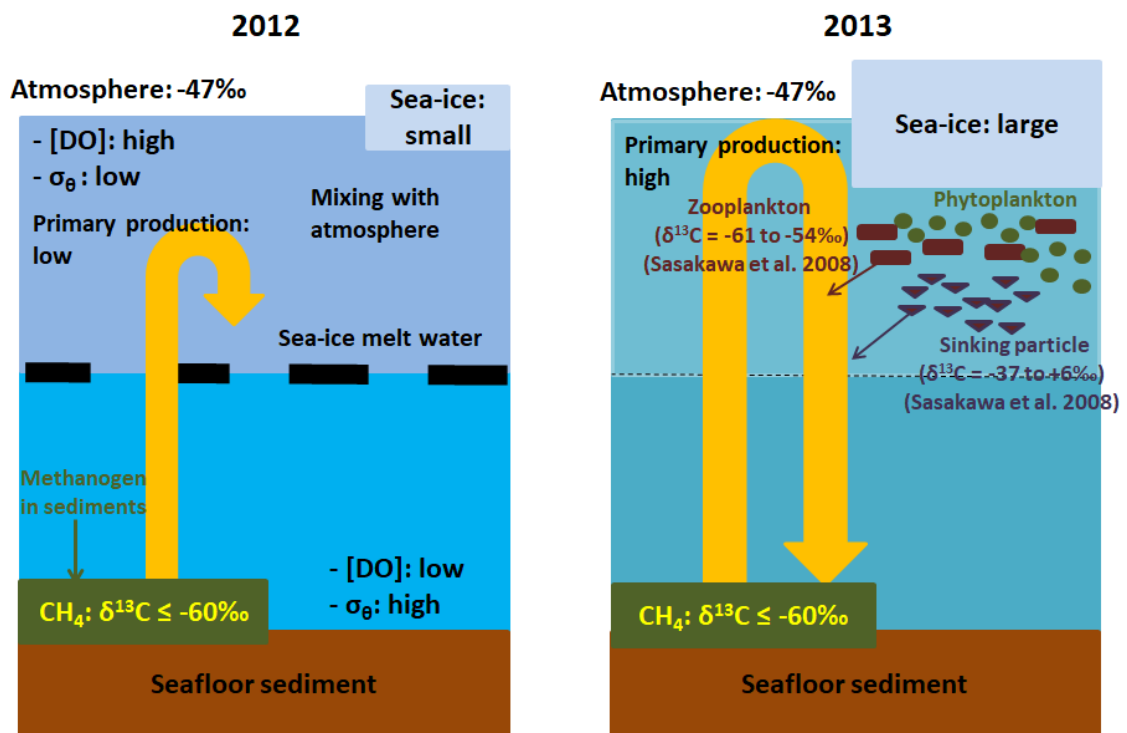


**Figure 4-6.** Schematics of dissolved CH<sub>4</sub> dynamics in the Chukchi Sea in 2012 and 2013.



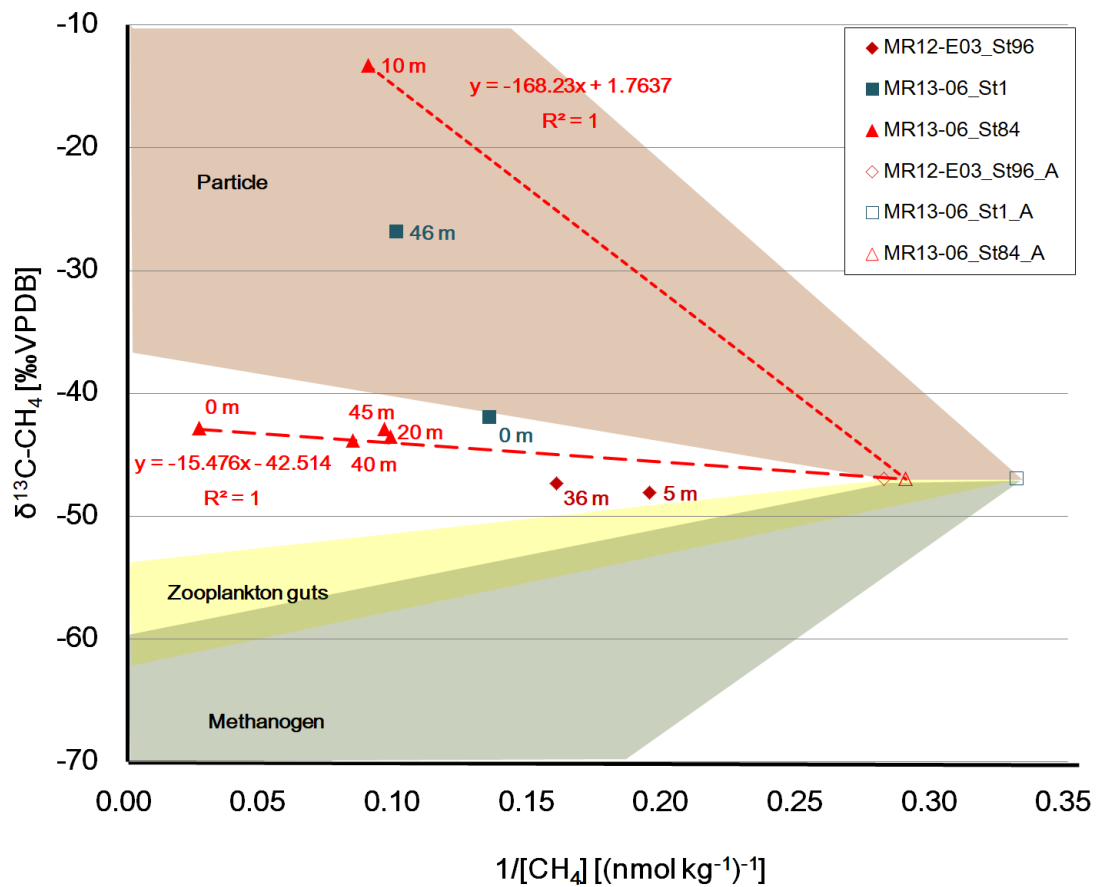


**Figure 4-7.** Relationship between inverse of dissolved  $\text{CH}_4$  concentration ( $1/[\text{CH}_4]$ ) and three end-members (Zs: sinking particle from zooplankton body ( $\delta^{13}\text{C}$  = from -37 to +6‰VPDB: Sasakawa et al., 2008); Zg: zooplankton guts ( $\delta^{13}\text{C}$  = from -61 to -54‰VPDB: Sasakawa et al., 2008); M: methanogen ( $\text{CO}_2$  reduction pathway) ( $\delta^{13}\text{C}$  = from -110 to -60‰VPDB: Whiticar et al., 1986, 1999; Sugimoto and Wada 1993)) in Bering Strait in 2012 (at station 96) and 2013 (at stations 1 and 84). Data from dissolved  $\text{CH}_4$  are drawn as closed symbols and calculated values for the surface water equilibrated with the atmosphere (A) are drawn as open symbols. Straight lines show mixing lines between 0 m and atmospheric equilibrium, and between 0 m and atmospheric equilibrium station 84 in 2013.

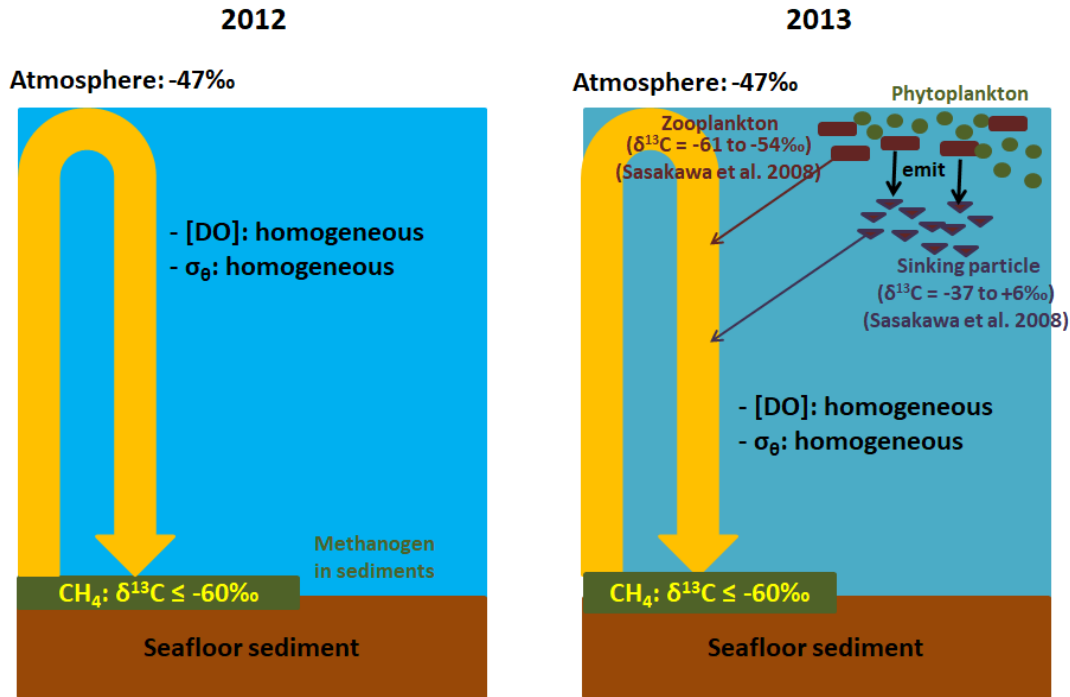


**Figure 4-8.** Schematics of dissolved  $\text{CH}_4$  dynamics in the Bering Strait in 2012 and 2013.

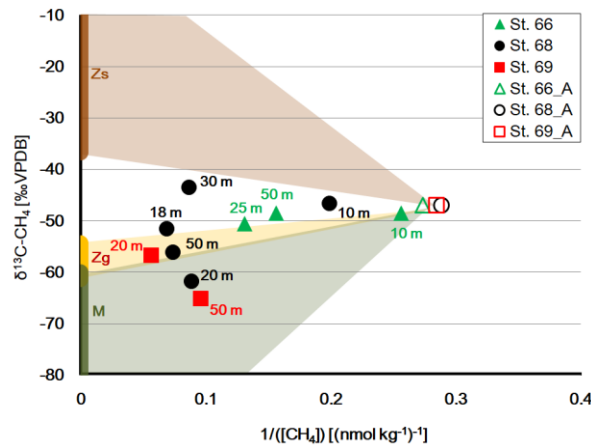


**Figure 4-9.** Relation between inverse of dissolved  $\text{CH}_4$  concentration ( $1/[\text{CH}_4]$ ) and  $\delta^{13}\text{C}-\text{CH}_4$  values in 10–50 m depth at stations 66, 68, and 69. Data from 10–50 m depth are drawn as closed symbols and calculated values for the surface water equilibrated with the atmosphere (A) is drawn as open symbols. Three zones show mixing between each of three end-members (Zs, sinking particle from zooplankton body ( $\delta^{13}\text{C}_{\text{Zs}}$  = from -37 to +6‰; Sasakawa et al. 2008); Zg, zooplankton guts ( $\delta^{13}\text{C}_{\text{Zg}}$  = from -61 to -54‰; Sasakawa et al. 2008); M, methanogen ( $\text{CO}_2$  reduction pathway) ( $\delta^{13}\text{C}_{\text{M}}$  = from -110 to -60‰; Whiticar et al. 1986, 1999; Sugimoto and Wada 1993)) and the surface water.

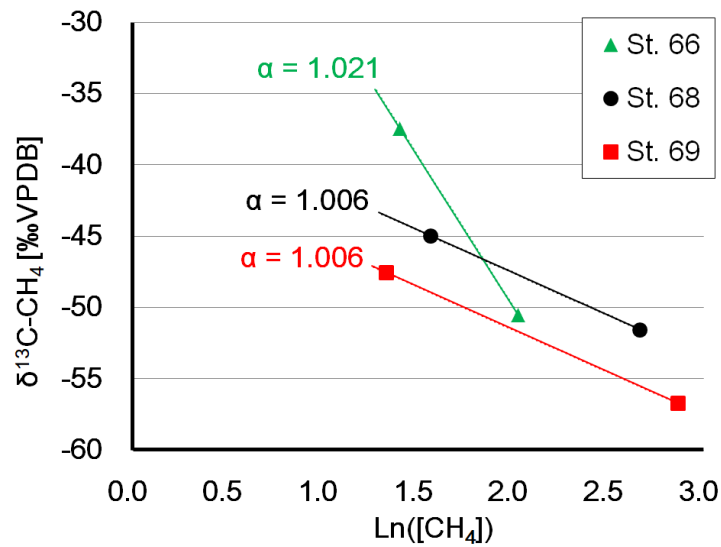


**Figure 4-10.** Oxidation curve between CH<sub>4</sub> concentration maximum in 10–50 m depth and 0–10 m depth.

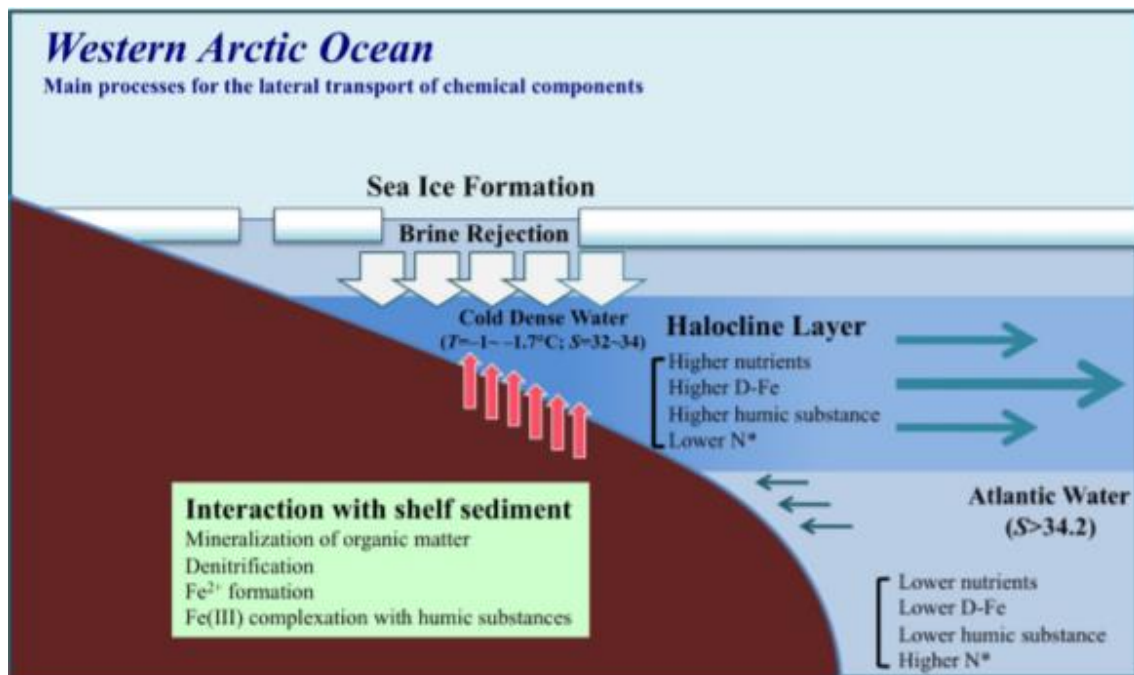


**Figure 4-11.** Schematic representation of the three main processes leading to the lateral transport of chemical constituents in the halocline layer of the western Arctic Ocean: (1) brine rejection during sea-ice formation; (2) dissolved (D)-Fe, nutrients, and humic DOM supplied from shelf sediments to the overlying brine water in the shelf region; and (3) lateral transport from shelf to basin of D-Fe, nutrients, and humic DOM in the halocline layer (Hioki et al. 2014).

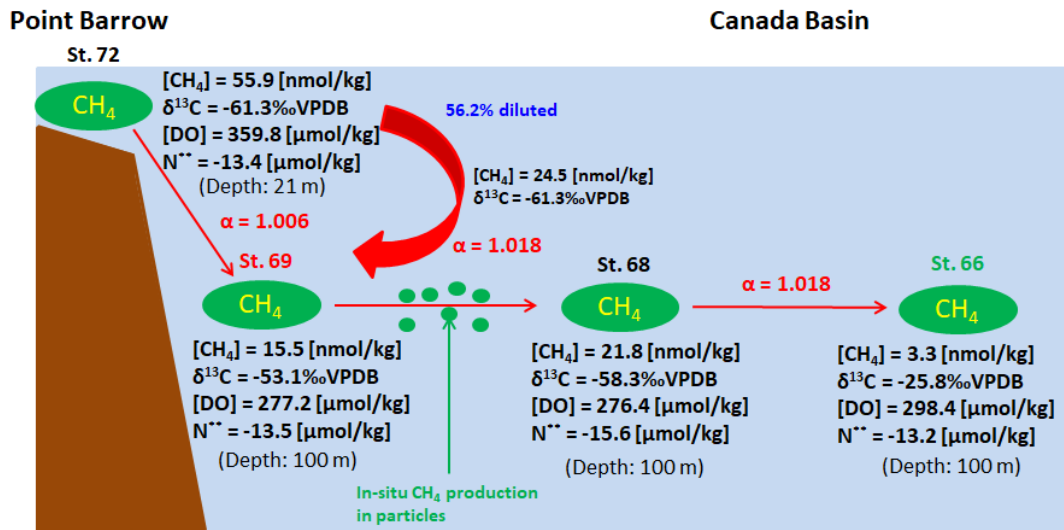


**Figure 4-12.** Schematic of CH<sub>4</sub> transportation from continental area to deeper area based on information of St. 72 (Depth: 21 m), 69, 68, and 66 (Depth: 100 m) on MR12-E03 cruise

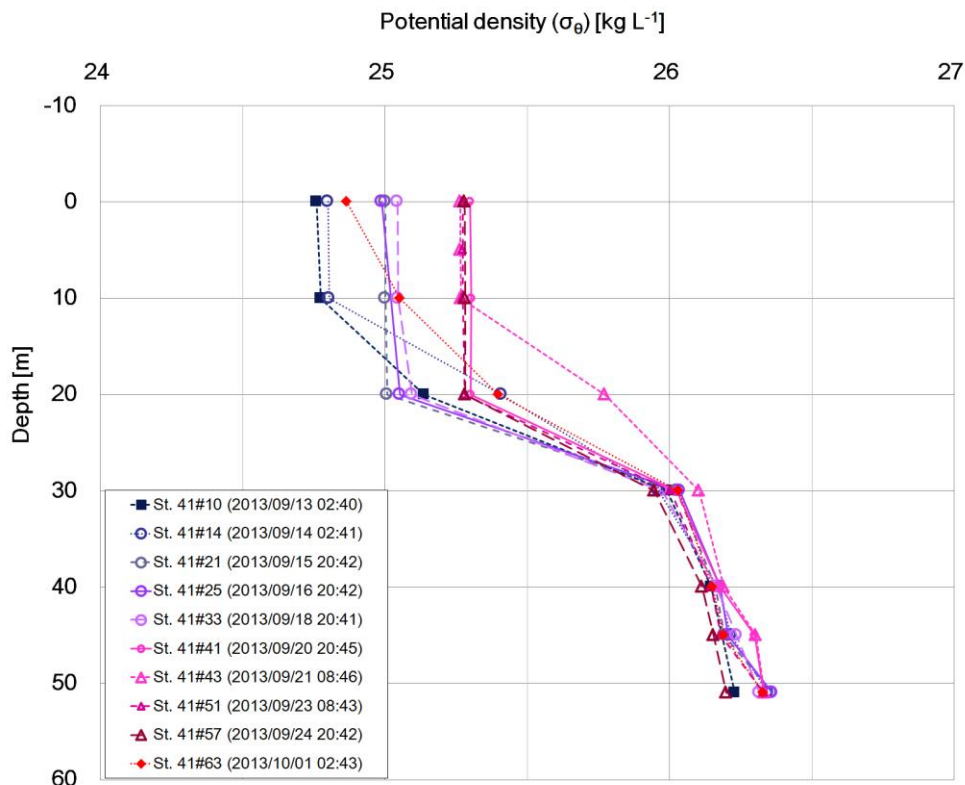


**Figure 4-13.** Vertical distributions of potential density ( $\sigma_\theta$ ) in fixed-point observation in 2013.

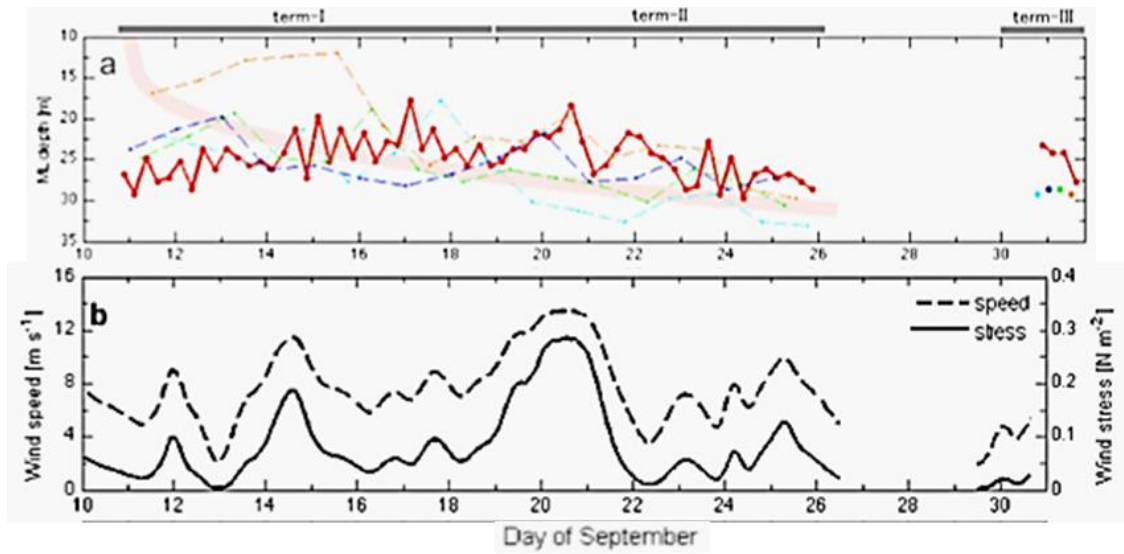


**Figure 4-14.** Time series of (a) Mixed layer (ML) depth (m) and (b) surface wind speed (dashed) ( $\text{m s}^{-1}$ ) and wind stress (solid) ( $\text{N m}^{-2}$ ). In (a), ML depth is defined as an average depth of  $\sigma_\theta = 25.5\text{--}25.9$  isopycnal. Red, blue, green, orange, and sky blue colored line denote the daily CTD stations to the center, north, south, east, and west, respectively. In (b), wind stress magnitude is defined as  $\text{ABS}(\tau) = \rho_a c_D \text{ABS}(v^2)$ . Where  $\rho_a$  is the air density and  $c_D$  is the drag coefficient. Term I, II, and III is 10–18 September, 19–26 September, and 30 September and 1 October, respectively (Kawaguchi et al. 2015).

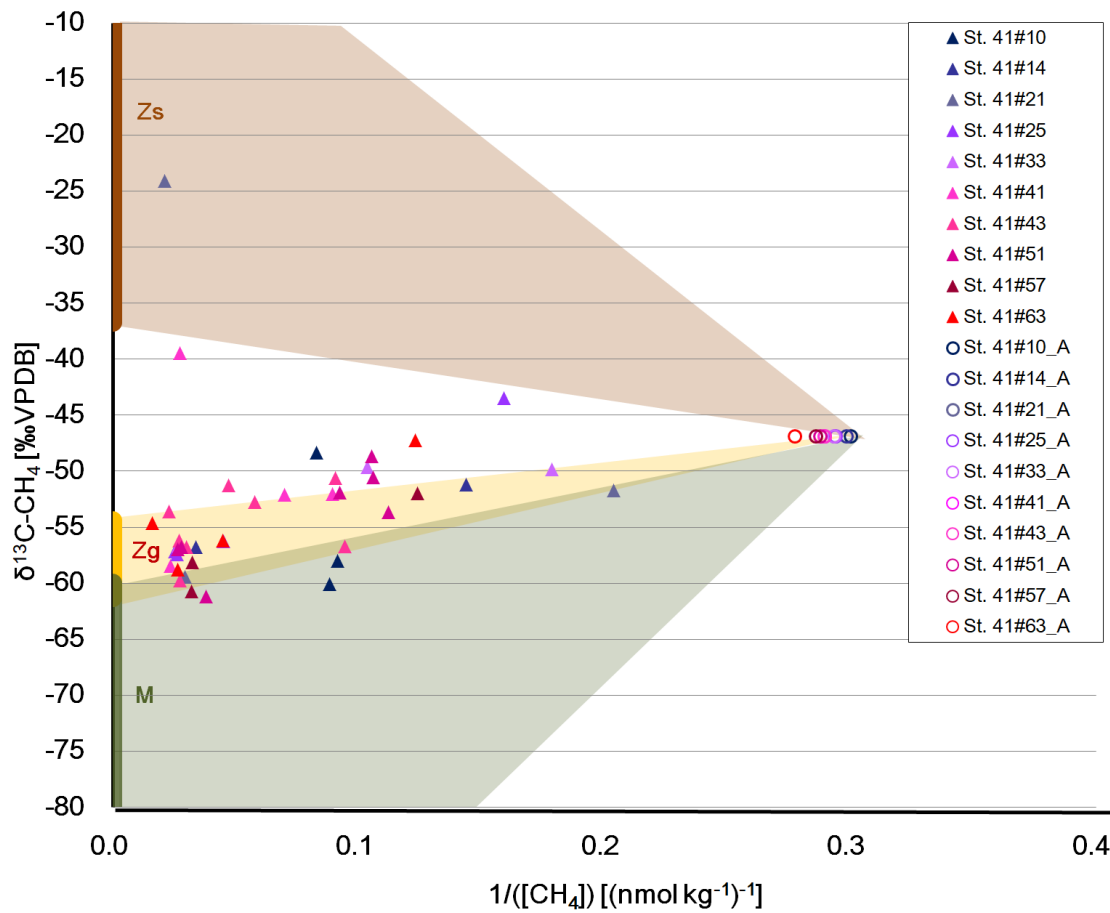


**Figure 4-15.** Relationship between inverse of dissolved CH<sub>4</sub> concentration and three end-embers (Zs: sinking particle from zooplankton body ( $\delta^{13}\text{C}$  = from -37 to +6‰VPDB: Sasakawa et al., 2008); Zg: zooplankton guts ( $\delta^{13}\text{C}$  = from -61 to -54‰VPDB: Sasakawa et al., 2008); M: methanogen (CO<sub>2</sub> reduction pathway) ( $\delta^{13}\text{C}$  = from -110 to -60‰VPDB: Whiticar et al., 1986, 1999; Sugimoto and Wada 1993)) in fixed-point observation in 2013.

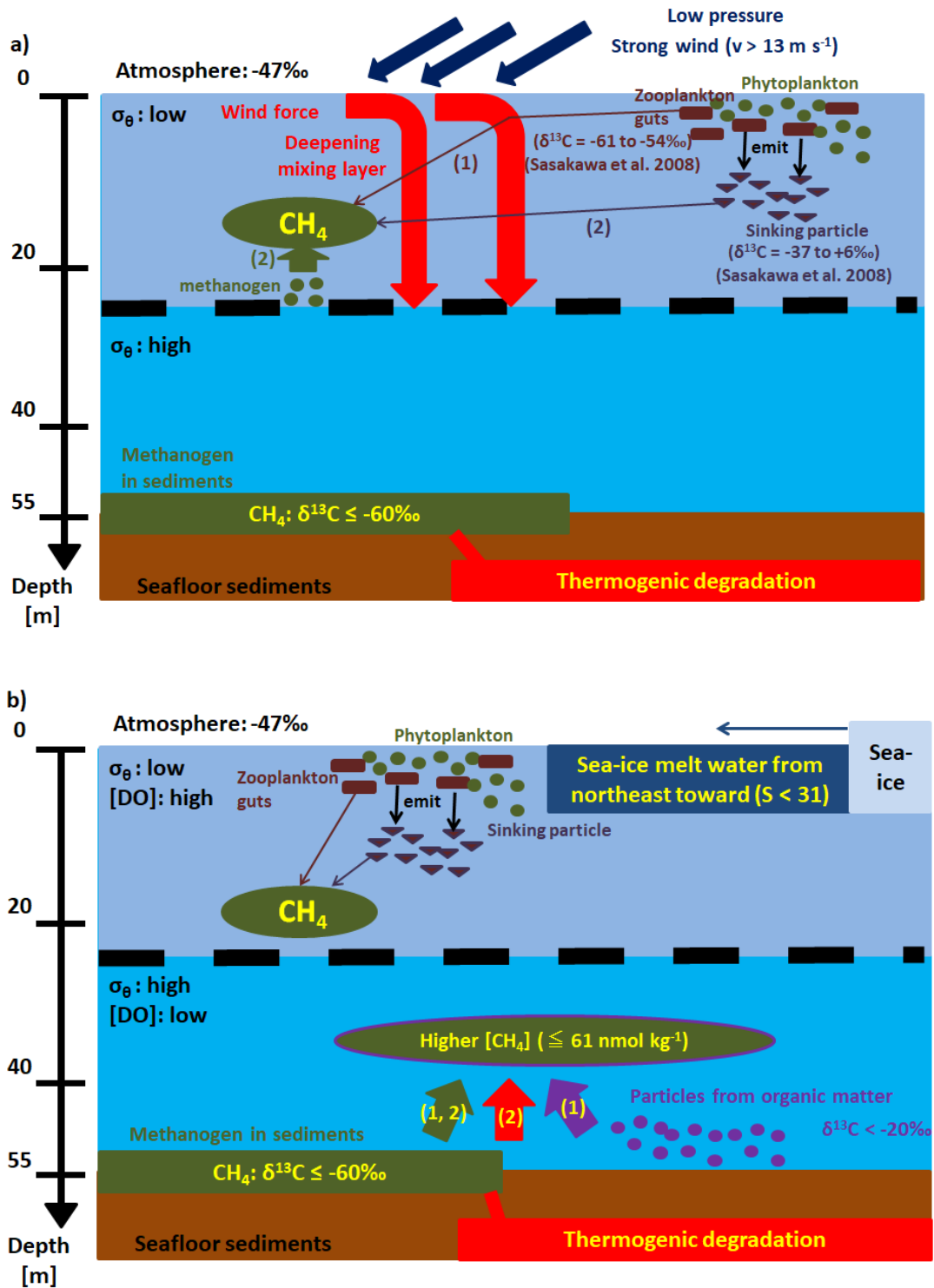


**Figure 4-16.** Schematics of dissolved CH<sub>4</sub> dynamics in FPO during (a) September 21<sup>th</sup> and (b) October 1<sup>st</sup>.

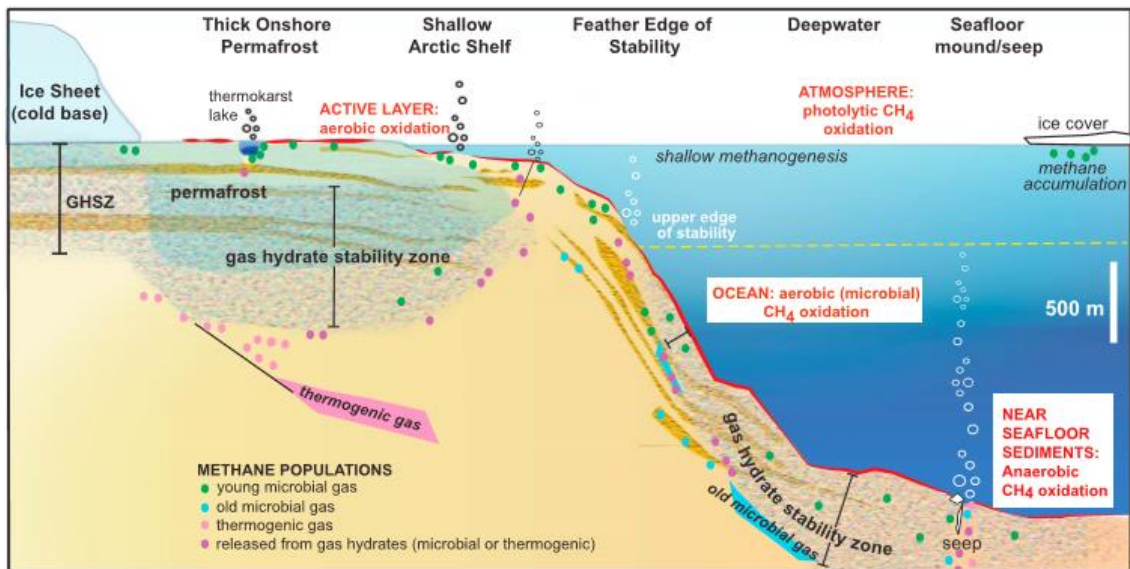


**Figure 4-17.** Schematic of methane hydrate dynamics and methane distributions in different physiographic provinces. This diagram is updated from Ruppel [2011a] with the addition of subglacial hydrates and methane accumulation under ice. The most climate-susceptible hydrates are associated with (1) thawing subsea permafrost beneath Arctic Ocean shelves that were unglaciated at the Last Glacial Maximum (LGM) and (2) dissociating gas hydrates on upper continental slopes, respectively corresponding to Sectors 2 and 3 of Ruppel [2011a] (Ruppel and Kessler 2017).

## Tables

**Table 4-1.** Distribution of dissolved CH<sub>4</sub> concentrations, δ<sup>13</sup>C values, and α values at St. 66, 68, 69 (at 100 m depth) and 72 (at 21 m depth).

Station	Depth (m)	[CH <sub>4</sub> ] (nmol kg <sup>-1</sup> )	δ <sup>13</sup> C (‰VPDB)	α
66	100	3.3	-25.7	1.018
68	100	21.8	-58.3	-*
69	100	15.5	-53.1	1.006
72	21	55.9	-61.3	-*

(\*: α values in these points cannot be calculated because of increasing CH<sub>4</sub> concentrations)



## Chapter 5: Conclusion

### 5.1 Summary of this study

I analyzed concentrations and  $\delta^{13}\text{C}$  values of dissolved  $\text{CH}_4$  in the western Arctic Ocean during the R/V Mirai cruise of August–October in 2012 and 2013 (MR12-E03 and MR13-06 cruises, respectively), when the sea-ice extent was minimal. Surface water was found to be supersaturated with  $\text{CH}_4$  in all cases, suggesting that the western Arctic Ocean behaved as a potential  $\text{CH}_4$  source to the atmosphere during summer time. Dissolved  $\text{CH}_4$  concentrations in surface water in 2013 were 2–3 times higher than in 2012. This reason might be considered as vertical transportation of  $\text{CH}_4$  from bottom layer to surface layer due to weaker stratification by freshwater. In the Chukchi Sea in 2012, higher  $\text{CH}_4$  concentration in the bottom layer were produced mainly by methanogens in continental shelf sediments, as indicated by their accompanying  $\delta^{13}\text{C}$  values ( $< -60\text{‰}$ ), after which they might be partially transported to the atmosphere. On the other hands, in 2013, gradients of concentration and  $\delta^{13}\text{C}$  value of dissolved  $\text{CH}_4$  were not found. Furthermore,  $\text{CH}_4$  in surface layer might be influenced by plankton activity due to higher primary production by nutrient supply from bottom to surface. Therefore, these facts suggested that  $\text{CH}_4$  was influenced by vertical mixing between bottom layer and surface layer, and plankton activity in surface layer in 2013. In the Canada Basin in 2012, maxima of  $\text{CH}_4$  concentration were detected at 10–50 m and 100–200 m depths. Profiles of  $\delta^{13}\text{C}$ , DO concentration and  $\text{N}^{**}$  values indicate that shallower  $\text{CH}_4$  maxima were produced by guts in zooplankton, sinking particles, and phytoplankton metabolite (e.g., DMSP), whereas deeper  $\text{CH}_4$  maxima were produced by

methanogen in continental shelf sediments, with transportation horizontally to the Canada Basin with effects from both CH<sub>4</sub> production by particle and biological CH<sub>4</sub> oxidation. Results obtained from this study clarified the horizontal and vertical profiles of dissolved CH<sub>4</sub> in the western Arctic Ocean. During the fixed point observation in 2013, concentrations and  $\delta^{13}\text{C}$  values of dissolved CH<sub>4</sub> in bottom layer were higher and lower than in surface layer, respectively. Especially, Vertical mixing occurred at windy condition by low pressure and this produced the highest CH<sub>4</sub> concentration in the surface layer (17.2 nmol kg<sup>-1</sup> with  $\delta^{13}\text{C} = -52.9\text{‰}$ ), which suggested that CH<sub>4</sub> was transported from bottom of mixing layer and might be produced by zooplankton guts and/or methanogen. These results are expected to contribute to our understanding of impact of sea-ice melting to greenhouse gas dynamics and the feedback effects to Arctic climate change.

## 5.2 Future works

I clarified the spatial and temporal profiles of dissolved CH<sub>4</sub> in the summertime western Arctic Ocean based on information of concentration and  $\delta^{13}\text{C}$  values. However, factor for obtaining CH<sub>4</sub> production processes in more detail and longer scale may be still limited based on only this information. Thus I think that below things should be conducted as future works.

- (1) Investigating the profile of  $\delta\text{D}$  values which help to clarify CH<sub>4</sub> production processes via methanogen (CO<sub>2</sub> production process and acetate fermentation process).
- (2) Investigating concentration and  $\delta^{13}\text{C}$  value of carbonate (HCO<sub>3</sub><sup>-</sup>) which also help to

clarify CH<sub>4</sub> production processes via methanogen.

- (3) Investigating CH<sub>4</sub> profile in sediments, which provide the information of originally CH<sub>4</sub> state and CH<sub>4</sub> emission process from sediment (including CH<sub>4</sub> hydrate) to seawater column and oversea atmosphere.
- (4) Investigating the profile of clumped-CH<sub>4</sub> (<sup>13</sup>CH<sub>3</sub>D), which reflects CH<sub>4</sub> formation temperature and information of verifying effect by thermogenic CH<sub>4</sub> production processes in deeper sediments.
- (5) Calculation using simulation model (e.g.; marine ecosystem isotopomer model, ocean circulation model and coupled ocean–atmosphere general circulation model) for developing to quantify CH<sub>4</sub> production processes, CH<sub>4</sub> dynamics in ocean and ocean–atmosphere interaction of CH<sub>4</sub>.

## **Acknowledgements**

I gratefully acknowledge to all the people who have supported my research and life. They encouraged, advised and worried me, and I could spend the greatest time of my life with them.

**My supervisors:** Prof. Naohiro Yoshida and Assoc. Prof. Keita Yamada.

**Members and persons concerned in Yoshida Group:**

**Staffs (including past time):** Assoc. Prof. Sakae Toyoda, Prof. Yasuko Kasai, Prof. Naohiko Ohkouchi, Assoc. Prof. Yuichiro Ueno, Assis. Prof. Shohei Hattori, Dr. Mayuko Nakagawa, Dr. Alexis Gilbert, Dr. Florian Breider, Dr. Miyuki Tahata, Dr. Maxime Julien, Dr. Liu Qi, Dr. Naizhong Zhang, Dr. Chisato Yoshikawa, Dr. Koki Maeda, Dr. Kentaro Yamada, Dr. Midori Yano, Dr. Chen Wu

**Past students:** Dr. Milhail Vasiliev, Ms. Nozomi Suzuki, Dr. Arata Mukotaka, Dr. Tomohiro Sato, Ms. Erena Hayashi, Dr. Hiroyuki Haraguchi, Dr. Tumendelger Azzaya, Dr. Yun Zou, Dr. Tarin Nimmanwudipong, Dr. Kota Kuribayashi, Mr. Tomoaki Umemura, Ms. Hitomi Abe, Ms. Akari Toyoda, Ms. Sanae Ishii, Mr. Kazuki Ohishi, Mr. Shingo Komatsu, Mr. Akira Inagaki, Mr. Wataru Takeya, Mr. Keiichi Kuzunuki, Mr. Kenji Doi, Mr. Yuki Sato, Mr. Takayoshi Yamada, Mr. Tamaki Fujinawa, Mr. Yuto Sugiuchi, Mr. Kohei Takeda, Ms. Sakiko Ishino, Mr. Kazuki Kamezaki, Mr. Yuta Tan, Mr. Daiki Sayama, Mr. Hiroki Tajima, Mr. Jun Hasegawa, Mr. Yuki Kajimoto, Mr. Syuichiro Matsushima, Mr. Yuki Mineta, Mr. Sho Fujiwara, Mr. Hiroaki Hamashima, Mr. Yuma Watanabe, Mr. Takahito Kakimoto, Mr. Keisuke Shimizu, Mr. Atsushi Hirakawa, Mr. Masaki Watanabe, Mr. Naoyuki Kawakami, Mr. Yoshio Nunez Palma, Mr. Fukutaro Iijima, Ms. Xu Jiaxin, Mr. Kohei Kamei, Mr. Jo Fushimi, Mr. Kenta Miyazawa, Ms. Asuka Tsuruta, Mr. Tatsunori Osone, Mr. Tomoya Matsui, Ms. Kanon Ngazu Kobayashi, Ms. Yu Okumura, Mr. Ryota Misawa, Mr. Kengo Maeto, Mr. Keisuke Furukawa

**Secretaries:** Mrs. Mitsuko Nishijima, Mrs. Hiromi Daimon, and Mrs. Chieko Endo.

**Collaboration researchers:** Dr. Daisuke Sasano, Mr. Naohiro Kusugi, Dr. Masao Ishii, Prof. Hisayuki Yoshikawa, Dr. Akihiko Murata, Dr. Hiroshi Uchida, and Dr. Shigeto Nishino.

I am supported by the scientists and crews of the MR12-E03 and MR13-06 cruises on R/V Mirai, JAMSTEC, for sampling and providing the hydrographic and nutrient data. They carefully supported me for observation, analyzing data, discussion, and life in these research cruises. This study was conducted under the Green Network of Excellence (GRENE) Arctic Climate Change Research Project. It was also supported

financially by JSPS KAKENHI 23224013 and by the Global COE program “From Earth to Earths” of the Ministry of Education, Culture, Sports, Science and Technology, Japan. When I was writing this thesis Dr. Martin Schoell well discussed with me and gave me important advices. In this work, Figures 2-1, 3-1, 3-2 and 3-6 were drawn using “Ocean Data View” (<http://odv.awi.de/>) software.

Lastly, the completion of this work would not have been possible without the support from my friends and family. I gratefully thank my Father, Mother, younger sister, Grandfather, Grandmother, uncle, aunt, cousins. My study life has been developed without their help and encouragements.

## References

- Aagaard K, Weingartner TJ, Danielson SL, Woogate RA, Johnson GC, Whitledge TE (2006) Some controls on flow and salinity in Bering Strait. *Geophys Res Lett* 33, L19602.  
doi:10.1029/2006GL026612
- Alperin MJ, Reeburgh WS, Whiticar MJ (1988) Carbon and hydrogen isotope fractionation resulting from anaerobic methane oxidation. *Global Biochem Cycles* 2:279–288.
- Arrigo KR, Dijken van G (2011) Secular trends in Arctic Ocean net primary production. *J Geophys Res* 116 C09011. doi: 10.1029/2011JC007151
- Coleman DD, Risatti JB, Schoell M (1981) Fractionation of carbon and hydrogen isotopes by methane-oxidizing bacteria. *Geochim Cosmochim Acta* 45:1033–1037.
- Damm E, Helmke E, Thoms S, Schauer U, Nothig E, Bakker K, Kiene RP (2010) Methane production in aerobic oligotrophic surface water in the central Arctic Ocean. *Biogeosci*:7, 1099–1108.
- Damm E, Kiene RP, Schwarz J, Flack E, Dieckmann G (2008) Methane cycling in Arctic shelf water and its relationship with phytoplankton biomass and DMSP. *Mar Chem* 45–59.
- Damm E, Mackensen A, Budeus G, Faber E, Hanland C (2005) Pathways of methane in seawater: Plume spreading in an Arctic shelf environment (SW-Spitsbergen). *Continental Shelf Research* 1453–1472.
- Damm E, Rudels B, Schauer U, Dieckmann G (2015) Methane excess in Arctic surface water-triggered by sea ice formation and melting. *Nature*. doi:10.138/srep16179
- Database of JAMSTEC.
- Dlugokencky EJ, Bruhwiler L, White JWC, Emmons LK, Novelli PC, Montzka SA, Masarie KA, Lang PM, Crotwell AM, Miller JB, Gatti LV (2009) Observational constraints on recent increases in the atmospheric CH<sub>4</sub> burden. *Geophys Res Lett* 36 L18803. doi: 10.1029/2009GL039780
- Dlugokencky EJ, Nisbet EG, Fisher RE, Lowry D (2011) Global atmospheric methane: budget, changes and dangers. *Phil Trans R Soc A* 369:2058–2072.
- Fenwick L, Capelle D, Damm E, Zimmermann S, Williams WJ, Vagle S, Tortell PD (2017) Methane and nitrous oxide distributions across the North American Arctic Ocean during summer, 2015. *J Geophys Res Oceans* 122:390–412. doi:10.1002/2016JC012493
- Florez-Leiva L, Damm E, Farias L (2013) Methane production induced by dimethylsulfide in surface water of an upwelling ecosystem. *Progress in Oceanography* 112-113:38–48.
- Fransson A, Chierici M, Nojiri Y New insights into the spatial variability of the surface water carbene dioxide in varying sea ice conditions in the Arctic Ocean. *Cont Shelf Res* 29:1317–1328.  
doi:10.1016/j.csr.2009.03.088
- Gong D, Pickart RS (2015) Summertime circulation in the eastern Chukchi Sea. *Deep Sea Res Part 2*

118:18–31.

- Grant NJ, Whiticar MJ (2002) Stable carbon isotopic evidence for methane oxidation in plumes above Hydrate Ridge, Cascadia Oregon Margin. *Global Biogeochem Cycles* 16:4. doi:10.1029/2001GB001851
- Gruber N, Sarmiento JL (1997) Global patterns of marine nitrogen fixation and denitrification. *Global Biogeochem Cycles* 11 (2):235–266.
- Harada N (2016) Review: Potential catastrophic reduction of sea ice in the western Arctic Ocean: Its impact on biogeochemical cycles and marine ecosystems. *Global and Planetary Change* 136:1–17.
- Hioki N, Kuma K, Morita Y, Sasayama R, Ooki A, Kondo Y, Obata H, Nishioka J, Yamashita S, Kikuchi T, Aoyama M (2014) Laterally spreading iron, humic-like dissolved organic matter and nutrients in cold, dense subsurface water of the Arctic Ocean. *Nature* 4:6775. doi: 10.1038/srep06775.
- Holmes ME, Sansone FJ, Rust TM, Popp BN (2000) Methane production, consumption, and air-sea exchange in the open ocean: An evaluation based on carbon isotopic ratios. *Global Biogeochem Cycles* 14(1):1–10.
- Hopcroft R, Bluhm B, Gradinger R (2008) Arctic Ocean Synthesis: Analysis of Climate Change Impacts in the Chukchi and Beaufort Seas with Strategies for Future Research. Univ. of Alaska Fairbanks, Inst. of Mar. Sci., 184 pp., North Pacific Research Board, Anchorage, Alaska
- Intergovernmental Panel on Climate Change AR4 (2007)
- Intergovernmental Panel on Climate Change AR5 (2013)
- Jacob DJ (1999) Introduction to Atmospheric chemistry. Princeton University Press.
- Karl DM, Beversdorf L, Bjorkman KM, Church MJ, Martinez A, Delong EF (2008) Aerobic production of methane in the sea. *Nature Geoscience* 1. www.nature.com/naturegeoscience
- Karl DM, Tilbloom BD (1994) Production and transport of methane in oceanic particulate organic matter. *Nature* 368:732–734.
- Kastner M, Kvenvolden KA, Lorenson TD (1998) Chemistry, isotopic composition, and origin of a methane-hydrogen sulfide hydrate at the Cascadia subduction zone. *Earth Planet Sci Lett* 156:173–183.
- Kawaguchi Y, Nishino S, Inoue J (2015) Fixed-Point Observation of Mixed Layer Evolution in the Seasonally Ice-Free Chukchi Sea: Turbulent Mixing due to Gate Winds and Internal Gravity Waves. *Journal of Physical Oceanography* 45: 836–853.
- Kikuchi, T (2012) R/V Mirai Cruise Report MR12-E03, edited by T. Kikuchi and S. Nishino 190pp., JAMSTEC, Yokosuka, Japan
- Kvenvolden KA (1993a) GAS HYDRATES – Geological Perspective and Global Change. *Reviews of Geophysics* 31(2):173–187.
- Kvenvolden KA, Lilley MD, Lorenson TD, Barnes PW, McLaughlin E (1993b) The Beaufort Sea

- continental shelf as a seasonal source of atmospheric methane. *Geophysical Research Letters* 20(22):2459–2462.
- Lapham L, Marshall K, Magen C, Lyubchich V, Cooper LW, Grebmeier JM (2017) Dissolved methane concentration in the water column and surface sediments of Hanna Shoal and Barrow Canyon, northern Chukchi Sea. *Deep-Sea Res II* 144: 92–103, <http://dx.doi.org/10.1016/j.dsr2.2017.01.004>
- Lelieveld J, Crutzen PJ, Dentener FJ (1998) Changing concentration, lifetime and climate forcing of atmospheric methane. *Tellus Ser B* 50:128–150.
- Macdonald RW (1976) Distribution of low-molecular weight hydrocarbons in southern Beaufort Sea. *Environmental Science and Technology* 10:1241–1246.
- Martens CS, Albert DB, Alperin MJ (1999) Stable isotope tracing of anaerobic methane oxidation in the gassy sediments of Eckernförde Bay, German Baltic Sea. *Am J Sci* 299:589–610.
- McGuire AD, Anderson LG, Christensen TR, Dallimore S, Guo L, Hayes DJ, Heimann M, Lorenson TD, Macdonald RW, Roulet N (2009) Sensitivity of the carbon cycle in the Arctic to climate change. *Ecological Monograph* 79(4):523–555.
- McGuire AD, Macdonald RW, Schuur EAG, Harden JW, Kuhry P, Hayes DJ, Christensen TR, Heimann M (2010) The carbon budget of the northern cryosphere region. *Current Opinion in Environmental Sustainability* 2:231–236.
- Myhre CL, Ferre B et al (2016) Extensive release of methane from Arctic seabed west of Svalbard during summer 2014 does not influence the atmosphere. *Geophys Res Lett* 43:4624–4631. doi:10.1002/2016GL068399
- Nishino S, Kikuchi T, Fujiwara A, Hirawake T, Aoyama M (2016) Water mass characteristics and their temporal changes in a biological hotspot in the southern Chukchi Sea. *Biogeosciences* 13:2563–2578. doi:10.5194/bg-12-2563-2016
- Nishino S, Shimada K, Itoh M (2005) Use of ammonium and other nitrogen tracers to investigate the spreading of shelf waters in the western Arctic Ocean. *J Geophys Res* 110 C10005. doi: 10.1029/2003-JC002118
- Oremland RS (1979) Methanogenic activity in plankton samples and fish intestines: A mechanism for in situ methanogenesis in oceanic surface waters. *Limnol Oceanogr* 24(6):1136–1141.
- Permentier F-JW, Christensen TR, Sorensen LL, Rysgaard S, McGuire AD, Miller PA, Walker DA (2013) The impact of lower sea-ice extent on Arctic greenhouse-gas exchange. *Nature Climate Change* 3:195–202. doi:10.1038/nclimate1784
- Prince MJ, Blanch HW (1990) Bubble Coalescence and Break-up in air-sparged bubble columns. *AIChE Journal* 36(10): 1485–1499.
- Quay PD, King SL, Stutsman J, Wilbur DO, Steele LP, Fung I, Gammon RH, Brown TA, Farwell GW, Grootes PM, Schmidt FH (1991) Carbon isotopic composition of atmospheric methane:



- Fossil and biomass burning source strength. *Global Biogeochem Cycles* 5:25–47.
- Rau GH, Sweeney RE, Kaplan IR (1982) Plankton  $^{13}\text{C}$ :  $^{12}\text{C}$  ratio changes with latitude: differences between northern and southern oceans.
- Rehder G, Brewer PW, Peltzer ET, Friederich G (2002) Enhanced lifetime of methane bubble streams within the deep ocean. *Geophys. Res. Lett.* 29 15:1731. doi:10.1029/2001GL013966
- Ruppel CD, Kessler JD (2017) The interaction of climate change and methane hydrates. *Rev. Geophys.* 55:126–168. doi:10.1002/2016RG000534
- Sansone FJ, Popp BN, Gase A, Graham AW, Rust TM (2001) Highly elevated methane in the eastern tropical north Pacific and associated isotopically enriched fluxes to the atmosphere. *Geophys Res Lett* 24:4567–4570.
- Sasakawa M, Tsunogai U, Kameyama S, Nakagawa F, Nojiri Y, and Tsuda A (2008) Carbon isotopic characterization for the origin of excess methane in subsurface seawater. *J Geophys Res* 113, C03012. doi:10.1029/2007JC004217
- Savichev AS, Rusanov II, Pimenov NV, Zakharova EE, Veslopolpva EF, Lein AL, Crane K, Ivanov MV (2007) Microbial processes of the carbon and sulfur cycles in the Chukchi Sea. *Mikrobiologiya* 76(5):682–693. doi:10.1134/S00262617070S0141
- Shakhova N, Semiletov I, Leifer I, Sergienko V, Salyuk A, Kosmach D, Stubbs C, Nicolsky D, Tumskoy V, Gustafsson O (2014) Ebullition and storm-induced methane release from the East Siberian Arctic Shelf. *Nature Geoscience* 7. doi: 10.1038/NGEO2007, [www.nature.com/naturegeoscience](http://www.nature.com/naturegeoscience)
- Shakhova N, Semiletov I, Panteleev G (2005) The distribution of methane on the Siberian Arctic shelves: Implications for the marine methane cycle. *Geophys Res Lett* 32 L09601. doi:10.1029/2005GL022751
- Shakhova N, Semiletov I, Salyuk A, Yusupov V, Kosmach D, Gustafsson O (2010) Extensive Methane Venting to the Atmospheric from ediments of the East Siberian Arctic Shelf *Science* 327:1246 doi: 10.1126/science.118221
- Sugimoto A, Wada E (1993) Carbon isotopic composition of bacterial methane in a soil incubation experiment: Contributions of acetate and  $\text{CO}_2/\text{H}_2$ . *Geochim Cosmochim Acta* 57:4015–4027
- Tilbrook BD, Karl DM (1995) Methane sources, distributions and sinks from California coastal waters to the oligotrophic North Pacific gyre. *Mar Chem* 49:51–64.
- Tsunogai U, Ishibashi J, Wakita H, Gamo T, Watanabe K, Kajimura T, Kanayama S, Sakai H (1998) Methane rich plumes in Suruga Trough (Japan) and their carbon isotopic characterization. *Earth Planet Sci Lett* 160:97–105.
- Tsunogai U, Yoshida N, Ishibashi J, Gamo T (2000) Carbon isotopic distribution of methane in deep-sea hydrothermal plume, Myojin Knoll Caldera, Izu-Bonin arc: Implications for microbial methane oxidation in the oceans and applications to heat flux estimation. *Geochimica et*

- Cosmochimica Acta 64(14):2439–2452.
- Valentine DL, Blanton DC, Reeburgh WS, Kastner M (2001) Water column methane oxidation adjacent to an area of active hydrate dissociation, Eel River Basin. *Ceochimica et Cosmochimica Acta* 65(16): 2633–2640.
- Verzhbitsky V, Savostina T, Frantzen E, Little A, Sokolov SD, Tuchkova MI (2008) The Russian Chukchi Sea shelf. *GEO ExPro* 5(3): 36–41 (full article available at <http://www.geo365.no/TGS-Chukchi/>).
- Wanninkhof R (1992) Relationship Between Wind Speed and Gas Exchange Over the Ocean. *J. Geophys Res* 97, C5, 7373–7382.
- Watanabe S, Higashitani N, Tsurushima N, Tsunogai S (1995) Methane in the Western North Pacific. *J Oceanogr* 51:39–60.
- Whiticar MJ (1999) Carbon and hydrogen isotope systematics of bacterial formation and oxidation of methane. *Chemical Geology* 161:291–314.
- Whiticar MJ, Faber E, Schoell M (1986) Biogenic methane formation in marine and freshwater environments: CO<sub>2</sub> reduction vs. acetate fermentation – isotope evidence. *Geochim Cosmochim Acta* 50:693–709.
- Wiesenberg DA, Guinasso NL, Jr. (1979) Equilibrium Solubilities of Methane, Carbon Monoxide, and Hydrogen in Water and Sea Water. *Journal of Chemical and Engineering Data* 24(4):356–360.
- Yamada Y, Fukuda H, Uchimiya M, Motegi C, Nishino S, Kikuchi T, Nagata T (2015) Localized accumulation and a shelf-basin gradient of particles in the Chukchi Sea and Canada Basin, western Arctic. *J Geophys Res Oceans*. doi:10.1002/2015JC010794
- Yamada K, Yoshida N, Nakagawa F, Inoue G (2005) Source evaluation of atmospheric methane over western Siberia using double stable isotopic signatures. *Org Geochem* 36:717–726.
- Yoshida O, Inoue HY, Watanabe S, Noriki S, Wakatsuchi M (2004) Methane in the western part of the Sea of Okhotsk in 1998–2000. *J Geophys Res* 109 C09S12. doi: 10.1029/2003-JC001910
- Yoshikawa C, Hayashi E, Yamada K, Yoshida O, Toyoda S, Yoshida N (2014) Methane sources and sinks in the subtropical South Pacific along 17°S as traced by stable isotope ratios. *Chemical Geology* 382: 24–31.
- Zhang J, Zhan L, Chen L, Li Y, Chen J (2015) Coexistence of nitrous oxide undersaturation and oversaturation in the surface and subsurface of the western Arctic Ocean. *J Geophys Res Oceans* 120:8392–8401. doi:10.1002/2015JC011245
- Zhou J, Tison JL, Camat G, Geilfus NX, Delille B (2014) Physical controls on the storage of methane in landfast sea ice. *The Cryosphere* 8:1019–1029. doi:10.5194/tc-8-1019-2014